



**Politecnico  
di Torino**

Politecnico di Torino  
Mining Engineering  
A.Y. 2020/2021

# **3D geomechanical characterization for a safe design of an open pit exploitation**

Supervisors:

Prof. Marilena Cardu

Dr. Daniele Martinelli

Dr. Marcelino Linares Gonzalez

Candidate:

Giorgia Pasqualone

## INDEX

INTRODUCTION .....	1
1. MINING LEGISLATION .....	2
1.1. Italian regulation of the mining activities .....	2
1.2. Regional law of 1998, August 8 <sup>th</sup> .....	3
1.3. Current quarry plan at Varese Province .....	4
1.3.1 Main definitions .....	5
1.3.2 Technical Standards .....	7
1.4. Technical restrictions .....	9
1.4.1 Distances .....	9
1.4.2 Perimeter of the area .....	9
1.4.3 Waste material .....	10
1.4.4 Stages of exploitation.....	10
1.4.5 Vegetable soil .....	10
1.4.6 Water drainage.....	11
1.4.7 Service roads.....	11
1.4.8 Protection of aquifers.....	11
1.4.9 Protection of human health from noise impact.....	12
1.5. Overview of the mineral deposits available in Varese Province.....	12
2. CASE STUDY: ATE C2 – TRAVEDONA MONATE .....	15
2.1. Framework of the area .....	15
2.2. Technical constrains from legislation .....	16
2.3. Project of exploitation .....	19
2.3.1 Exploitation design .....	20
2.3.2 Morphological recovery.....	21
2.3.3 Exploitation method.....	22

2.3.3.1	Overburden removal.....	22
2.3.3.2	Excavation of the material .....	23
2.3.3.3	Material conveyance .....	24
2.3.3.4	Crushing.....	24
2.4.	Work model.....	24
2.5.	Work plan.....	25
2.5.1	Phase 1 .....	26
2.5.2	Phase 2 .....	27
2.5.3	Phase 3 .....	28
2.5.4	Phase 4 .....	28
2.5.5	Phase 5 .....	29
2.6.	Limestone exploited from the Faraona quarry .....	29
3.	SLOPE STABILITY ASSESSMENT .....	31
3.1.	Limit equilibrium method .....	33
3.2.	Numerical modelling.....	35
3.2.1	Continuum models.....	36
3.2.2	Discontinuum models .....	37
3.2.3	Criticalities in slope numerical modelling .....	38
4.	FARAONA QUARRY: THE DESIGN PROCESS .....	39
4.1.	Geological data.....	39
4.1.1	Ternate formation .....	40
4.1.2	Geological environment.....	41
4.2.	Structural data .....	42
4.3.	Instability phenomena during the excavation phase .....	44
4.3.1	Instability phenomena occurred in 2017 and adaptation of the excavation technique.....	45

4.3.2	Instability phenomena occurred in 2018.....	46
4.3.3	Instability phenomena occurred in 2019.....	47
4.3.4	Present situation.....	48
4.4.	Geotechnical model.....	50
4.5.	Stability analyses carried out .....	52
4.5.1	Slope stability analysis 2011.....	53
4.5.2	Slope stability analysis 2019.....	56
4.5.3	Considerations on the existing stability analyses .....	58
5.	CONTINUUM MODELLING OF THE FARAONA QUARRY .....	60
5.1.	Model preparation .....	61
5.1.1	Geometry .....	61
5.1.2	Meshing .....	63
5.1.3	Staging .....	65
5.2.	Input data.....	66
5.2.1	Rock mass parameters .....	66
5.2.2	Loads and boundary conditions .....	68
5.3.	Results.....	69
5.3.1	Displacements.....	69
5.3.2	Equivalent plastic strain.....	70
5.3.3	Material status.....	71
5.4.	Remarks on the continuum modelling .....	73
6.	DISCONTINUUM MODELLING OF THE FARAONA QUARRY .....	74
6.1.	Model preparation .....	74
6.1.1	Geometry .....	74
6.1.2	Meshing .....	77
6.1.3	Staging .....	78

6.2.	Input data.....	78
6.2.1	Joint properties.....	79
6.2.2	Material properties .....	81
6.2.3	Boundary conditions .....	82
6.3.	Results.....	83
6.3.1	Displacements.....	83
6.3.2	Principal stresses.....	85
6.3.3	Joint stress.....	87
6.4.	Remarks on the overall discontinuum modelling.....	88
7.	BACK ANALYSIS FOR THE EAST FACE.....	90
7.1.	Model preparation .....	90
7.1.1	Geometry .....	90
7.1.2	Meshing .....	91
7.1.3	Staging .....	91
7.2.	Input data.....	93
7.2.1	Joint properties.....	93
7.2.2	Material properties .....	94
7.2.3	Boundary conditions .....	95
7.2.4	Back-analysis data .....	95
7.3.	Results.....	96
7.3.1	Displacements .....	96
7.3.2	Joint stress.....	103
7.4.	Remarks on the detailed discontinuum modelling and back-analysis ..	105
8.	CONCLUSIONS .....	106
	REFERENCES .....	108
	ACKNOWLEDGEMENTS.....	111



# INTRODUCTION

According to the *Legambiente 2021 Quarry Report*, in Italy there are currently 4,168 authorized quarries. In detail, the aggregate quarries and those of limestone and gypsum represent over 64% of the total authorized quarries in Italy, a percentage that exceeds 81% analysing the amounts extracted. For instance, 26.8 Mm<sup>3</sup> of limestone are extracted annually for the construction sector. This sector, so delicate due to the impacts and the interests of many subjects, is governed at national level by a Royal Decree of Vittorio Emanuele III of 1927. With the D.P.R. 616/1977 the administrative functions related to the quarry activities were transferred to the Regions, and regional regulations were gradually approved to control the sector.

In this scenario, the need for an extension of a limestone quarry developed. The quarry is located in the Municipality of Travedona Monate, in the Province of Varese. The demand of material for the cement factory managed by Holcim Italia SpA required an expansion of the exploitation of the Faraona quarry, paying particular attention to a "safe" design both for workers and from a purely legislative point of view.

However, a planning of the exploitation cannot always be kept during the extraction, as changes can occur, which require an adaptation of the exploitation plan. An important and flexible tool for obtaining good results is numerical modelling, which, through the reconstruction of the three-dimensional model with specific software, allows to model the behaviour of the rock to evaluate the stability of the pit. The existing 2D model returned a good idea of the scenarios, nevertheless this work is based on a more accurate and complex series of 3D-FEM and 3D-DEM analyses to better describe the overall and local stability of the new slopes forming the extension of the quarry.

# 1. MINING LEGISLATION

The economy based on minerals has unique aspects, and, in particular, all mining activities are characterized by a given level of uncertainty. Each exploitation is peculiar and the production of minerals for industry represents an essential element for the economy of a country. Therefore, the demands for expansion of mining operations for increasing profits collide with the environmental and political restrictions of the state where the deposit is located.

To proceed with an expansion of a field exploitation, the reference regulatory context has to be examined. Each country has its own legislation: in Italy, for example, the main law dates back to the period before the Second World War and provides a distinction between different types of extraction. Currently the regulation has undergone considerable changes, delegating most of the planning and supervision tasks to the Regions, which opted for planning on a provincial basis.

At the European level, mining activities are considered in a unitary way, within the policy of raw materials, as it is believed that each mineral has its own specific use and function in the European production system, without favouring particular types of goods. Within the Community policy, a specific action is also envisaged for the reduction of the consumption of raw materials, through recycling or reuse, as well as the replacement of high impact materials with others of lesser interference with the environment.

## 1.1. Italian regulation of the mining activities

The exploitation of minerals from quarries and mines represents a significant activity both economically and in terms of environmental impact. Rocks and minerals represent for many industrial sectors the raw material necessary for the production of goods. The Italian legislation dates to the Royal Decree n. 1443/1927, which provides a clear distinction based on the type of material extracted. Mines

are those activities in which first category materials are extracted (i.e. minerals that can be used for the extraction of metals, metalloids, graphite, phosphates, alkaline and magnesium salts, alumite, micas, feldspar, kaolin and bentonite); while quarries are those in which second category materials are extracted (i.e. peat, materials for building constructions).

Based on the recent changes made to the Italian constitution, the competences relating to the exploitation of non-energy minerals have been transferred to the Regions; the reference standards are the Presidential Decree of July 24<sup>th</sup>, 1977, n. 616; Legislative Decree March 31<sup>st</sup> 1998 n.112 and Legislative Decree June 22<sup>nd</sup> 2012 n.83.

The substantial difference between mining and quarrying activities, from a conceptual point of view, is extremely clear: the mines are owned by the State, as an unavailable asset (and then were moved to the Regions), whereas the quarries are left in availability of the landowner, with the provisions of article 826 of the Civil Code. The mining activity must not meet any limits for the principle of ownership, as the deposit of a first-class mineral belongs to the State, and the private individual cannot claim possession.

## **1.2. Regional law of 1998, August 8<sup>th</sup>**

The law governs the regional planning in the field of research and exploitation of minerals from quarries and mines and the relative activity in the Lombardy Region in execution of the national law D.P.R. n. 616 of July 24<sup>th</sup> of 1977 (art. 62).

The planning of mining activities is implemented through plans at the provincial level, divided by type of material extracted. These plans state location, quality and amount of usable resources.

The Provinces, in order to draw up the plans, must first consider: the geological and hydrogeological conditions of the environment;

- the current intended use of the areas related to existing infrastructures and planning tools;
- the consistency and the characteristics of the deposits, as a non-renewable resource. For these resources, surface and depth compatible with the planning must be identified;
- the requirement of maximum environmental compatibility and reuse planning;
- the existing mining activities.

The plans can be divided into different sectors (sand and gravel, clay, ornamental stones, rocks for industrial uses, crushed stone and peat) and have a maximum duration of 20 years for the stone sector and 10 years for the other sectors.

The Plans locate the areas where quarrying activities are planned (named Territorial Extractive Areas – A.T.E., and any reserve quarries for public works and recovery quarries) and identify their main characteristics, such as the maximum extractable quantities, the type of extraction (groundwater or dry), the maximum depth that can be reached, the final destination of the areas at the end of the environmental rehabilitation, the presence of any constraints and any other requirements.

Finally, the quarry plans include the technical regulations, which contain, among other things, general and detailed rules for the exploitation of quarries and rules relating to environmental rehabilitation.

### **1.3. Current quarry plan at Varese Province**

The provincial quarry plan of Varese, approved in 2008, was updated with the D.G.R. X/1093 of June 21<sup>st</sup> of 2016 (published on July 14<sup>th</sup> of 2016 n.28), based on the results of the Strategic Environmental Assessment procedure initiated by DGR n. IX/4851 of February 13<sup>th</sup> of 2013 (Varese quarry plan 2016).

The quarry plan of the province of Varese was drawn up in accordance with the "*Requirements for the formation of provincial quarry plans*" issued by the

Lombardy Region with the resolutions of the Regional Council n. 6/41714 of February 26<sup>th</sup> of 1999 and n. 6/49320 of March 31<sup>st</sup> of 2000, in application of art.5 of the Regional Law n. 14 of August 8<sup>th</sup> of 1998 and in compliance with the contents of art.6 of the same law. In particular, the quarry plan:

- identifies the exploitable areas;
- identifies the A.T.E., including those located in protected areas pursuant to Regional Law n.86 of November 30<sup>th</sup> 1983;
- defines the production areas at the provincial level;
- identifies the reserve areas of aggregates, to be used exclusively for the occurrences of public works;
- identifies the depleted quarries to be subjected to environmental rehabilitation;
- establishes the intended use of the areas for the period of the production processes and their final destination at the end of the mining activity;
- determines, for each A.T.E., the types and amounts of substances exploitable from a quarry, in relation to existing mining activity, consistency of orebody, product characteristics, processing technologies, basins of users (provincial-national);
- establishes the general regulations applicable to all mining activities for the exploitation and environmental recovery that must be observed for each basin in relation to hydrogeological characteristics, geotechnical and the type of substances exploitable.

### **1.3.1 Main definitions**

A.T.E.: Territorial Extractive Area: the unit of reference in which mining activities are permitted during the period of validity of the quarry plan; it may include either or more productive settlements consisting of quarry, plants and connected activities. They are identified in Annex A and marked by the acronym ATE + sector + progressive identification number (ex. ATEc2).

Extractive area: it is the area where the exploitation has been planned. It is identified within the mining area in Annex A and recognised by the initials E.

Quarry: it is the unit inside the A.T.E. characterized by the homogeneity of the activity. Identification is in Annex A and marked by the initials C + number.

Plant and storage area: they are included in the A.T.E. used for activities of processing, transformation and temporary storage of the extracted and/or worked material. They are identified in Annex A and marked by the initials Is.

Area devoted to service facilities: they are included in the A.T.E. and used as structures related to mining. Service areas can be located either inside or outside the mining area. They are identified in Annex A and marked by the initials S1 in the case of offices, garages, warehouses and by S2 in the case of access roads, perimeter tracks e manoeuvring areas.

Area of respect: area, included in the A.T.E., surrounding the areas previously defined, necessary to ensure a correct relationship between the intervention area and the adjacent territory. They are identified in Annex A and marked by the initials T1 if it is subject in whole or in part to the Sector connected to the A.T.E., by the initials T2 in case of other areas and T3, in case of a transit area of respect, is identified where the urban plan provides for an alternative urban destination.

Recovery quarry: closed quarry where temporary recovery is allowed of the mining activity for the sole purpose of allowing its environmental rehabilitation according to times and methods established in the environmental refurbishment project. They are identified in Annex B and identified by the initials R + sector + number progressive.

Reserve quarry: quarry intended for the production of aggregates to be used exclusively for occurrences of public works.

Exploitable orebody: part of the provincial territory affected by the presence of quarry mineral resources without unavoidable constraints and obstacles that prevent their exploitation. They are identified in Annex D by the initials G + number + sector.

### 1.3.2 Technical Standards

The planning project of the A.T.E., referred to the Regional Law n. 14/1998, must contain several elements:

- a planimetric survey on a suitable scale of the area with the identification of all public services uses and infrastructures and of reference points of the morphology; mining project with geological and hydrogeological report on the land involved in exploitation, also through geognostic and geophysical investigations, with identification of the lithostratigraphic sections and of the geotechnical and geomechanical characteristics;
- a technical report on the exploitation project that specifies the consistency of the mineral deposit; the depth of the free and/or confined aquifer; the time phases of exploitation, the techniques and method of exploitation of the orebody also related to its characteristics and potential of the equipment used; the possible location of the landfill areas, if required by the type of material and exploitation methods with identification of their main characteristics; stability calculations of the safety profiles of the walls during and at the end of the exploitation; graphic tables showing the main lots and the situation at the end of the exploitation;
- a design of the works necessary for environmental rehabilitation during and at the end of the exploitation, a technical report specifying the planned works, construction times, costs planned, the final layout of the quarry area connected to the neighbouring areas, the destination of exploited land; graphic tables showing the individual phases of environmental recovery, the final structure and the destination of the area at the end of the rehabilitation.

According to the art. 14 of the Regional Law n. 14/1998, the executive project must contain:

- a plan survey in scale (ex: 1:500. 1:1000 or 1:2000) of the area covered by the request for authorization, as well as the previously exploited areas and the neighbouring areas with the representation of all services and infrastructures;

- a mining project with a technical report of the exploitation project, based on the geological, hydrogeological and geotechnical data, where the maximum excavation depth is specified; the characteristics of the aquifer; the excavated volume and the average annual production expected; the phases of exploitation over time, the techniques of exploitation linked to the characteristics and potential of the equipment used; the possible location of landfill areas if required by the type of material and exploitation methods, with an indication of their main characteristics; the stability checks of the soil profiles during and at the end of the exploitation and a technical report on the preliminary analysis of the main problems of safety related to the execution of the project with an indication of the design solutions adopted to minimize the dangers for employees as well as to ensure compliance with the relevant regulations to prevent accidents and protect the working environment in accordance with the current legislation;
- a project of the environmental recovery during and at the end of the exploitation, consisting of a technical report specifying the planned works, the program of their maintenance during and at the end of the exploitation, the times of construction, expected costs, morphology and final destination of the land exploited; graphic tables at the same scale of those of the exploitation project showing the single phases of environmental rehabilitation, the final layout and destination of the area at the end of environmental rehabilitation works;
- a program of environmental mitigation interventions with an indication of the criteria and the operating methods designed to reduce the interference of mining with the surrounding environment;
- an economic and financial program, containing: the qualitative characteristics of the material with the certification programs; the use and destination of marketable products; the techniques for extraction, loading and hauling of the material, the equipment used, the characteristics and the potential of the processing plants together with indication of their structural and flow diagram; investment programs relating to machinery and plants

whose introduction must also be aimed at improving the safety conditions of workers and the protection of the working environment.

## **1.4. Technical restrictions**

### **1.4.1 Distances**

The distances from works and artefacts are those provided by the current regulations of Mining Police. The minimum distance from housing must be determined by the impact predictions acoustic and the effects of vibrations, for which reference is made to current legislation, as well as on the basis of interventions aimed at reducing the visual and acoustic impact and dispersion of dust. Regarding the property boundaries, the minimum distance between the exploitation limit and the perimeter of the available area must be 10 m; for ornamental stone quarries this distance is set at 5 m. Where the height of the bench is less than 10 m, the abovementioned minimum distance must be not less than 4 m. The minimum distance from places surrounded by walls is set at 20 m and can be reduced up to 10 m by agreement between neighbours. The above distances are intended to be measured horizontally from the upper edge of the excavation and they are determined after checking the stability conditions of the slopes.

### **1.4.2 Perimeter of the area**

The perimeter of the exploited area, where accessible, must be fenced with a wire mesh not less than 1.80 m or with other means prescribed by the authorization provision. Warning signs of danger, showing the presence of mining activity, must be placed along the fence at intervals not exceeding 50 m. The project area has to be checked in order to verify the possibility of leaving some portions of the fence raised from the ground by 20-30 cm to allow the passage of wild animals. The entrances to the quarry must be closed outside the working hours. In order to avoid accidental falls from the edge of the quarry due to poor visibility, it must be kept free from shrub vegetation at least 3 m.

All the safety measures required by current legislation on mining safety and accident prevention and at work must be adopted – expect for more restrictive laws, referring to particular cases – regarding the carrying out of excavation works, loading and hauling of materials and security signs to third parties.

### **1.4.3 Waste material**

The waste material, including material that cannot be considered soil, must be placed in the quarry area during and at the end of exploitation, or be valorised as a by-product for different uses, if the morphological arrangement and environmental recovery work are not necessary. The topsoil is not a quarry waste and must be completely relocated on site during and at the end of the mining activity.

### **1.4.4 Stages of exploitation**

The exploitation of the quarries must take place in phases, with a duration to be established by authorization provision, in order to ensure the progressive environmental recovery and ecological continuity. In particular, in all stages of exploitation, it must be avoided, as far as possible, lighting and disturbing activities during the night, in order to minimize negative interference with respect to the animals.

### **1.4.5 Vegetable soil**

The removal of the topsoil must proceed together with the exploitation phases, in order to limit the negative effects on landscape and damage to crops and vegetation. The topsoil must be temporarily stored in the quarry or in the immediate surrounding area to be relocated in the quarry area following the project of exploitation. The deed of authorization must indicate the place of storage if it is not in the quarry area. The authorization must also provide the requirement to carry out periodic checks and any interventions on the topsoil temporarily set aside, so that it does not settle non-native plant species, whether the masses are located inside or outside the area. Temporary accumulations of topsoil must not exceed 3 m in height with a base with a shorter side not exceeding 3 m. Due to the morphology of the places or to other technical reasons, it is not possible to keep the soil as shown above

or it is not possible to separate the soil vegetable from the topsoil; then, after verifying the chemical-physical conditions of the soil at the time of repositioning, the appropriate corrections must be made, favouring compounds of organic origin.

#### **1.4.6 Water drainage**

The entry of run-off rainwater into the quarry must be avoided by carrying out adequate collection and drainage works connected to the existing natural and/or artificial water network.

If necessary, rainwater falling within the quarry area must be disposed of through an adequate network of drainage channels kept in efficiency. If the morphology of the places does not allow to avoid the entry of water into the quarry surface the internal network must be adequately sized in order to ensure proper disposal.

#### **1.4.7 Service roads**

The minimum size and maximum slope of the service road for the circulation of vehicles must be suitably sized and indicated in the project according to the construction characteristics and use of the excavation equipment, loading and transport of employees and the safety requirements of the work and employees

#### **1.4.8 Protection of aquifers**

For each mining area, the Province prescribes, where necessary, works and measures for the definition and hydrochemical and hydrodynamic monitoring of groundwater. The technical characteristics and methods of implementation of these works, the frequency of phreatometric measurements and analysis as well as the hydrochemical parameters to be detected are established in the authorization. The results of the analysis and measurements must be sent by the operator of the mining activity, to the Quarry Office of the Province and the competent Municipality.

To limit the effects of reducing the permeability of the aquifer, the water coming from the sorting and washing plant, when not treated in recycling plants, must be placed in different tanks suitable for sedimentation, clarification and disposal,

indicated in the authorization provision, without prejudice to the current regulations on the protection of waters.

#### **1.4.9 Protection of human health from noise impact**

The operation of the mining activity must take place while ensuring compliance with the noise limits, both absolute and differential. The production management projects of the areas must include a plan of monitoring of the effects, in terms of acoustic impact, both of fixed sources of the quarry activity, and of the effects of induced traffic. Where the acoustic monitoring highlights critical issues regarding exposure to the noise of the population in a direct or induced way, the acoustic mitigation measures necessary to bring the exposure of the population must be implemented. The opportunity for further mitigation measures has to be evaluated, in cost-benefit ratio logic, to contain the increases in noise levels which, although not leading to an overcoming of the limits, were particularly consistent.

### **1.5. Overview of the mineral deposits available in Varese Province**

The quarry plan previously described and in force since 2016 has identified 13 areas of interest in this Province for the extraction of different types of minerals (the previous schedule for mineral extraction was updated to 2008). For each A.T.E. the total volume of the mineral deposit, the extractable volume according to the plan and eventually the amount of reserves were estimated. Figure 1.1 summarizes the location of the quarries: the active quarries are shown in blue, the quarries in the rehabilitation phase in green and the other currently unexploited deposits in red.

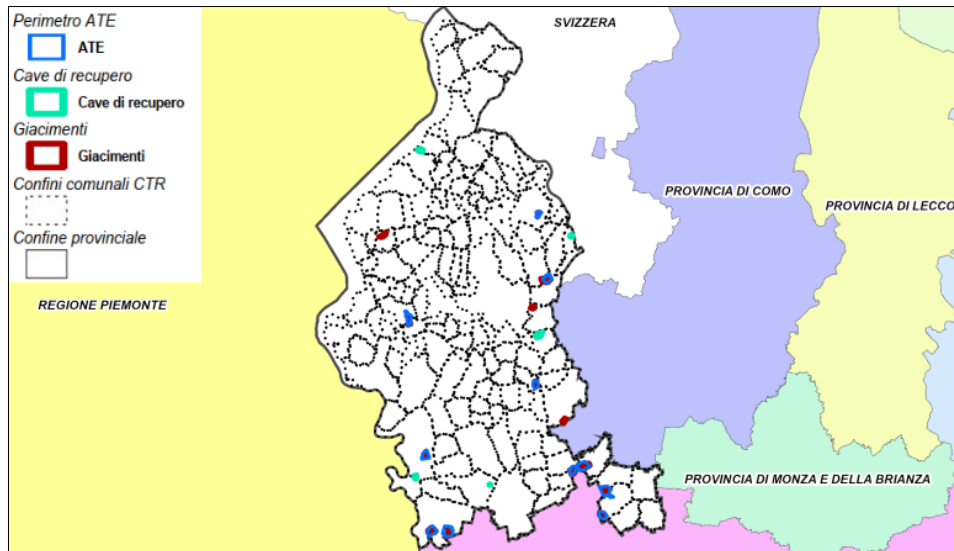


**Figure 1.1 – Map of the Varese Province with the A.T.E. (blue line), recovery quarries (green line) and other deposits (red line). (Source: <http://cartografia.provincia.va.it>).**

For each A.T.E., the typology of the mineral and its volumes (available deposit, mining volume and reserves) were estimated. In Table 1.1, specifically, the Area with the letter “g” represents a sand and gravel quarries, which are the most frequent in this area; the letter “c” indicates rocks for industrial uses (i.e. to produce cement) and the letter “o” identifies the ornamental stones.

**Table 1.1 – List of all the A.T.E. in Varese Province with data of available deposit, planned volume and reserves. (Varese quarry plan 2004).**

<b>ATE</b>	<b>City</b>	<b>Available deposit (m<sup>3</sup>)</b>	<b>Planned volume (m<sup>3</sup>)</b>	<b>Reserves (m<sup>3</sup>)</b>
ATEg1	Lonate Pozzolo	5,380,000	4,000,000	1,380,000
ATEg2	Lonate Pozzolo	3,957,000	3,957,000	0
ATEg3	Ubaldo	2,800,000	2,000,000	800,000
ATEg4	Gerenzano Ubaldo	3,200,000	2,000,000	1,200,000
ATEg5-C5	Gorla Minore Marnate	4,600,000	2,600,000	2,000,000
ATEg5-C6	Cislago	3,900,000	2,600,000	1,300,000
ATEg6	Gornate Olona Lonate Ceppino Venegono Inferiore	2,700,000	2,000,000	700,000
ATEg7	Cantello	6,350,000	2,300,000	4,050,000
ATEg8	Somma Lombardo	4,250,000	3,400,000	850,000
ATEc1	Casale Litta	0	0	0
ATEc2	Travedona Monate Ternate	3,989,000	3,989,000	0
ATEo1-C13	Cuasso al Monte	158,000	158,000	0
ATEo1-C14		254,000	254,000	0
<b>Recovery quarries</b>	<b>City</b>	<b>Available deposit (m<sup>3</sup>)</b>	<b>Planned volume (m<sup>3</sup>)</b>	<b>Reserves (m<sup>3</sup>)</b>
Rg1	Vizzola Ticino	237000	237000	0
Rg2	Vedano Olona	173000	173000	0
Rg3	Somma Lombardo	0	0	0
Rg4	Samarate	100000	100000	0
Rg5	Viggiù	100000	0	0

## **2. CASE STUDY: ATE C2 – TRAVEDONA MONATE**

The subject of this thesis is the assessment of the stability conditions of the Faraona quarry, belonging to the ATEc2 of Travedona Monate and Ternate, following the expansion works. For this quarry, the quarry plan estimates the potential extraction of 6,780,000 m<sup>3</sup> of material, for the next two decades.

The exploited rock is a limestone, which is inserted into the second category according to the mining legislation. According to this category, the quarry plan prescribes further technical indications to be respected. In particular, the maximum height and/or depth of excavation, the maximum height of each bench wall, the minimum width of the relative tread and the slope of the walls.

### **2.1. Framework of the area**

The ATEc2 sheet describes the technical characteristics of the Faraona quarry, but it is necessary to consider a more general framework of the area to better understand the need for expansion in the exploitation of limestone by the company Holcim Italia S.p.A. (since 2015 following merger it became LafargeHolcim S.p.A.). This company carries out its activity through:

- cement units, one of which is organised as a complete cycle with a kiln in Ternate (VA) and a grinding station in Merone (CO),
- 5 aggregate quarries, (including Faraona quarry and Santa Marta mine),
- 11 concrete plants,
- cement import terminals.

The Santa Marta mine allowed the extraction of marlstone and was active until 2013; then, according to the provincial exploitation plan, the volume available for

exploitation ended. Currently the works for the environmental rehabilitation are under completion, especially in terms of morphological remodelling.

The exploitation of the Faraona quarry has undergone several expansions over time. Thanks to the aerial images available on the Lombardy Region cartographic portal (3D Geographic viewer) it is possible to verify that starting from 1975 both Faraona quarry and Santa Marta mine have been already partially exploited (Figure 2.1).



Figure 2.1 - Evolution of the area of Faraona quarry and Santa Marta mine. Comparison of aerial photos of 1975 and of 2018.

## 2.2. Technical constrains from legislation

According to the mining legislation, specific requirements have to be followed for the design and the exploitation of a quarry. In particular, the inclination of the bench, in case of breakdown stratification, must coincide, once the appropriate stability checks have been carried out, with the progress of the layers. Exceptions to the previous standard can be granted in case of inclination of the walls lower than  $35^\circ$  and lack of joints or discontinuities filled with fine material. The excavation works have been performed taking care of the global stability of the excavation face

and of the correct environmental rehabilitation. The exploitation geometry must in any case be verified on site as a function of the local and general long-term stability of the walls, according to current legislation and to technical requirements of the environmental recovery designed, in accordance with the final destination. However, the following parameters must not be exceeded:

- maximum height of the bench: 20 m
- minimum width of the bench: 2/5 of the height of the bench.

The inclination of the excavation faces under their evolution, as well as the minimum width of each individual bench, must be commensurate with the equipment and techniques adopted and are determined according to safety requirements.

The height of the benches during the exploitation must not exceed the limits indicated in the plan that identify each individual mining area. The exploitation of quarries can take place from top to bottom, by descending slices, starting from the upper limit of the authorized area, to ensure a progressive recovery of the quarry face. The upper edge of the excavation must always be reachable with appropriate tracks or ramps that can be travelled by vehicles. The ramps must be kept efficient until the completion of the environmental recovery for any following maintenance and control interventions. Where the morphology of the area does not allow this, the upper excavation edge must be accessible with a suitable equipment from the floor of the highest bench of the quarry face.

Table 2.1 (included within Varese quarry plan 2018) summarizes all the technical characteristics of the Faraona quarry site and the data to size the mining project. The project involves an open pit excavation in an area very close to another site (Santa Marta mine), inactive since 2013. Following some legal disputes on the planning of the area, the ATec2 data have been modified in 2018. In particular, the size of the mining area has been further expanded (from 224,000 m<sup>2</sup> to 352,000 m<sup>2</sup>) and consequently all the volumes have also been changed (the old technical parameters are indicated under brackets).

**Table 2.1 – Technical data of Faraona quarry based on the provincial plan.**

<b>ATEc2 Report</b>	
<b>General data</b>	
<b>Commodity sector</b>	Rocks for industrial purposes
<b>Quarry</b>	C12 - Holcim Italy spa
<b>City</b>	Travedona Monate - Ternate (VA)
<b>Specific place</b>	Faraona
<b>References in regional cartography (C.T.R.) (1:10000)</b>	A4b5 Ispra; A4c5 Varese Lake
<b>Features of the site</b>	
<b>Existing reference</b>	ATEc2
<b>Total area of the site (m<sup>2</sup>)</b>	645,261 (575,000)
<b>Mining area (m<sup>2</sup>)</b>	352,944 (224,000)
<b>Average altitude (m)</b>	345 (338 North; 360 South)
<b>Legal restrictions (national and European)</b>	Cultural heritage (L.D. 42/04); SPA- Varese lake (Dir. 79/409/EEC); SCI - Brabbia swamp and Comabbio lake (Dir. 92/43/EEC)
<b>Framework</b>	Inside a core area of the Regional Ecological Network
<b>Geological formation</b>	Bioclastic limestone (Travedona formation)
<b>Mining project</b>	
<b>Available volume (2009) (m<sup>3</sup>)</b>	8,990,000 (3,989,000)
<b>Available volume (next two decades) (m<sup>3</sup>)</b>	6,780,000 (3,989,000)
<b>Residual volume (m<sup>3</sup>)</b>	2,210,000 (0)
<b>Mining technique</b>	Open pit excavation
<b>Geometrical parameters</b>	Maximum height: 15 m
	Minimum tread: H/2 or > 4 m
<b>Maximum altitude of excavation (m)</b>	375 (360)
<b>Minimum altitude of excavation (m)</b>	275
<b>Mitigation measures</b>	The wooded area between S. Marta mine and the limit of the Faraona quarry is constrained. It must be guaranteed the continuity with the ecological network during the mining operations. In case of presence of bird nests such as kingfishers, European bee-eaters or and sand martins, near a pile, the loading operations must be suspended. Pay attention to the stormwater coming from the mining site and try to reuse the water of the basin inside the quarry.
<b>Morphological recovery</b>	Guarantee the continuity of the ecological network in the North area (connection between the Varese, Biandronno and Monate lakes). At the same time, S. Marta mine must be recovered.

As required by law, the area of Faraona Quarry was planned for zoning. Therefore, the Faraona Quarry is divided, within the perimeter of the A.T.E. (indicated in blue) into an area of actual exploitation (shown in Figure 2.2 with the letter “a” in red); a buffer zone T2 (shown in Figure 2.2 with a red grid) and an area for traffic and service (blue dots in Figure 2.2).

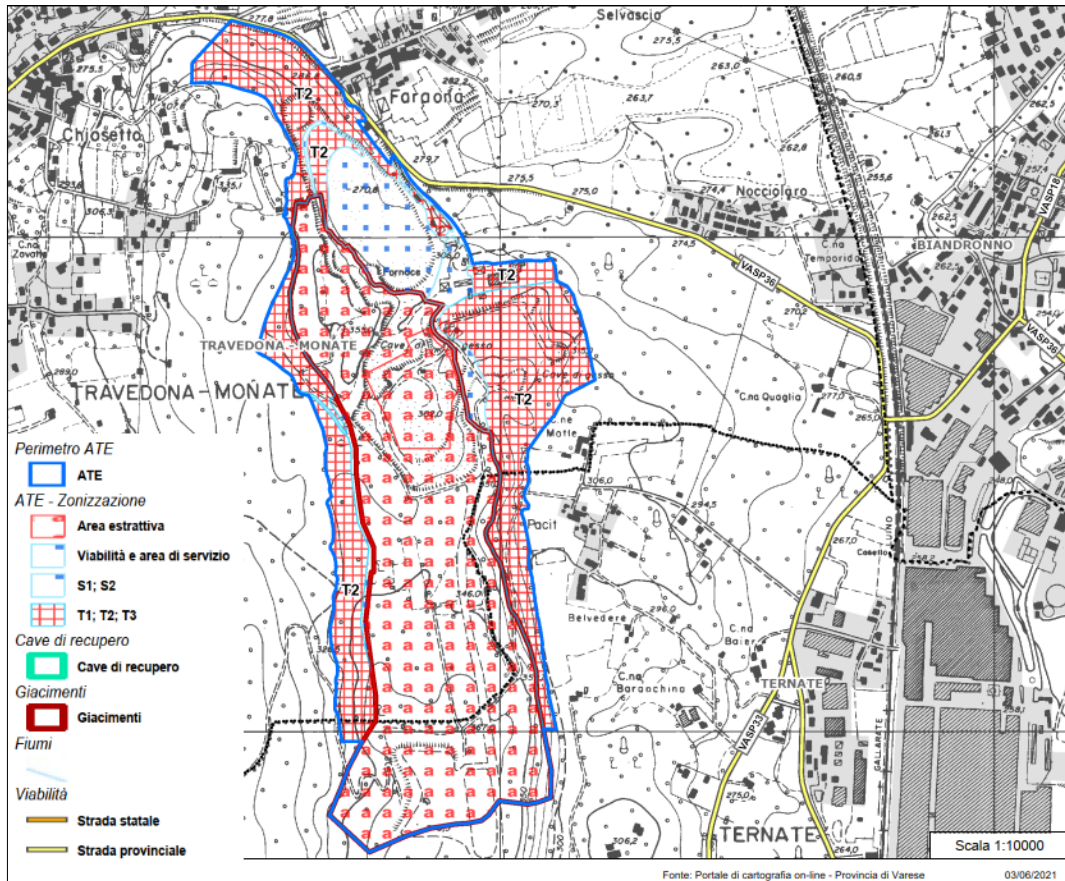


Figure 2.2 – Zoning of the ATEc2 (Source: <http://cartografia.provincia.va.it/> ).

Starting from the legislative constraints, an exploitation plan was developed which followed the general technical and site-specific requirements contained in the quarry plan of the Province of Varese.

### 2.3. Project of exploitation

This project has the fundamental purpose of guaranteeing the supply of raw material for the production of concrete at the Ternate plant. In the design it has been decided

to plan the exploitation and the environmental recovery according to stages from North to South, in order to "isolate" the northern part from the remaining of the quarry. The design choices have been made considering the technical parameters of previous projects and the results of specific studies on environmental and safety aspects. The report of the ATE c2, previously quoted (see section 2.2), allows the extraction of 4,800,000 m<sup>3</sup> of material on a total area of 25.4 ha, including the ATE area already subject to previous mining activity.

Based on the expansion project, the total volume of limestone that can be exploited amounts to 3,988,003 m<sup>3</sup> of which 3,905,677 m<sup>3</sup> in the current project and 82,326 m<sup>3</sup> already exploited in 2009. Figure 2.3 shows an overview of the Faraona quarry in July 2021, with the exploited face proceeding in the East area.



Fig. 2.3 – Overview of the Faraona quarry (situation updated to July 2021).

### 2.3.1 Exploitation design

The extraction of the material starts as mentioned in the North area of field, already affected by previous exploitation works and proceeds as follows:

- excavation of the area from top to bottom (275 m);
- loading and hauling of the material to the Ternate plant through the existing internal road.

The walls in moraine material have height between 10 ÷ 40 m in South and in West area. The walls in limestone have a height between 45 ÷ 55 m, with variable inclinations. The maximum excavation height is between 355 m and 275 m of the final yard at the bottom excavation.

The service ramp, outside the exploitation area, is in correspondence to the South-West boundary and is linked to the runway of connection with the factory. This road allows the access for the maintenance of the recovered areas. A main access road to the exploitation area is used to transport the material to the factory. The beginning of the ramp is provided by the intersection point of the current connecting road of Faraona quarry and Santa Marta mine. From this point, the development is expected to the South and then to the West towards the North until reaching an altitude of 310 m.

The proposed road layout is designed in order to ensure access to the area under exploitation throughout the period of activity, avoiding the interference of transport with the areas recovered to the North. Finally, this path allows to minimize the hauling distance, thus leading to a reduction in impacts (dust, noise, emissions, fuel consumption, etc.). An 8-10 m wide service road on the East face at an altitude of about 330 m is designed to guarantee the access the recovered areas.

### **2.3.2 Morphological recovery**

At the same time as the exploitation activities go on, the morphological remodelling of the depleted areas using the moraine material coming from the uncovering phase, is managed. The final morphological situation of the area, once the exploitation and morphological recovery activities have been completed, it is characterized by:

- final shape at an altitude of approximately 289 m, with slope connections contained with the walls at an altitude of about 295-300 m;
- keeping the main road and the auxiliary ramps;

- development of additional roads to allow the connection with the ramps and routes of external circulation, access to the flat area and to facilitate maintenance of recoveries and the future usage of the site;
- current artificial lake with the function of water collection tank at an altitude of about 280 m in order to allow natural outflow towards the outside;
- system of channels for the collection and conveyance of water rain towards the collection tank;
- use of soil as needed, even from the outside (5-10%), in order to guarantee a good result of the interventions vegetational recovery.

The total volume to be exploited is 4,816,514 m<sup>3</sup>, of which 3,905,677 m<sup>3</sup> of limestone and 910,837 m<sup>3</sup> of overburden, to be reused mainly for morphological recovery and, if the conditions are right, a limited part can be exploited in the production process.

### **2.3.3 Exploitation method**

The excavation is developed open pit, according to methods widely tested over the last few years that have allowed to obtain good production results and a high degree of safety while carrying out the excavation.

#### **2.3.3.1 Overburden removal**

The first stage of processing consists of overburden removal in areas not affected by mining yet. The overburden consists in moraine with a thickness varying from a few tens of cm at East up to 20-25 m in the West sector.

The removal takes place with an excavator equipped with a backhoe bucket that directly loads the material on dumpers that convey it to the unloading area, in forecast of its use for the final recovery of the area. Before proceeding with the excavation of the moraine material, it is necessary to remove the vegetation and recover the vegetal material that covers the whole area of expansion of the mining activity. The works for overburden removal have to be planned before the end of exploitation of the previous phase in order to ensure the continuity of limestone

production for the plant. A period of 6 to 12 months is necessary for this preliminary phase.

### 2.3.3.2 Excavation of the material

The project evolves according to descending horizontal slices, from top to bottom, keeping a height of the benches of 5-8 m, with a D&B technique. This configuration allows a greater safety during all phases of exploitation of the material. The D&B scheme provides, in its standard configuration, a mesh of 2.5 m x 2.5 m of vertical holes having a 76 mm diameter and a 5.35 m length (for the bench of 5 m), which will be adapted to operational needs. The holes are loaded with slurry-type explosives and triggered with high intensity micro-delayed electric detonators or with Nonel detonators. Figure 2.4 shows an example of a blasting scheme and firing pattern for a 5 m high bench.

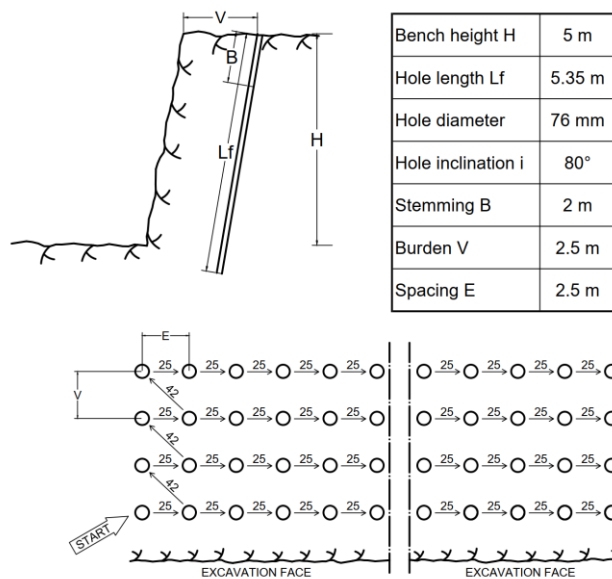


Fig. 2.4 – Example of a blasting scheme and firing pattern for a 5 m high bench.

In the areas close to the final spit, controlled blasting is adopted to limit the effect of the vibrations due to blasts on the areas around the quarry not affected by excavation; the technique generally adopted to this aim is pre-splitting. Over-sized blocks, not suitable for dumpers or having dimensions greater than the opening of the crusher, are reduced by means of a hydraulic hammer. However, considering the layering of the material, the presence of such blocks is quite remote. The loose

material is collected by an excavator and loaded into dumpers which transport it to the feed hopper of the primary crusher in the plant area.

In the areas planned for expansion, not yet affected by mining activity, in the start-up phase, the overburden is removed. The excavation of the moraine material takes place by means of a hydraulic backhoe excavator and is loaded directly onto dumpers for its conveyance into the exhausted quarry area, where it is used for morphological rehabilitation.

### **2.3.3.3 Material conveyance**

The excavated material is then moved on the yards by excavators, which load the dumpers for transport to the crushing plant. For the preparation (levelling) of roads a wheel loader is used.

The dumpers cover the internal road and then take the current connecting road between the Faraona quarry and the processing plant, without any interference with public roads. Near the unloading area, a weighing machine is installed that is used for the daily control of the amount of extracted material.

### **2.3.3.4 Crushing**

At the crushing plant, the limestone from the Faraona quarry, in mixed size, is crushed in a HAPRA hammer crusher with a capacity of 800 t/h and an installed power of 1200 kW. The constancy in terms of raw material quality is continuously analysed by a gamma ray spectrometer which corrects any deviations of one or more elements. The hailing of the crushed and controlled material takes place via conveyor belts, which move it to the pre-homogenization plant, with a total capacity of 85,000 t.

## **2.4. Work model**

- Some infrastructures, necessary for this project, mainly consist of:
- Traffic routes: a main access route is developed to the exploitation area which is used for hauling the material to the plant and is connected to the

current connection track between Faraona quarry and Santa Marta mine at the intersection of the southern border of the authorized exploitation area. These service roads allow the future access to the area for the implementation of any maintenance operations and for ensuring the usage of the site.

- Water regulation works: the meteoric run-off waters, coming from the upper edge of excavation, are channelled through a collecting system, arranged at the foot of the walls and combined with transversal channels; the bench is also made in a small counter-inclination to convey the flows towards the collection tank at an altitude of 280 m.
- Service area: it is planned to use the service area of the Santa Marta mine equipped with office, services, canteen, plant for washing the vehicles, etc.
- Fencing structures: the fencing and signage system is built according to the regulations in force in order to guarantee ongoing safety and the future safe usage of the site.

The planned activities are the continuation of the activity carried out in the past and therefore the same technical-operational organization used in the past is adopted. The exploitation activities are normally carried out over a shift of 8-9 h/d, 5 d/w, for a total of about 240 d/y. Depending on the requirements, in particular for the activities of loading and transport, the working hours are planned to be increased up to a maximum of 2 shifts/d (16 h/d). In fact, the annual production can vary according to the requests of mineral from the concrete plant and the current trend of the concrete market. The project assumed an average annual production of 480,000 m<sup>3</sup> compatible with the yard's standard operating configuration. Any increases in demand can be met by increasing the working hours/d, up to a maximum of 2 shifts/d (16 h/d).

## **2.5. Work plan**

The planning of activities involves five steps to ensure the contemporaneity of the exploitation and the environmental rehabilitation of areas excavated to reduce the

exposed areas and the consequent impact on landscape. The program foresees the achievement of the exploitation in about 9 years and a subsequent period of 2 years for completing the recovery works. This time depends on the real situation and on the raw material requirements of the Ternate plant, which is a function of the market trends.

The time schedule was defined by estimating an average requirement of the plant of 480,000 m<sup>3</sup>/y and considering the reserves again available in the Santa Marta mine. To ensure continuity of raw materials coming to the Ternate plant, the authorization process is implemented according to lots. For this purpose, 2 main lots, L1 and L2, have been identified for which the process authorization of L1, can be started immediately, while for L2, an additional period of approximately 6 months were considered for completing all administrative formalities required.

### **2.5.1 Phase 1**

The first phase of the ATEc2 production management project covers an area of approximately 72,000 m<sup>2</sup> to exploit 476,875 m<sup>3</sup> of material. Phase 1 interests the northern part of the current quarry. The excavation is carried out, as already mentioned, proceeding according to the horizontal slices from top to bottom, with heights of the bench of limited thickness (5/8 m). The excavation geometry is characterized by the creation of 10 m high benches, interspersed with a flat area of 5 m in width, with differentiated inclination for West and East faces. More precisely, during this phase, the West face is exploited with an inclination of the single bench equal to 60° and an average inclination of the face of 48°.

During this phase, a temporary road is built on the East side of the quarry, as a continuation of the road that enters into the quarry on the North-East side. The road has a width of 16 m and an inclination of 10%. During the next phase, in which the construction of a new road is planned, the East face is completely remodelled and the limestone, on which the road is developed, is fully recovered. Since the East and South parts of the area covered by phase 1 undergo remodelling, during the subsequent phase 2 of enlargement to eliminate the provisional viability, the

geometry of these 2 faces (East and South) foresees, without prejudice to the height of the bench of 10 m, a general inclination of each wall less than 50° (about 48°).

Phase 1 of the project can be defined as a preparatory step for the real exploitation. The goal of this planning is to create an adequate volume for recovering the morainic material, which is exploited in the following stages, and to speed up the final recovery of the northern part of the quarry.

In terms of volume, the extracted limestone corresponds to 476,875 m<sup>3</sup> and therefore the pit at the bottom of the excavation is available for filling with the removed overburden, which will be extracted in the next phase. At the end of this phase, approximately 6 months before the completion of the limestone exploitation, it is necessary to start the overburden removal from the area to be exploited during phase 2.

### **2.5.2 Phase 2**

This phase lasts about 1.5 years and covers a surface of 105,000 m<sup>2</sup> for the exploitation of a volume of limestone of 633,425 m<sup>3</sup>. The phase is developed in the central-southern sector of the quarrying area, with a retraction of the excavation face to the South of about 170 m. Phase 2 corresponds to the first overburden removal in the new area not affected by the previous exploitation activities.

The geometry of the faces is the same as phase 1, but the inclination of the benches assumes an average value of 55° (instead of 50°). This phase concerns, as mentioned, the ex-novo exploitation of the quarry and provides the removal of 20 cm of overburden and a thickness of moraine material, variable from a few meters in the East sector up to 25-30 m in the West. The topsoil is set in areas adjacent to those of excavation; it is subsequently reused for completing the environmental recovery. The overburden is used for the morphological recovery of the North area of the quarry, where the excavation bottom level of 275 m has already been reached. The recovery project involves the filling of the bottom of the quarry up approximately the altitude of 289 m. The excess overburden, approximately 92,000 m<sup>3</sup>, is used to realize an internal road between the altitudes 320 and 299 m, to ensure the access to the final excavation yard. The aim of the road is twofold, on one hand

to have two alternative accesses to the bench at the bottom of the excavation and to reduce or eliminate the circulation of dumpers near the recovered areas.

To reach the new site, a road has been built from the southern sector of the quarry following the West side up to an altitude of 320 m. During this second phase, recovery operations are environmentally planned in correspondence with the northern sector of the mining sector, by using the topsoil and the resulting morainic material from the overburden removal works. Operationally, the environmental recovery proceeds from North to South, at the same time as the exploitation progresses towards South.

### **2.5.3 Phase 3**

The third phase of the excavation, which lasts about 2.5 years, concerns the activities of overburden removal in phase 2 and the exploitation of 908,823 m<sup>3</sup> of limestone. The overburden used to create the road between 320 m and 299 m is removed and is put to permanent position in the North, where exploitation has been exhausted. The uncovering material used for the morphological recovery of the northern area of the quarry where the excavation bottom level of 275 m had already been reached, is subject to remodelling according to the final morphology of the project. As part of these interventions, a small lake is created at an altitude of 285 m for collecting the rainwater.

### **2.5.4 Phase 4**

This excavation phase lasts about 1.5 years and involves a surface of about 118,000 m<sup>2</sup> for the exploitation of a volume of 569,899 m<sup>3</sup> of limestone. The exploitation develops further in the South sector of the quarry, with retraction of the excavation face up to the limit of the mining area.

An intermediate square is realised at an altitude of 330÷320 m in the southern part of the mining area. Access to the excavation area is guaranteed through the main road that develops on the South and West face, with an elevation of 356 m approximately, up to 327 m.

The overburden is planted in the North area, where the excavation bottom level of 275 m has already been reached for storing the whole volume, approximately 510,500 m<sup>3</sup>. Also in this phase, the amount of topsoil, deriving from the screening operations, is used for the recovery.

### 2.5.5 Phase 5

This phase lasts 4 years and covers an area of about 118,000 m<sup>2</sup> for the exploitation of 1,316,655 m<sup>3</sup> of limestone. It represents the final phase of exploitation within the mining area provided in the quarry plan and also includes the final phase of morphological recovery.

Once this phase has been completed, remodelling is carried out with the moraine material in order to obtain the final morphology of the area. Subsequently, all the adjustment interventions are completed (traffic routes, rainwater control, etc.) and together with the re-naturalization interventions of the whole sector.

## 2.6. Limestone exploited from the Faraona quarry

Based on the exploitation project, which was described in Section 2.5, the overall project of this A.T.E. has been valued in 224,400 m<sup>2</sup>. The exploitable volume reaches 3,905,677 m<sup>3</sup>. Table 2.2 summarizes the data relating to the volume both overall and relative to each phase. It should be noted that the production of moraine to be reused for the environmental rehabilitation amounts to 18% of the tout-venant.

**Table 2.2 -Volumes extracted from the Faraona quarry based on exploitation project.**

Stage	Limestone (m <sup>3</sup> )	Moraine material (m <sup>3</sup> )	Total (m <sup>3</sup> )
F1	476,875	0	476,875
F2	633,425	398,231	1,031,656
F3	908,823	1,140	909,963
F4	569,899	510,467	1,080,366
F5	1,316,655	999	1,317,654
<b>Total (m<sup>3</sup>)</b>	<b>3,905,677</b>	<b>910,837</b>	<b>4,816,514</b>

The exploitation project has a duration of about 9 years. The volume of approximately 910,800 m<sup>3</sup> of morainic material and topsoil is used for the morphological recovery of the northernmost area. The design has in fact provided that exploitation and recovery take place in lots from North to South, in order to partially anticipate the recovery in the North side.

All the exploited material is directly moved to the crushing plant and destined for the production of concrete. The average production expected in the project is of about 1,200,000 t/y distributed on average over the 12 months of activity, corresponding to about 100,000 t/month. Since the exploited material is completely intended for the production of the concrete, which is conditioned by market trends, the mentioned production corresponds to the maximum value under standard conditions. The average production capacity of the crushing and screening plant is about 800 t/h spread over about 12 h/d.

### 3. SLOPE STABILITY ASSESSMENT

The term landslide indicates a movement of masses of soil or rock down the slope (Cruden, 1991). This definition refers to movements of masses both on natural slopes and on excavated (artificial) faces. Movements can occur by collapsing, toppling, sliding, expanding or flowing. As regards the excavation faces, being artificial slopes, their analysis aims to determine an average height and inclination of the faces to guarantee the stability of the excavation in the short term, during the execution phases, and in the long-term. In general, it is possible to carry out the assessment according to two levels: the overall stability of the slope (large scale) and the stability of the single benches (local scale).

The knowledge of the causes that contribute to the genesis of the landslide phenomenon is of fundamental importance both for choosing the stabilization interventions of the natural slopes and for containing the excavation faces, as well as for adequately preventing further phenomena of instability in similar geological conditions. The main causes of instability can be divided into predisposing causes, which are intrinsic factors of instability linked to the lithological and/or structural characteristics, and triggering causes, which act on the slope causing the landslide phenomenon (i.e. intense rainfall/overpressures, seismic activity).

The failure of the slope along a given surface occurs when the resultant of the forces opposing the movement (shear strength of the materials constituting the mass), is less than the resultant of the forces that favour the movement itself (shear actions mobilized along the surface). In this case the factor of safety, defined as the ratio between the stabilizing forces and the driving forces along a certain surface, has a value lower than 1. The elements that can lead to the instability of the slope are classified into elements that contribute to increase the tangential forces mobilized and elements that contribute to decrease the shear strength of the material (Gattinoni et al., 2004).

The study of the slope stability of an excavation face involves the definition of a geomechanical model capable of describing the modalities in which the phenomenon occurs, the causes of potential instability and the strength mechanisms of the material involved, capable of counteracting the loss of static balance. A rock mass can be defined as a set of isolated blocks of a rock matrix, having a certain geometry determined by the different discontinuities that separate it. The rocky matrix represents a portion of intact material that constitutes blocks separated by the discontinuities (Goodman 1989).

Considering an approach based on the rocky matrix or on the rock mass in the complex depends on the scale of the problem to be faced. If the rock mass volume is large, for example if an entire slope or the global development of an excavation face is analysed, its behaviour is governed by the combined set of discontinuities and intact rock. On the other hand, on the scale of the single bench, the discontinuities of the system can assume a greater importance.

The stability assessment can be carried out with different calculation methods, depending on the type of possible instability phenomena. Preliminary analyses can be carried out for the determination of the overall geomechanical assessment and characterization. Subsequent analyses of the parametric type allow to define the influence that the various geomechanical parameters have on the conditions of stability (sensitivity or back analysis). There are numerous methods for this type of analysis. These methods can be of a static or evolutionary type: for example, the analysis conducted with the limit equilibrium methods examines the possibility of initial movement and does not consider the evolution of the system. With numerical analysis, on the other hand, the behaviour of the system is simulated following more realistic hypotheses of the phenomenon.

### 3.1. Limit equilibrium method

These methods investigate the stability of a sliding surface chosen a priori (flat, circular or curvilinear), which can also be hypothetical, for example if the slope instability is still in a potential or real phase and if the landslide phenomenon has already taken place in whole or in part. The stability analysis of the portion of the slope between the sliding surface and the topographic surface takes place by applying the equilibrium conditions provided by the static law (translation and rotation). The approach involves admitting that in limit equilibrium conditions (called incipient failure), the shear strength mobilized along the sliding surface is equal to the maximum shear strength that can be mobilized along the same surface (peak or residual depending on the conditions). Since reference is made to a rock mass, the shear strength depends on the nature of the material, but also on the characteristics of the discontinuity systems.

Limit equilibrium methods introduce the concept of factor of safety (FoS) as an index of the degree of stability. This coefficient is the ratio between the maximum shear strength of the material and the mobility strength. Under limit equilibrium conditions, FoS takes a unitary value. If the sliding surface is not known, the purpose of the stability analysis is to identify the internal surface of the mass characterized by the minimum factor of safety.

Hoek and Bray (1981) schematized a method of calculating the factor of safety of a sliding block. For a shear failure, as the sliding occurs along a joint/discontinuity, the surface must be defined by using a proper strength criterion such as Mohr-Coulomb, where the shear strength along the surface is expressed in terms of cohesion  $c$  and friction angle  $\varphi$ . The block acts along the sliding surface with the action of an effective normal stress  $\sigma'$  and consequently the shear strength  $\tau$  is obtained as follows:

$$\tau = c + \sigma' \cdot \tan\varphi$$

Figure 3.1 shows a  $\sigma' - \tau$  plot, where the cohesion is defined as the intercept on the vertical axis and the friction angle is defined as the slope of the line.

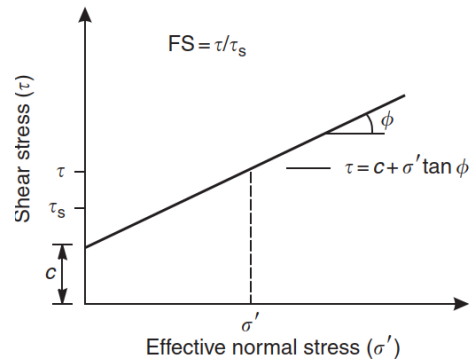


Figure 3.1 – Normal stress – shear stress plot (Hoek and Bray 1981).

An example of calculation of the factor of safety for a slope is represented in Figure 3.2. The forces acting along the sliding surface are divided into a parallel and a perpendicular component to the surface itself. The same procedure is also performed for the weight components of the moving block. In this way there will be the subdivision of the forces into non-slip forces and mobilizing forces.

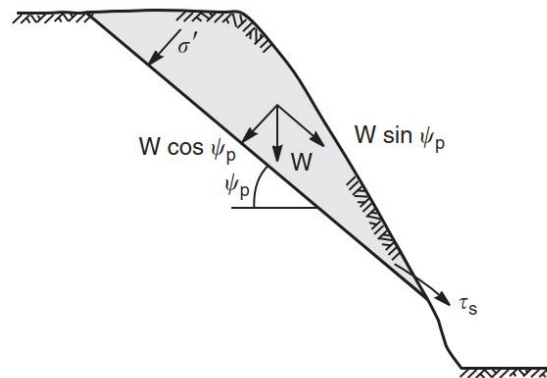


Figure 3.2. Resolution of the force  $W$  into two components parallel and perpendicular to sliding surface (Hoek and Bray 1981).

The stability of the block will be quantified through the relationship between resisting forces and unstable forces, which follows the expression (Hoek and Bray 1981):

$$FoS = \frac{\text{Resisting forces}}{\text{Driving forces}} = \frac{c \cdot A + W \cdot \cos \psi_p \tan \phi}{W \cdot \sin \psi_p}$$

This methodology can be applied to several conditions, including the presence of water acting along the sliding surface or external forces. The water pressure, for

example, can generate the opening of a tension fracture which will be decisive in the creation of an additional unstable force, causing a reduction of factor of safety. Water might also influence the friction of the joint in case of filled joints or presence of clayey materials into the openings: in this case the cohesion might decrease, as well as the friction angle.

### **3.2. Numerical modelling**

The modelling of a geotechnical problem, such as the stability analysis of an open pit excavation, is generally a complex operation. The phenomena of instability can be induced by gravitational forces, rainfalls or by a combination of decay processes in the shear strength of the material. All these causes can be concomitant, but even when the instability is apparently attributable to a single cause. The analysis of a slope requires a detailed geomorphological, hydrogeological and geotechnical characterization (Lancellotta, 2008).

Most of the challenges encountered in modelling a rock mass are due to the fact that the rock is a natural and heterogeneous material, and its physical and geotechnical characteristics can only be established through in-situ investigations. The rock mass is generally defined as D.I.A.N.E., i.e. Discontinuous, Anisotropic, Inhomogeneous and Non-Elastic (Hudson 1997).

The complex combination of the elements constituent the materials (mainly attributable to the geological history) and the difficulty of a mathematical representation led to the development of numerical modelling in geomechanics (Jing 2003). Then modelling a rock mass, it is necessary to include the physical processes and to represent the problem through partial differential equations, the constitutive laws of the material and the related parameters, any pre-existing stress state, the presence of fracturing and the variation of properties in case of anisotropic material and the effects resulting from anthropogenic perturbation (for example, the variation of the profile during the excavation).

Numerical analysis methods are capable of processing complex conditions, such as inelastic stress-strain behaviour, anisotropy and changes in geometry. The representation of a rock mass can be carried out by using two different approaches: in the first the rock mass is represented as a homogeneous and continuum (continuum equivalent approach); in the second the model represents more faithfully the reality by including the blocks of intact rock separated by a pattern of joints or faults with specific orientations (discontinuum approach). While the first is easier to model, as the geometry basically represents just the boundaries and eventually the contacts between different lithologies, the second is more complex but is able to represent in a more effective way the kinematic chains between the blocks. Depending on the nature of the rock mass (e.g. blocky, chaotic or massive), there is a better approach to be used.

### **3.2.1 Continuum models**

In a continuum numerical model, as already said, the material is considered as globally continuous. In rock slopes, the system is represented as an equivalent continuum in which the effect of the discontinuities reduces the elastic properties and strength of the intact rock and consequently of the rock mass. This process is performed through the use of rock mass classifications (e.g. RMR, GSI, Q), where depending on the overall rock mass quality, the values of the mentioned data are accordingly reduced. Each element is assigned a material model with specific characteristics. As an example, considering a limestone rock mass with a Young's modulus  $E_i$  of 60 GPa and a GSI equal to 60 (corresponding to a blocky rock mass with 3 joint sets and fair surface conditions), the equivalent stiffness  $E_m$  for using a continuum model is reduced to 31.2 GPa. This means that the deformability of the mass is higher, so it is expectable to obtain larger displacements compared to a model with intact rock parameters: this allows to represent more the reality, but on the other hand in a blocky rock mass most of the deformations occurs along joints. Therefore, in some cases, the discontinuum approach is preferable when more localized instabilities have to be examined, while the continuum equivalent to assess the general large-scale behaviour of the system.

### 3.2.2 Discontinuum models

A discontinuous model is developed in case of presence of discontinuities in the rock mass. A discrete elements code allows to elaborate a model with innumerable discontinuities, but it is not recommended to simulate cases of chaotic and fragmented rock masses (GSI lower than 40). The whole domain of the problem is divided into blocks. Each block can assume a rigid or deformable behaviour: this aspect is important because while using rigid blocks the model can handle larger number of discontinuities, but blocks cannot deform internally and generally cannot be characterized by a well-defined in-situ stress. On the other hand, deformable blocks can represent more accurately the reality but in order to simulate the deformability of the blocks a mesh and more computational capability is required. The treatment of data from the structural surveys of the rock mass has a fundamental importance, as the model must in any case have a manageable size during the computation phase. This is obtained by selecting the families of discontinuities that could cause relevant kinematics. Another important aspect is the calibration of the model on the basis of the results obtained and the real behaviour of the material.

The management of the block interfaces involves two different approaches:

- a soft-contact approach that provides for a certain stiffness of the block at the discontinuity (for example a set of rigid spheres with a reduced friction angle and low stress levels);
- a hard-contact approach, in which the interpenetration between elements is not considered physical (as for the propagation of a wave).

The development of these discontinuous codes in slope stability analyses represented a true evolution in modelling a rock mass. Nevertheless, the need to limit the number of discontinuities still represents a critical factor, even though with modern computers this problem is reducing more and more.

### 3.2.3 Criticalities in slope numerical modelling

As described in the previous paragraphs, numerical modelling can be considered as a powerful tool to describe different geomechanical problems such as slope stability. Especially in the latest year, the number of commercially available codes considerably increased, and the GUI of each software became more user friendly. This might lead to underestimate the possible criticalities that numerical modelling can hide behind its extreme usefulness. Some of the most critical aspects to be taken into account can be summarized as follows (Lorig et al., 2009):

- the maximum allowable size of the model limits the discretization of the boundaries, possibly influencing the final result;
- the initial in-situ conditions are not fully known and can only be reconstructed by site surveys and investigations. Through numerical modelling it is possible to vary the initial stress conditions in order to seek for the condition that simulate the real situation. It is anyway important to note that most of slope failures are gravity-driven, so the effect of the existing stress is less important. During the exploitation of a quarry, the rock mass might change its tension-deformative behaviour. An example could be the effective persistence of a discontinuity as the excavation face advances;
- the boundary conditions can be real or fictitious, since in the stability analyses the domain cannot have an infinite extension but must be artificially truncated. The deformation at the base of the model must be fixed in both horizontal and vertical directions to inhibit rotation of the model. This type of criticality can be overcome in a 2D model, assuming an infinite lateral extension, while for the 3D case the same solution cannot be adopted. It is therefore necessary to select a wider area of the model, so at the borders it is not so influenced by what happens within the model itself;
- the effect of water is another important aspect: it is essential therefore to evaluate the actual flow and pressure of water through the joints;
- the excavation sequence in the modelling phase is generally simplified but the most critical stages must still be considered.

## **4. FARAONA QUARRY: THE DESIGN PROCESS**

Holcim Italia SpA deals with the exploitation in the area located between the municipalities of Ternate and Travedona Monate. Specifically, the mining area is enclosed between Comabbio Lake and Monate Lake. Originally the area was occupied by a large glacier that extended over the Verbano region. This formation excavated the lake cones where the lakes are now located and a large morainic amphitheater that delimits the southern part of the area has been created.

The mining activity concerns the carbonate formation of the dome following the retreat of the glacier. This dome has a North-South orientation and represents the watershed between Lake Monate and Lake Comabbio.

### **4.1. Geological data**

The limestone, exploited at the quarry, belongs to the Eocene formation called “Ternate formation”, whose two outcrops in the Faraona quarry and in the Santa Marta mine can be observed. The geological formation consists of a succession of organogenic limestones with granular support, interspersed with a grey-green marl, whose origin is referable to episodes of currents and submarine landslides; this formation has a total thickness of about 400 m. Marly lenses of various sizes were also observed: they range from centimetres to metric and in some cases have a stratification in agreement with that of limestone. The thickness of these lenses is between 0.3 - 0.5 m. Pockets of polygenic conglomerates with marly cement and irregular trend can also be found.

Above, in contact with the carbonate formation, one Quaternary formation is observed, consisting of detrital materials, mostly loose or poorly cemented, with different grain size and composition, with rounded and slightly flattened coarse pebbles, showing a glacial-morainic deposition.

Figure 4.1 shows an overview of the open pit at Faraona quarry. In the upper part the overburden with the development of visible vegetation is noticeable, while below there are the limestone strata.



**Figure 4.1 – Overview of the West face of Faraona quarry (July 2021).**

The lithological diversity of the clasts (granites, gneisses, mica schists, etc.) also indicates a typically glacial deposition environment. Such materials are in contact with the Ternate formation, with gradually increasing thicknesses from East to West. On the eastern side of the hill, the morainic deposits are reduced to a few decimetres, while on the western side they reach thicknesses of several tens of meters. During the exploitation, the detrital-moraine material must be totally removed, to allow the excavation of the underlying limestone formation. Later on, it is reused for the modelling of the benches and the morphological recovery of the construction sites (see Chapter 2).

#### **4.1.1 Ternate formation**

The Ternate formation emerges exclusively in the Province of Varese. It is mainly formed by the accumulation of resedimented marine sediments. Most of the geological formation is made up of limestone and marlstone from the Liassic, late Cretaceous and mid Eocene periods. These deposits contain coralline algae, larger

foraminifera (e.g. nummulitids) and other shallow water skeletal grains. This type of deposit allows to hypothesize the presence of a carbonate platform that is now completely eroded, in the area where the mining activity takes place (Coletti 2016).

Figure 4.2 resumes the lithological characteristics of the area of Travedona Monate and Ternate. The central area in orange is classified as "sandy silts with pebbles and boulders (moraine)", as it can be already seen in Figure 3.1. The zone in brown (right of the exploitation) has been classified as "limestone, calcareous marlstone". The green area (left of the exploitation) is instead classified as "silty sands with pebbles".

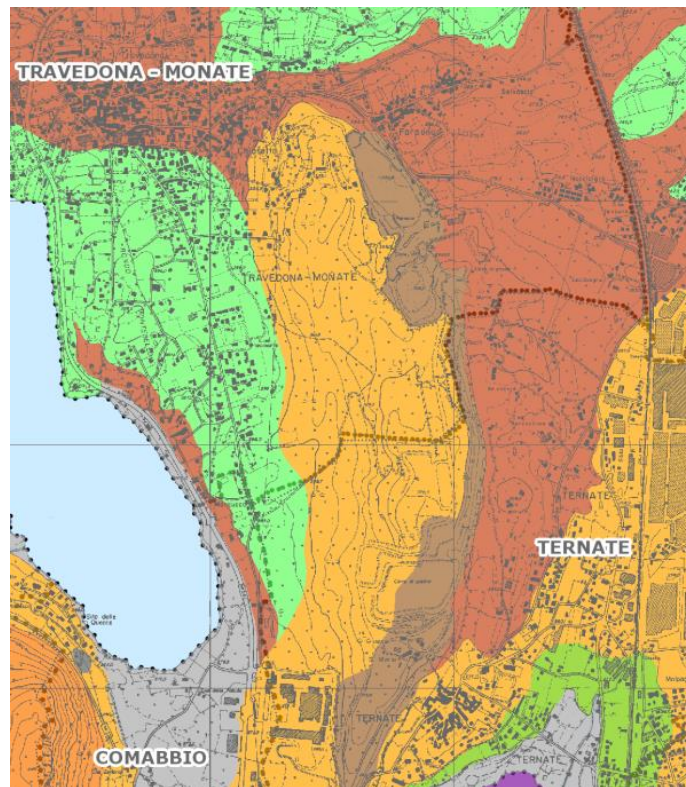


Figure 4.2 – Lithological map of the area of Travedona Monate – Ternate. The orange zone represents the sandy silt with pebbles and boulders (moraine) (Source: <http://cartografia.provincia.va.it/>).

#### 4.1.2 Geological environment

During the exploitation of the Santa Marta mine, a "V" profile has been found, which is a typical indicator of a valley engraved by a stream, instead of the classic "U" profile, typical of glacial valleys. Also, the stratifications confirm an evolution of the environment in erosion and subsequent fluvial resettlement, referred to the

environment fluvio-glacial. Finally, deposits are present, especially at the edges of the main lake basins, in a silty-clayey type, with rare pebbles, indicators of Quaternary deposits recent lake type.

The detrital-moraine formation is always commonly considered permeable for porosity and therefore represented as a sort of reservoir "sponge", on the underlying waterproof limestone. It seems that the water circulation occurs by infiltration of meteoric water and vertical percolation. Indeed, the morainic deposit is not homogeneous, on the permeability point of view. The permeability tests carried out over the years and the piezometers installed in various points in the area have confirmed the inhomogeneity of the formation.

## **4.2. Structural data**

Various geognostic surveys have been carried out in order to understand the development of the limestone formation in the area. For realizing the exploitation project described in Chap. 2 an in-depth study of the area has been carried out. Figure 4.3 shows the results of the surveys and the principal orientation of the limestone strata in the Faraona quarry.



faults that in the past favoured the erosive action of the meteoric waters, with the formation of voids which have been subsequently filled by clays. These weakness areas are the only responsible for the sliding that occurred in different years. Areas of weakness with the same characteristics are also visible in the West face of the quarry (see Figure 4.4 taken in July 2021).



Figure 4.4 – Area of weakness on the West face of Faraona quarry (July 2021).

### **4.3. Instability phenomena during the excavation phase**

Some phenomena of instability have occurred over the years during the exploitation at Faraona quarry, showing a potentially dangerous situation. A first episode, which involved a reduced volume of material, occurred in 2017; in 2019 a more extensive sliding forced to move to a different management of the excavation in order to carry out in-depth instability analyses of the whole area pertaining to East face. The geo-mechanical characteristics of the area were deeply studied, in order to highlight the various criticalities in terms of safety. Starting from these input data, a 2D model

of the area that was involved in a planar sliding in 2019 has been developed (see section 2.4).

#### **4.3.1 Instability phenomena occurred in 2017 and adaptation of the excavation technique**

On June 23<sup>rd</sup>, 2017 a serious instability problem that affected the East face of Faraona quarry has occurred.



**Figure 4.5 – Planar sliding of the material occurred in 2017 (Griffini 2018).**

Figure 4.5 shows the limited planar sliding of the material that occurred under the excavation bench at a height of 320 m. It has been found that the average position of the dipping layers, towards the West, determined the stratification and, also, the landslide. This aspect, when linked to the presence of some marly-clayey levels, leads to the formation of weakness surfaces, even when the inclination of the layers is relatively mild. However, it has been found that the marly-clayey levels and inclusions are centred in the stratigraphic half top of the deposit. In addition, the state of fracturing is also more intense at higher altitudes.

A more conservative excavation geometry compared to that of the original project has therefore been suggested. An example of the new profile is given in Figure 4.6, where the difference between the yellow line, that represents the design profile of the section, and the red line that remodelled the excavation can be noticed. The excavation in this area is, in any case, carried out very cautiously, carefully checking the presence and extension of the weakness planes within its progress.

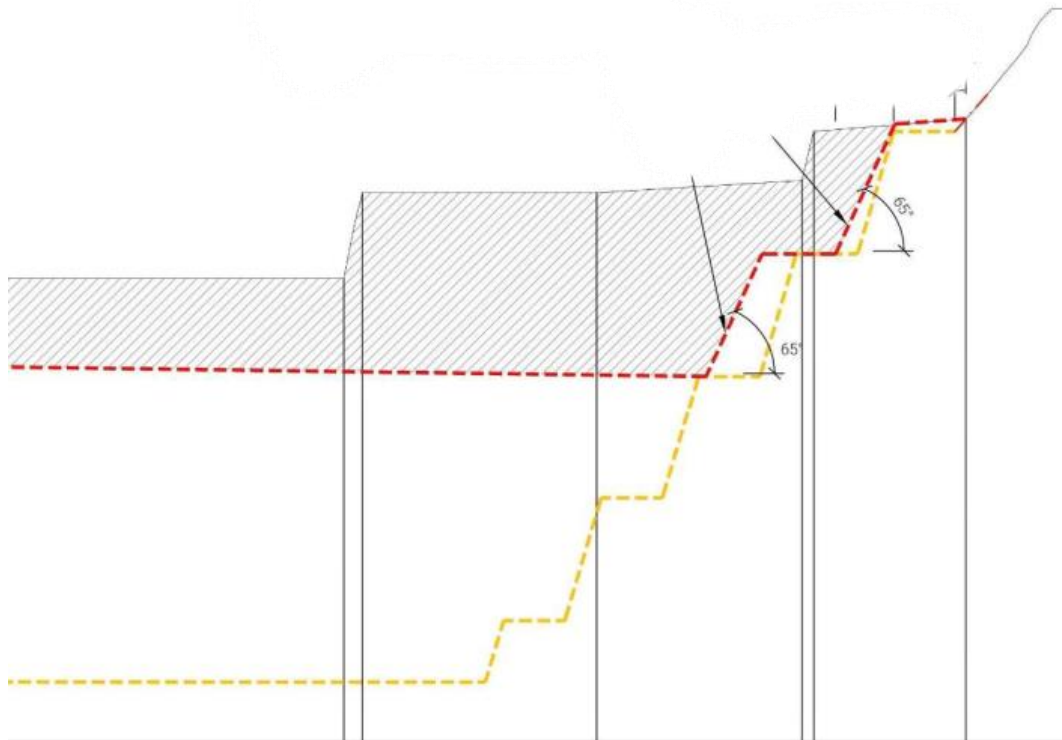


Figure 4.6 – Example of the new profile of the intermediate step (Griffini 2018).

### 4.3.2 Instability phenomena occurred in 2018

Although the solution described in Section 4.3.1, being able to guarantee the stability of the Eastern area of the quarry in the short term, in the long run problems related to the slow, but continuous, fragmentation of the final faces occurred, again caused by the breakdown arrangement of the strata and by the presence of marly-clayey levels.

In October 2018, a new phenomenon occurred on the bench at an altitude of 320 m (see Figure 4.7). The failure was characterized by a tensile fracture that developed

for about 10 m, with a maximum width of 4 m, a maximum thickness of 2 m and a total volume of about 40-50 m<sup>3</sup>.



Figure 4.7 – The red line describes the trend of the new tension crack in the East zone (Griffini 2018).

### 4.3.3 Instability phenomena occurred in 2019

On April 4<sup>th</sup>, 2019, another landslide of considerable extension occurred. This instability developed starting from the 320 m bench with the opening of a tensile fracture that developed for about 95 m in North-South direction (subparallel to the bench itself); this fracture developed in depth until reaching an extended sliding plane consisting of a marly-clayey level. The sliding plane is located at an altitude of 320 m from the bench, varying between 3.5 m at the North edge of the fracture and about 0.5 m at the South edge (see Figure 4.8).

The total surface (sliding surface + deposition area) is approximately 1,750 m<sup>2</sup> and the volume of material mobilized is approximately 1,000 m<sup>3</sup>. The landslide was due to an intense and persistent rainfall which occurred between April 3<sup>rd</sup> and 4<sup>th</sup>; the rain infiltrating the intensely fractured rock mass from the level of the bench of 320 m, reached the clayey level, saturating it and causing a slight increase in water pressure, with a drastic reduction in shear strength. The movement developed

downstream with a translation of 10 ÷12 m, stopping on the large lower bench (310 m).



Figure 4.8 – Tension crack in the left. Planar sliding in the right (Griffini 2020).

The sliding plane had a very low inclination, of about 14°-16°, with immersion towards East (275°÷280°) and was extremely persistent both in the direction of the maximum slope and in North-South direction.

#### 4.3.4 Present situation

The phenomena of instability described in the previous sections occurred with some regularity during the whole excavation of the East area of the quarry (see Fig. 2.3). In particular, after blasting, some tension cracks develop in the yard of the bench, thus creating problems of localized instability.

During the inspection carried out in July 2021, some tension cracks were clearly visible along the whole yard at an altitude of 320 m, after the blast. Figure 4.9 shows the tension cracks along the bench. In Fig.4.10 a detail of the tension crack is visible (average value of the opening 5÷10 cm).



**Fig.4.9 – Tension crack visible after a blast, July 2021.**



**Fig.4.10 – Detail of tension cracks, July 2021.**

#### 4.4. Geotechnical model

The geostructural characteristic of the whole extraction pole consist of a monocline structure that dips towards the West. The layers have an average inclination of about  $15^{\circ}\div 25^{\circ}$  with minimum values of about  $10^{\circ}$  and maximum values of about  $35^{\circ}$  (see Figure 3.3). Summarizing the data obtained in the various structural surveys, the families of discontinuities of the area, obtained from all the geomechanical-structural surveys performed from 2015 to 2019 (Griffini 2020), are the following (Figure 4.11):

- St family: coinciding with the stratification of the rock mass, dipping towards WSW-WNW ( $240^{\circ}\div 295^{\circ}$ ) with inclination between  $10^{\circ}$  and  $25^{\circ}$  ( $35^{\circ}$ ), average position  $280^{\circ}/22^{\circ}$ , with very high linear persistence, close to 100%;
- K2 family: immersion towards NNW-NE ( $355^{\circ}\div 040^{\circ}$ ) with inclination between  $65^{\circ}$  and  $85^{\circ}$ ), medium lying  $26^{\circ}/76^{\circ}$ , with medium persistence;
- K3 family: immersion towards ESE-SW ( $110^{\circ}\div 160^{\circ}$ ) with inclinations between  $55^{\circ}$  and  $80^{\circ}$ , average lying  $135^{\circ}/68^{\circ}$ , with low persistence;
- K4 family: immersion E-NE ( $50^{\circ}\div 90^{\circ}$ ) with inclinations between  $65^{\circ}$  and  $80^{\circ}$ , position average  $68^{\circ}/72^{\circ}$ , with low persistence;

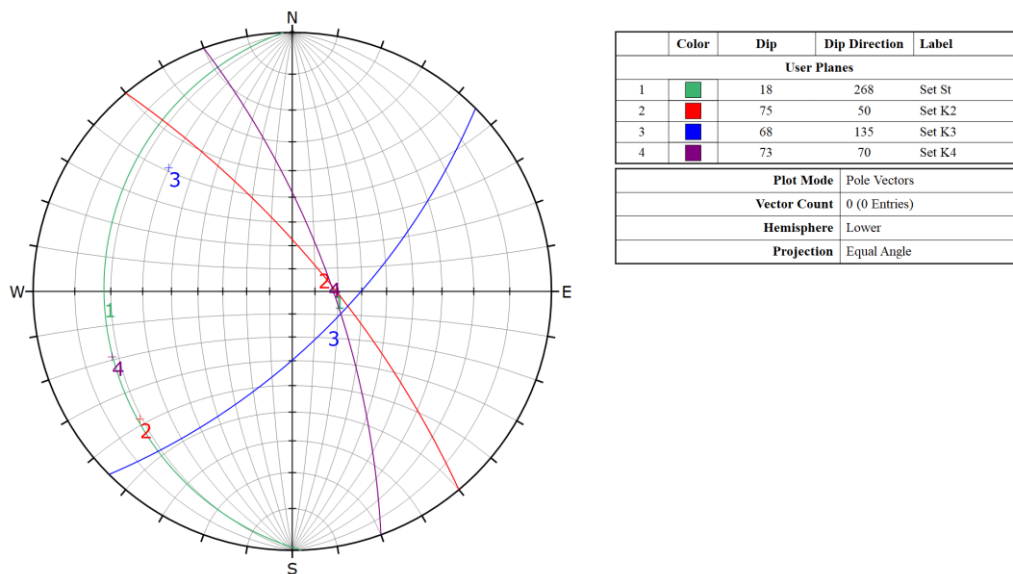
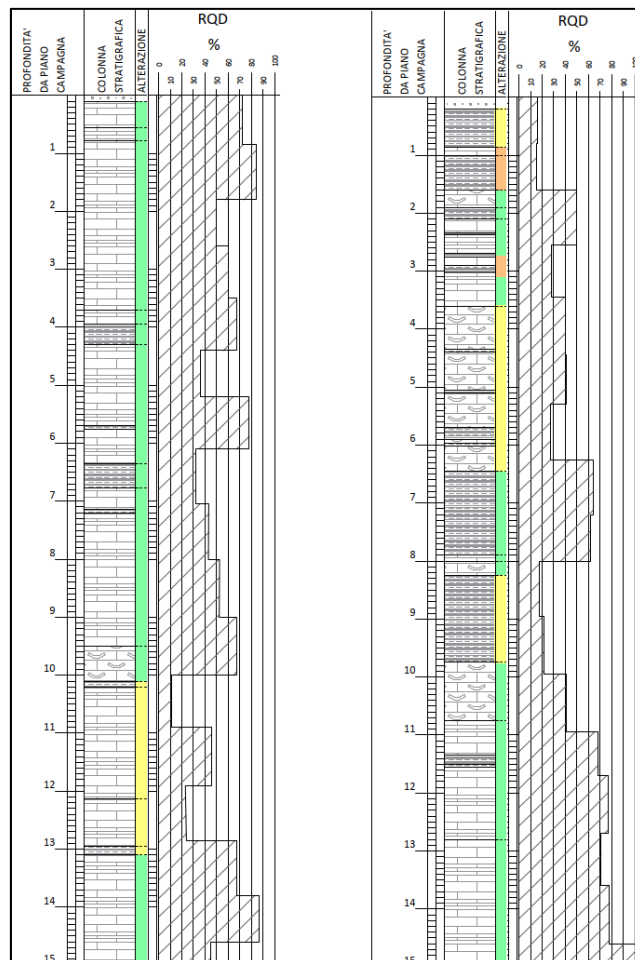


Figure 4.11 – Stereographical projections of the different families of discontinuities in the Faraona quarry (mean values of dip and dip direction for the joint sets).

The average position of the layers with immersion, towards the West, implies that the stratification is linked to landslides on the Eastern side of the mining area; this aspect, combined with presence of very continuous and extensive clayey levels, leads to the formation of areas of weakness with a relatively mild inclination of the layers ( $\geq 14-25^\circ$ ).

The investigations carried out during the excavations show that the levels and the included politics (clay) are concentrated in the stratigraphically upper half of the deposit (Figure 4.12). This assumption is also confirmed by some studies on the geological formation of Ternate (Mancin et al. 2001).



**Fig. 4.12 – Example of 2 stratigraphical logs obtained during the survey made in January 2019 (ref. S18-01 and S18-07). The green zones represent limestone and the yellow zones represent clayey zone. (Griffini 2020).**

In order to determine the presence of potentially persistent clayey levels even on significant extensions, in the Eastern area face, 7 continuous surveys have been carried out between December 2018 and January 2019, by using double cores barrels (type NT6S) and, in 4 of these, an inspection was carried out with an optical camera BHTV. Observation of the cores has in fact confirmed that the clayey levels, which constitute the potential plans of weakness, are more frequent in the stratigraphically upper half of the deposit.

These observations have been taken into account in the construction of the geological model and the geotechnical model used in the checking analyzes (see section 3.5), identifying the areas with a prevalence of widespread clayey levels in the project sections. The upper strip has a thickness of about 8-10 m and extends in depth below the exploitation area at an altitude of 330 m, up to about 315 m; a secondary band, with less frequent weak levels, has a thickness of 4-6 m and is located between 310 and 315 m. The two bands of weakness, being syngenetic to calcarenite deposits, have a concordant position with the position of the layers and therefore they deepen towards the West where they also show a decrease in average thickness.

#### **4.5. Stability analyses carried out**

The data collected in the Faraona quarry have been used to carry out 2 stability analyses of the area. The input data coming from 2 different rock mass characterizations are available, one from Altair report (2011) and the other from Griffini report (2020). Then, with the characteristic values of the geomechanical parameters of the rock matrix, integrated by the GSI values representative of the characteristics of the rock mass, the parameters of strength and deformability characteristic of the rock masses according to the Hoek envelope criterion (Hoek 2007) have been calculated. These geomechanical characterizations have been used as input data for those analyses, implemented through numerical models.

### 4.5.1 Slope stability analysis 2011

In 2011, a rock mass geomechanical characterization was carried out for preparing the expansion plan of the exploitation of the Faraona quarry. From the in-situ surveys, carried out in the adjacent area of the Santa Marta mine, 3 major joint sets were identified. The joint set St has a spacing equal to 15÷20 cm, instead the joint sets K2 and K3 have higher values (50÷70 cm). Figure 4.13 shows the stereographical representation of these main discontinuity sets.

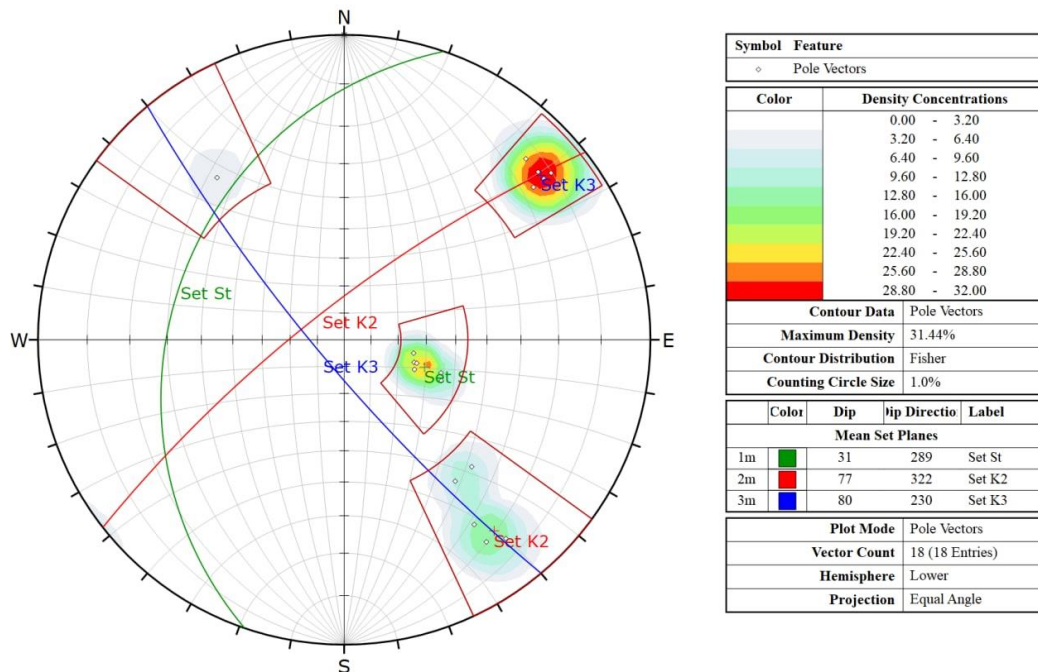


Fig. 4.13 – Stereographical representation of the structural survey carried out in 2011.

The models have been prepared with 2 different rock types: a limestone rock mass and a calcareous rock characterized by several weakness strata with clay (weaker material). Then, the equivalent continuum parameters have been calculated in order to proceed with the numerical modelling. The overburden has also been considered in the model. Table 4.1 resumes all the input data of the rock masses used for those models, whereas Table 4.2 presents the main parameters of the overburden.

**Table 4.1 – Intact rock and rock mass parameters of limestone, weakness strata and equivalent continuum material (Altair 2011).**

Parameter	Limestone	Weakness strata	Equivalent continuum material
Young's modulus - intact rock $E_i$	42 GPa	36 GPa	155 GPa
$m_i$	7	4	7
GSI	36	28	-
Young's modulus – rock mass ( $E_{rm}$ )	1428.97 MPa	967.54 MPa	1450 MPa
$m_b$	0,072	0,023	0.072
$s$	$2.33 \cdot 10^{-5}$	$6.14^{-6}$	$2.33 \cdot 10^{-5}$
Uniaxial compressive strength ( $\sigma_{cm}$ )	50 MPa	0.064 MPa	75 MPa
Unit weight of the rock mass ( $\rho$ )	2400 kg/m <sup>3</sup>	2400 kg/m <sup>3</sup>	2400 kg/m <sup>3</sup>

**Table 4.2 – Overburden parameters (Altair 2011).**

Parameter	Moraine overburden
Unit weight of the rock mass ( $\rho$ )	1700÷2000 kg/m <sup>3</sup>
Young's modulus (E)	0.8÷1.2 GPa
Cohesion	0
Friction angle	38°÷40°

The stability analysis is carried out using a FDM code (FLAC), starting from the previous parameters of the continuum equivalent models. The process is carried out with a 2D model in a particular critical cross section of the exploited area, in the middle of the Faraona quarry. The material has been modelled according to the linear elasto-plastic Mohr-Coulomb criterion.

The model considers and in-situ stage (before any excavation), then the exploitation is simulated with different stages: first the overburden is removed, then the excavation proceeds downwards from an elevation of 320 m to 275 m, in slices of 10 m (the last 2 slices are respectively 7 m and 8 m). Table 4.3 resumes the FoS obtained by the modelling for each stage, with the maximum value of total displacement.

**Table 4.3 – FoS and maximum displacement for each stage of excavation (Altair 2011).**

Stage	FoS	Max displacement (mm)
1 - Overburden removal	3.29	24.8
2 - Excavation to 320 m	3.29	26.4
3 - Excavation to 310 m	2.69	26.9
4 - Excavation to 300 m	1.84	27.0

5 - Excavation to 290 m	1.49	29.6
6 - Excavation to 283 m	1.41	28.5
7 - Excavation to 275 m	1.38	29.3

The FoS is always over the critical value of 1, therefore the model considers the layout stable for proceeding with the excavation. The displacements present some fluctuations, with the maximum value slightly lower than 3 cm in the last stage. Figure 4.14 shows 3 screenshots of the model of the final stage of exploitation as an example (geometry, total displacement with vectors and maximum shear strain increment).

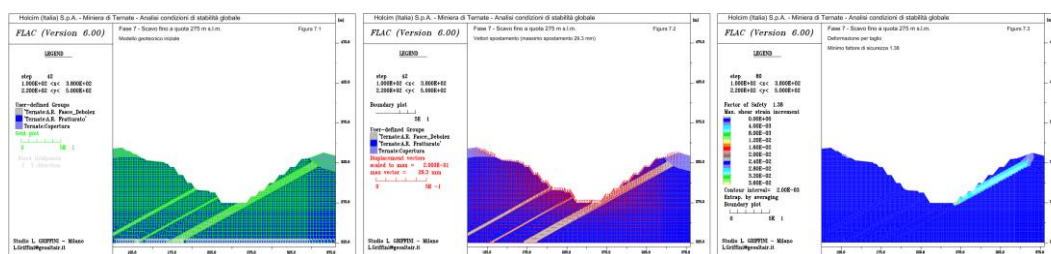


Fig. 4.14 – Example of the results of the 2011 models (geometry, total displacement with vectors and maximum shear strain increment) (Altair 2011).

For better considering the presence of the joint sets not included in the previous modelling, a discontinuum model has been prepared. In order to carry out a conservative analysis, the authors chose a high persistence to allow the formation of a larger number of blocks. Figure 4.15 shows the scheme of this approach with the formation of a potential planar sliding.

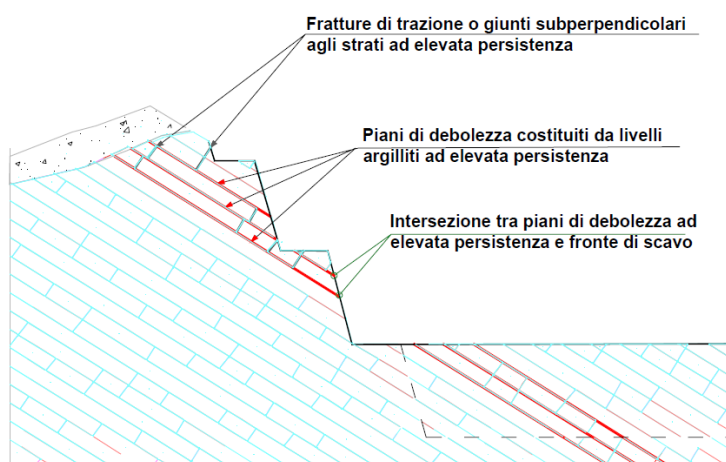


Fig. 4.15 – Scheme of the discontinuum model (the red lines represent the weakness zones) (Altair 2011).

For evaluating the slope stability, considering a discontinuum model, the authors implemented a model with UDEC code. The staging of the model is similar to the previous FDM model with a different slice height (15 m). The other difference is the orientation of the section, which in this case is opposite compared to the FDM section. An example of the obtained results is shown in Figure 4.16, in which it is evident the risk of planar sliding in the East face of the Faraona quarry due to the tabular shape of the formed blocks.

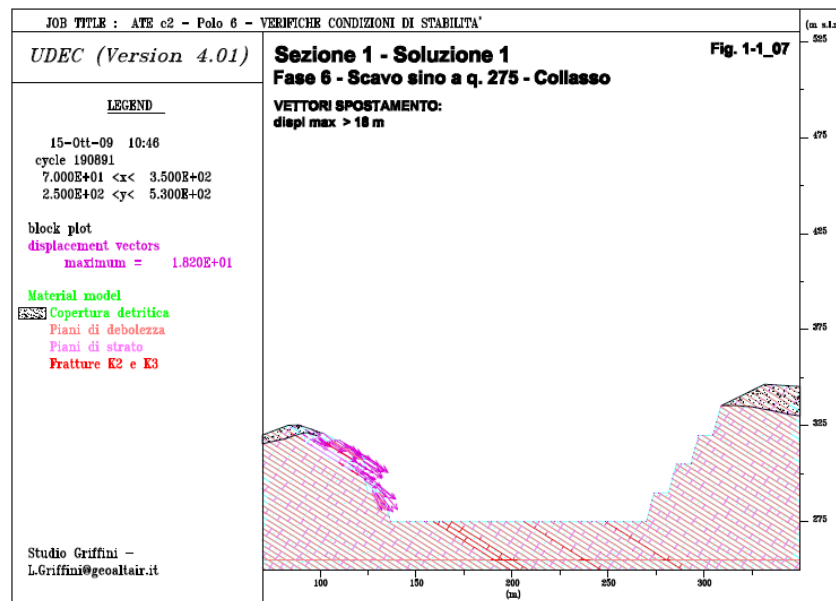


Fig. 4.16 – Example of results of the discontinuum model (displacement vectors). (Altair 2011).

#### 4.5.2 Slope stability analysis 2019

For the second slope stability analysis, carried out in 2019, another rock mass characterization has been implemented. Section 4.4 resumes all the discontinuity parameters of the 4 joint sets obtained from the new site surveying and characterization. In this new analysis, a 2D-DEM model is implemented; authors decided in this case to consider only 2 joint set parameters (Griffini 2020):

- St family: it is coinciding with the rock mass layering and dipping towards WSW-WNW (dip direction  $240^{\circ}\div 295^{\circ}$ ) with an inclination ranging between  $10^{\circ}$  and  $25^{\circ}$ . For the modelling an average  $dd/dip$  equal to  $280^{\circ}/22^{\circ}$  with a very high persistence close to 100% has been adopted;

- K4 family: this joint set is dipping towards E-NE (dip direction  $50^\circ \div 90^\circ$ ) inclined between  $65^\circ$  and  $80^\circ$ . For the modelling an average  $dd/dip$  equal to  $68^\circ/72^\circ$  with a low persistence has been adopted.

Table 4.4 summarizes the intact rock and rock mass parameters used for this second DEM modelling phase.

**Table 4.4 – Rock matrix and rock masses parameters (Griffini 2020).**

Rock matrix parameters					
$\sigma_t$ [MPa]	$m_i$			$E_i$ [GPa]	
35÷40	7.0			20.0	

Rock mass parameters					
Survey	$m_b$	$s$	$a$	$\sigma_c$ [MPa]	$E_{rm}$ [MPa]
RGS-01-19	1.322÷2.129	0.0094÷0.0357	0.502÷0.501	3.36÷7.53	7.05÷10.36
RGS-02-19	1.042÷1.678	0.0048÷0.0183	0.503÷0.501	1.2÷2.74	2.94÷5.44
RGS-03-19	0.647÷1.042	0.0013÷0.0048	0.506÷0.503	1.2÷2.74	2.94÷5.44
RGS-04-19	0.821÷1.322	0.0025÷0.0094	0.504÷0.502	1.7÷3.84	4.04÷7.05
RGS-05-19	0.647÷1.042	0.0013÷0.0048	0.506÷0.503	1.2÷2.74	2.94÷5.44
RGS-06-19	0.647÷1.042	0.0013÷0.0048	0.506÷0.503	1.2÷2.74	2.94÷5.44

The analyses have been performed by simulating the design, according to the different sequences of excavation corresponding to the formation of each bench. According to the official report, deformable blocks with a linear Mohr-Coulomb strength criterion have been considered for the modelling. The global stability is obtained by verifying the ratio between stabilizing and driving forces, obtaining a kind of Factor of Safety FoS ( $\gamma_R$ ). The results show that considering the characteristic peak parameters, the FoS is ranging between 1.27 in the initial state and 1.41 in the final stage; whereas considering the residual parameters the value of FoS is reduced to 0.91 in the initial state and to 1.25 in the final state (as an example, the pictures regarding the residual parameters are showed in Fig. 4.17). Considering the fact that the slope, according to this model, is stable at the end of the exploitation for both peak and residual strength, the excavation geometry has been adapted by removing totally the upper weakness layers in order to avoid the formation of planar sliding from the residual upper faces (Fig. 4.18).

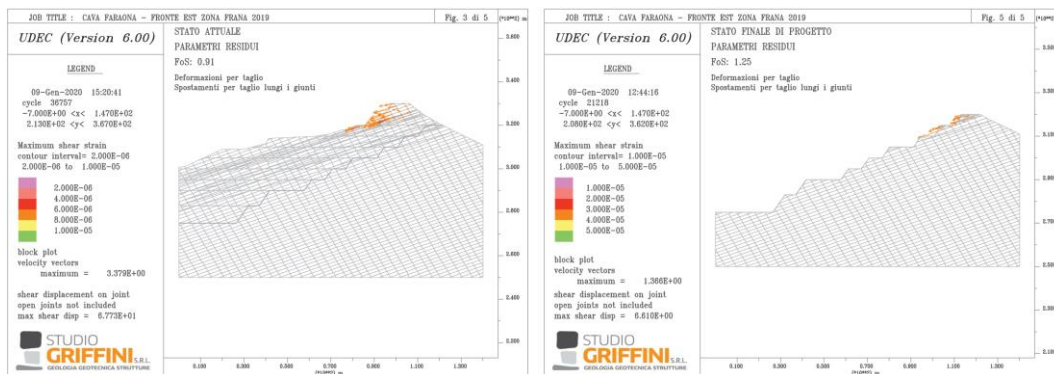


Fig. 4.17 – Results of the DEM model of the initial state (left) and final stage (right) considering the residual value of strength (Griffini 2020).

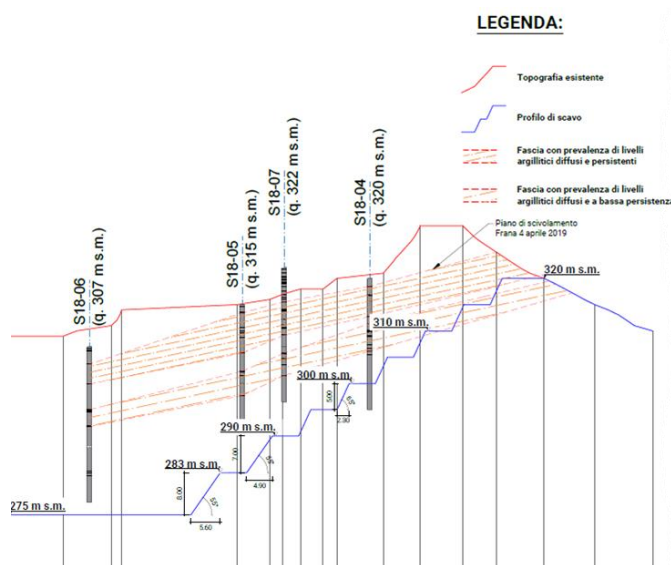


Fig. 4.18 – Proposed layout to avoid planar sliding on the top faces (Griffini 2020).

### 4.5.3 Considerations on the existing stability analyses

Comparing the 2 existing rock mass characterizations (2011 and 2019), the parameters have different value in terms of intact rock and rock mass. In 2011, the characterization regarded all the area of the Faraona quarry, therefore the investigation presents a large amount of data distributed in a large area. On the contrary, after the instability events in 2019, the survey has been focused on the East face: in this structural analysis, more attention has been adopted to identify the weakness zones.

Regarding the numerical modelling, as already said the analyses have been carried out in 2D: in particular in the first model, the adopted geometry is a middle cross

section of the whole quarry (including East and West face, visible as left and right slope in the models), instead in the second model the geometry is a cross section of the central East area, concentrating the calculation in the instable area (visible as a right slope).

Considering the uncertainties given by the different results obtained from the 2 modelling phases (the first with both continuum FDM and discontinuum DEM, while the second considering just the DEM), a 3D analysis would better describe the case. For this reason, this thesis considers a complete 3D numerical analysis by implementing the 2D analyses and the rock mass characterizations, coupled with the 3D design plans of the exploitation.

This new work has been organized in 3 different phases:

- 1) Large scale 3D-FEM (continuum equivalent) to evaluate the response of the rock mass to the different rock mass parameters given by the existing works from 2011 and 2020 and assess the global stability of the exploitation, also in terms of stress distribution and strains;
- 2) Large scale 3D-DEM (discontinuum) to confirm the results of the 2020 stability analysis by considering the complete geometry of the jointing (4 joint sets) and to assess the behaviour of the east slope object of frequent instability (see Section 4.3). To obtain suitable results for this last point, the jointing has been applied to the east area of the quarry and the rest of the model has been considered as a continuum equivalent. For this analysis deformable blocks have been used.
- 3) Small scale detailed 3D-DEM (discontinuum) to perform a back analysis on the joint parameters in order to cover all the possible scenarios which can occur during the exploitation. In this case, the model considers only the east area using rigid blocks with a denser joint pattern to obtain smaller blocks and better simulate the real situation.

## 5. CONTINUUM MODELLING OF THE FARAONA QUARRY

To build the continuum model of the Faraona quarry, the Midas GTS NX (2019 version 2.1) code was used. This code allows the evaluation of soil-structure based on finite element method. Examples of applications in geotechnical design are foundations, tunnels, soil consolidation, dams, seismic analyses and slope stability. The GUI is simple and user-friendly and the program is capable of working with remarkable performances in terms of speed of analysis and output return. Through Midas GTS NX all types of field conditions can be set using non-linear analysis methods (i.e. linear/non-linear static analysis, linear/non-linear dynamic analysis, seepage and consolidation analysis and slope safety analysis (Midas 2019).

The geometric model can be built in 2D or 3D directly by using the program tools (among other things, Boolean operators are available to merge, cut, intersect the various elements created) or by importing compatible files, such as DXF files. Figure 5.1 resumes the different objects can be created with this program. The simplest element is the point, while the most complex to process are the solid and the shell.

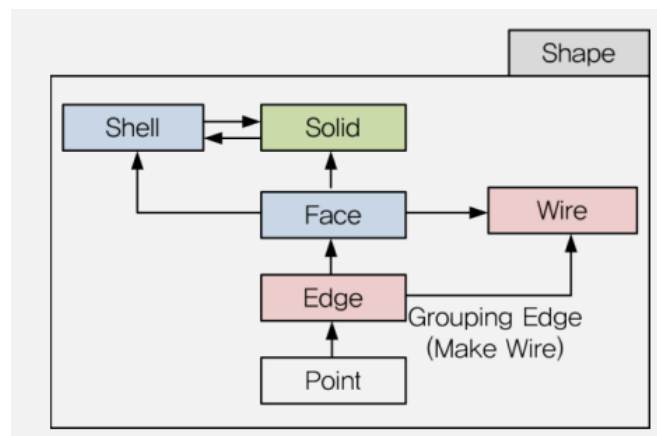


Fig. 5.1 Geometry ranking of the objects (Manual Midas GTS NX 2019).

As a first step it is necessary to define the characteristics of the material, specifically the general stiffness and properties of the ground and eventually of the structure.

The way to model the ground is to select the model type for each material. There are several possibilities of choosing the material type and model type, for example isotropic or orthotropic, elastic, Tresca, Mohr-Coulomb, von Mises, Hoek-Brown, etc (Midas 2019).

Regarding the meshing of solid rock structures, the 3D elements can be tetrahedrons, hexahedrons or hybrid (tetrahedral + hexahedron combination shape). The software is also able to handle 2D or 1D elements in order to discretize for example lining and bolts.

The code can provide different results, i.e. total displacement, effective stress, total stress, strain and equivalent plastic strain.

## **5.1. Model preparation**

### **5.1.1 Geometry**

The first step of the work consisted in preparing an overall continuum model by considering the whole geometry of the new extension of the quarry based on the design described in Chapter 2. This includes a detailed surface model that was built on the basis of the official drawings and of the regional map containing the isolines (one each 5 m).

The preparation of the surface has been then carried out using the code Rhino (version 7) which is a powerful tool able to create 3D surfaces based on the NURBS mathematical model, thus able to better interpolate missing areas with the existing isosurfaces. Figure 5.2 shows the obtained trace of the surface starting from the isolines.

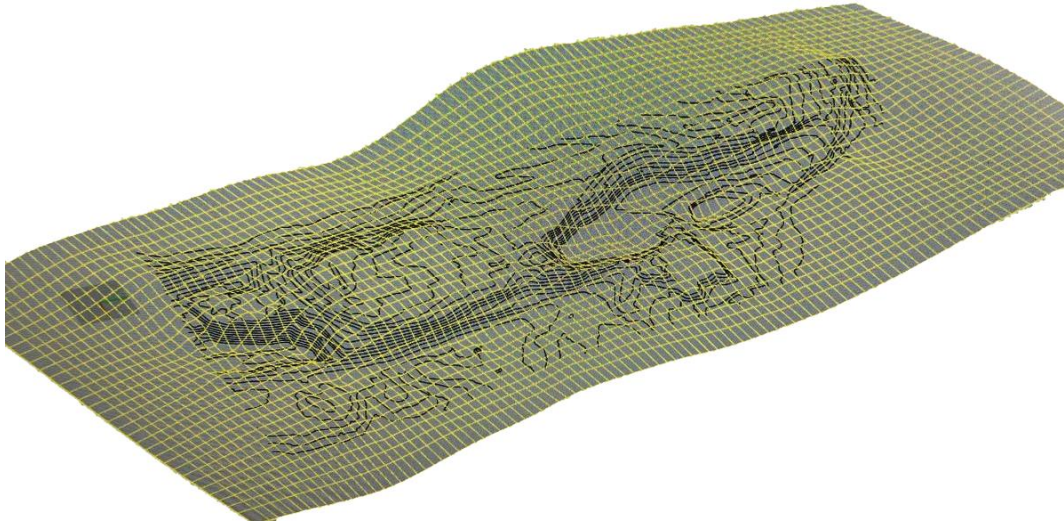


Figure 5.2 – Surface preparation in Rhino using the existing isolines.

Then, the surface has been imported into the Midas GTS NX 2019 code to be extruded in order to create the solid representing the modelled rock mass. Figure 5.3 shows the geometry of the global model of the Faraona quarry, which has an extension of  $2.5 \times 2.5 \text{ km}^2$ .

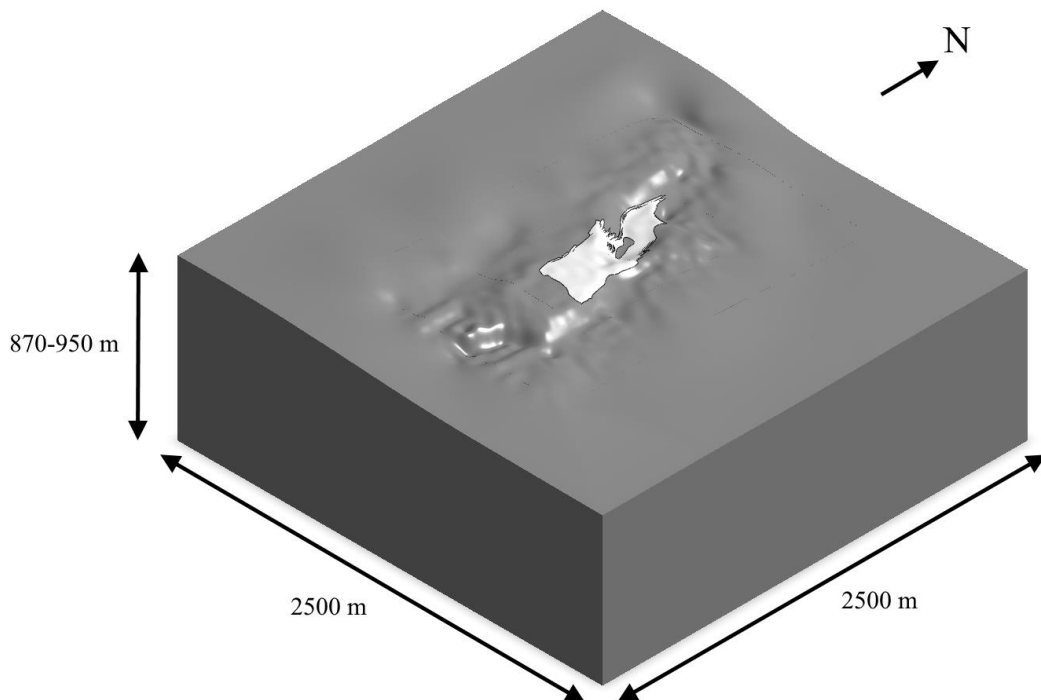
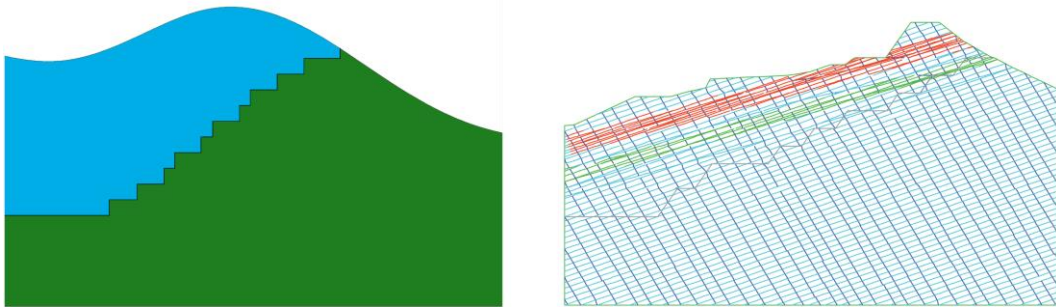


Figure 5.3 – Overall view of the 3D FEM continuum model. The exploitation area is represented in light grey. South from the quarry the depression caused by the trace of the Santa Marta mine is visible.

This large model allows to verify the overall stability and conditions of the quarry once exploited. The excavation phase in this case has been considered as performed in a unique stage, thus showing the final conditions of the rock mass after the exploitation. Moreover, considering the complexity of the model, the slopes have been considered as vertical with a height of 5 m according to the isolines derived from the final layout of the design (Fig. 5.4)



**Figure 5.4 – Comparison between the slopes modelling in the 3D continuum model (left) and the 2D models carried out by Griffini, 2020. The 3D model was built by considering an example section.**

### **5.1.2 Meshing**

All software that uses finite element methods require, after defining the geometries, to create the mesh. This is the only entity that is directly treated by the solvers used by the software, as the definition of the load, properties and boundary conditions can be done just in the mesh.

The elements used in Midas GTS NX models are solid to simulate the volume of rock considered in the calculations. For this model the elements used are tetrahedrons. In case of big models with irregular and complex geometries, the number of nodes and elements increases during the discretization in the link zones. Hence, it is necessary to control the dimension of the element (determined by the distance between the nodes) imposing larger distances in the less important zones (far from the excavations and close to the boundaries) and increasing the density of nodes in the parts of interest. Since the dimension of the Faraona quarry model is very large, the meshing stage has been performed by considering different areas: the excavated volume and the neighbouring slopes around it have been meshed by using a denser discretization in order to create a smoother and well-defined contour

and to obtain better results from the calculation. The remaining areas have been discretised more and more scattered. In average, the denser areas have an element size of 5-10 m, while in the external boundary the size reaches values over 100 m. This of course represents a weak point of the calculation, as this large size does not allow to get fine results, but as already mentioned this continuum equivalent model is produced for verifying the overall general assessment for getting an initial idea of the problem. Figure 5.5 shows the overall result of the meshing, in particular the increase of mesh size while moving away from the exploited area. This aspect is more significant looking at Figure 5.6, which represents a zoom of the previous figure over the exploited area.

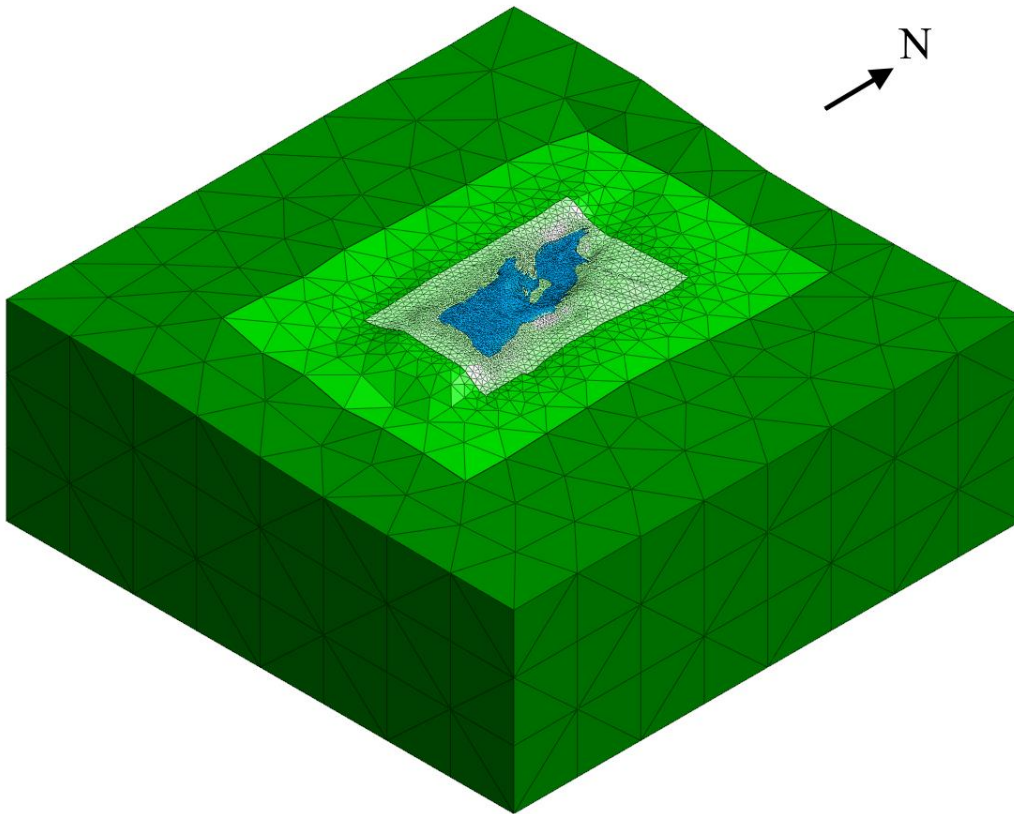


**Figure 5.5 – Overall view of the meshed model.**

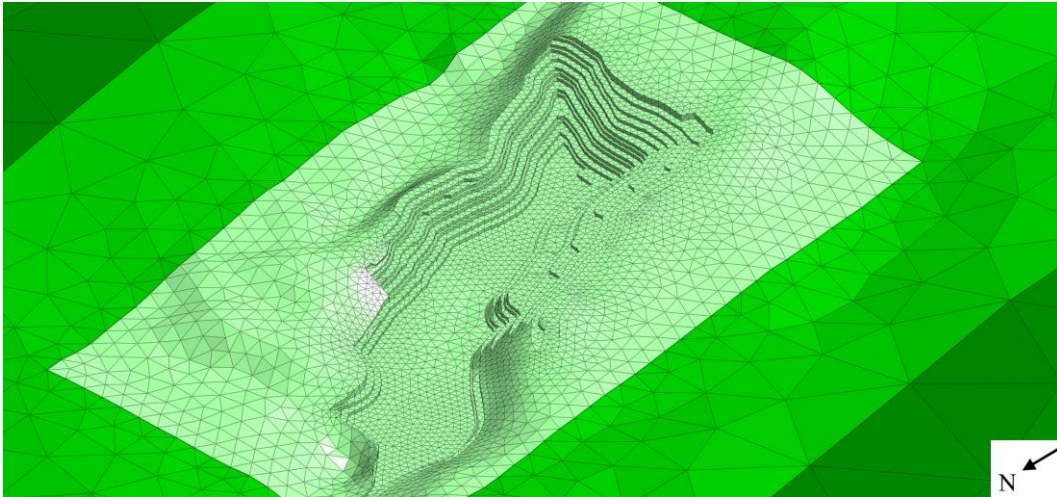


Figure 5.6 – Detail of the exploited area (the excavated volume has been removed to show the benches).

### 5.1.3 Staging

Since this is the first overall model of the quarry, only 2 stages have been considered: the in-situ stage which represents the initial condition with the surface modelled from the isolines of the regional cartography; the final layout after the exploitation of the quarry (residual slopes). No intermediate stages have been considered, because in this first modelling the goal was to establish what set of rock mass parameters are reliable for the refined slope stability analysis. Figure 5.7 shows the 2 stages of this model.

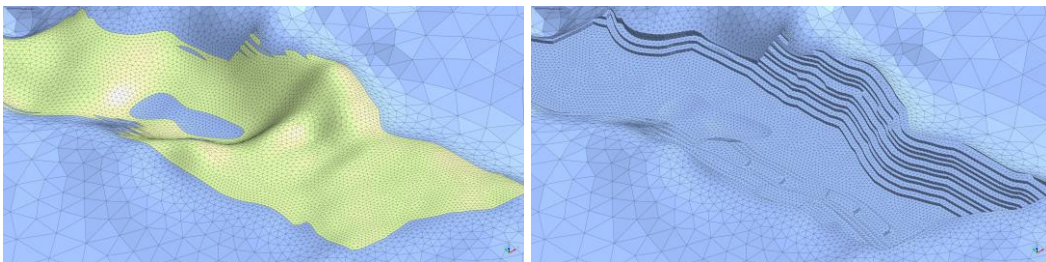


Fig.5.7 – In-situ stage (left) and final stage (right); the portion in yellow represents the mesh of the exploited volume.

## 5.2. Input data

### 5.2.1 Rock mass parameters

The existing geological model determined the presence of only one lithology (the exploited limestone) with an upper moraine layer which has been removed in the first phase of the exploitation. For modelling purpose, this top layer has been neglected as the goal of the stability analysis involves only the rock mass. Moreover, its depth is not relevant for the thickness of the limestone vein.

The rock mechanical data for the analysis have been obtained from 2 different characterizations of the rock mass: the geotechnical reports (Altair 2011 and Griffini 2020) include geomechanical parameters, obtained from different analyses, carried out in 2011 and in 2019. The data are listed in Table 5.1.

**Table 5.1 – Parameters of the intact rock.**

Parameter	Value (2011)	Value (2019)
Young's modulus - intact rock $E_i$	155 GPa	20 GPa
Poisson ratio	0.27	0.25
Uniaxial compressive strength ( $\sigma_{cm}$ )	75 MPa	75 MPa
Unit weight of the rock mass ( $\rho$ )	2400 kg/m <sup>3</sup>	2400 kg/m <sup>3</sup>
Hoek-Brown criterion parameter $m_i$	7	7

For this analysis the non-linear elasto-plastic Hoek-Brown criterion was adopted, which is widely used for describing rock masses with such characteristics. The data related to the intact rock have been then reduced accordingly to be used in a continuum equivalent model thanks to the GSI approach proposed by Hoek & Brown (2018). The treatment of these data has been carried out by using the code Rocscience RocData (version 5.013) to verify the Hoek-Brown criterion parameters for the rock mass starting from the ones used in the 2011 and 2019 analyses. The reports contain only partial indications about the quality of the rock mass: according to the analysis performed in 2011 the limestone rock mass has an estimated GSI of 36 which is reduced to 28 in the weakness zones, while in 2019 the estimation is missing. In order to assess the values for the new analysis in 3D, a back analysis of the parameters has been carried out to estimate the GSI by iterations also in the new characterization of 2019. The results are summarized in Figure 5.8 and Table 5.2.

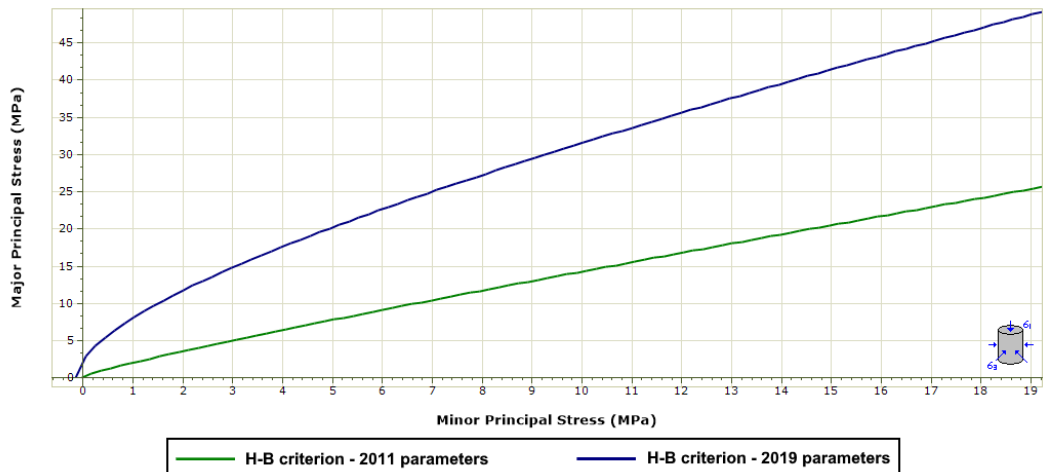


Fig. 5.8 – Comparison between H-B criterions with 2011 parameter and 2019 parameters of the rock mass.

Table 5.2 – Parameters of the rock mass used for the continuum modelling.

Parameter	Value (2011)	Value (2019)
Young's modulus – rock mass ( $E_{rm}$ )	1450 MPa	3000 MPa
Hoek-Brown criterion parameter $m_b$	0,072	0,65
Hoek-Brown criterion parameter $s$	$2.33 \cdot 10^{-5}$	$1.3 \cdot 10^{-3}$
Computed GSI (by iterations)	<5	33-39

Some criticalities are noticeable after the computation of the rock mass parameters and GSI:

- the Young's Modulus  $E_i$  of the intact rock ranges 20 GPa according to the 2019 characterization, and 155 GPa to that of 2011. The range is very wide and it cannot be easily justified (155 GPa seems to be exaggerated for this type of rock), especially because the  $E_{rm}$  is then lower in 2011 than in 2019. Based on the original data, the computed GSI would be equal to 39 from the analyses of 2019 and it cannot be calculated with the data of 2011 since, with a GSI of 5, the value would be 4.1 GPa, which is almost 3 times the one given in the 2011 report;
- the Hoek-Brown criterion parameters  $m_i$  is 7 for both the characterizations and appears suitable for the type of rock considered (limestone). On the contrary the rock mass parameters  $m_b$  and  $s$  are very different, appearing excessively small in the 2011 report (to obtain such values the GSI should

have been lower than 5 also in this case) and quite appropriate in the 2019 report.

These considerations raise the problem of relying on parameters that are scattered and with a high discrepancy: for this reason, the continuum equivalent model has been implemented with these 2 sets of geomechanical parameters to compare the results and to establish the more reliable rock mass characterization.

### 5.2.2 Loads and boundary conditions

Since the model considers a surface slope stability, there are no external loads included out of the gravity. Regarding the boundary conditions of the model, this FEM code allows the possibility of including different types of constraints. As the model has no external load and its extension is quite wide from the excavated area, there is no need of particular constraints, so it has been chosen to set a horizontal displacement ( $XY$ ) equal to 0 in the 4 sides and vertical displacement ( $Z$ ) equal to 0 in the bottom. Figure 5.9 shows the complete model with the meshes, the boundary conditions (indicated with blue and red arrows) and the gravity (indicated with the red downwards arrow in the middle).

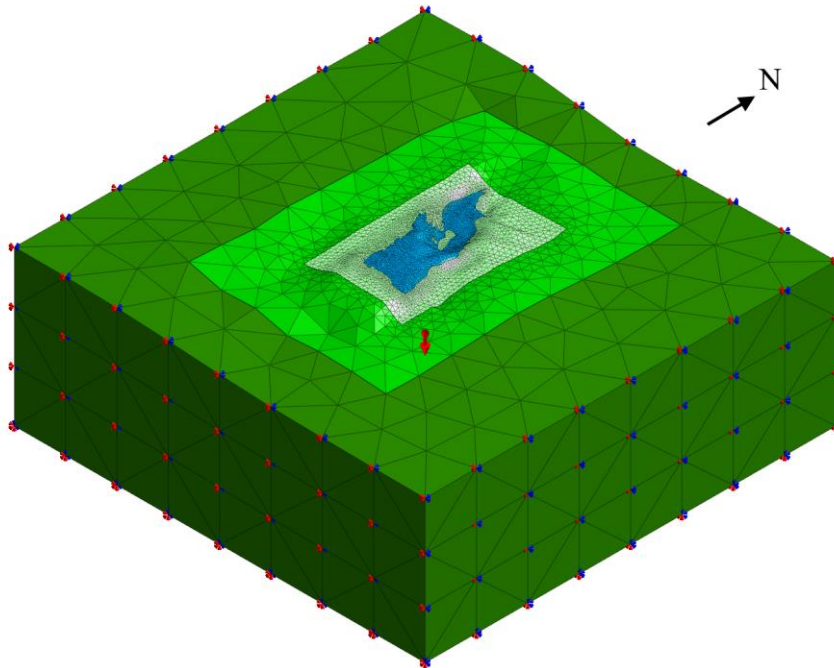


Fig. 5.9 – Boundary conditions and external load (gravity) of the continuum model.

## 5.3. Results

The results of the two models (identified as 2011 and 2019 depending on the used rock mass parameters) show a large discrepancy in the behaviour of the rock mass after the exploitation. In the next sections, the results of displacement, plastic strains and yielded zones are analysed in detail. Being this a continuum model with no external load other than the gravity, stresses are not considered in this part of the work.

### 5.3.1 Displacements

The displacements in the 2 models show a similar overall trend, but the magnitude is different. As a matter of fact, the 2011 model returns a maximum displacement almost double than the one of the 2019 model (80 mm vs 45 mm), as shown in Figure 5.10 and Figure 5.11. An important aspect to be considered coming from both the models is the direction of the displacement: results from a middle section of the Faraona quarry (Fig. 5.12 and Fig. 5.13) clearly show that the movement is generally oriented upwards and therefore the models are characterized by a heave effect of the residual slopes (end of the exploitation). This phenomenon is quite common in the continuum models with such characteristics especially due to lack of stress confinement after the exploitation. This effect underlines also the need of proceeding with a more accurate DEM model, in which the main displacements occur along the joints (sliding, toppling etc.).

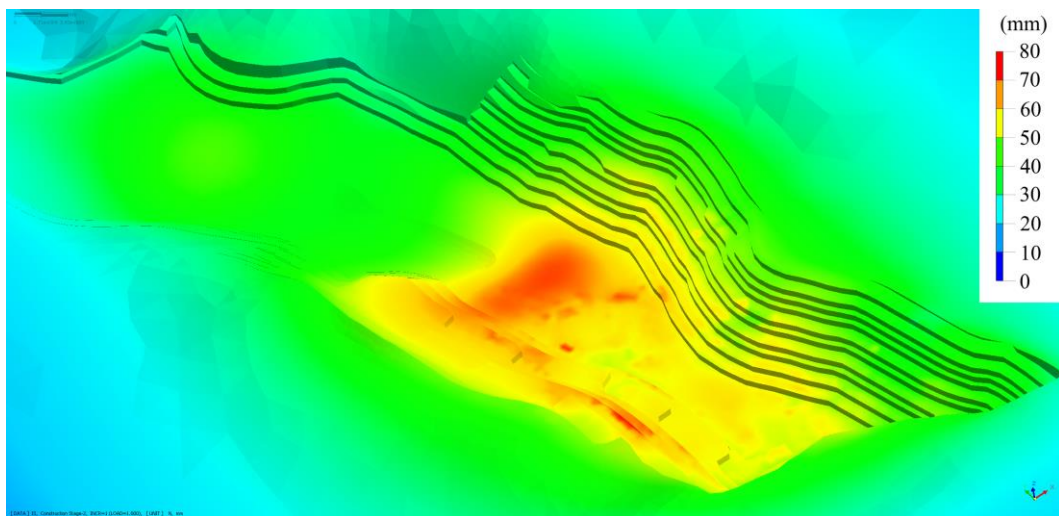
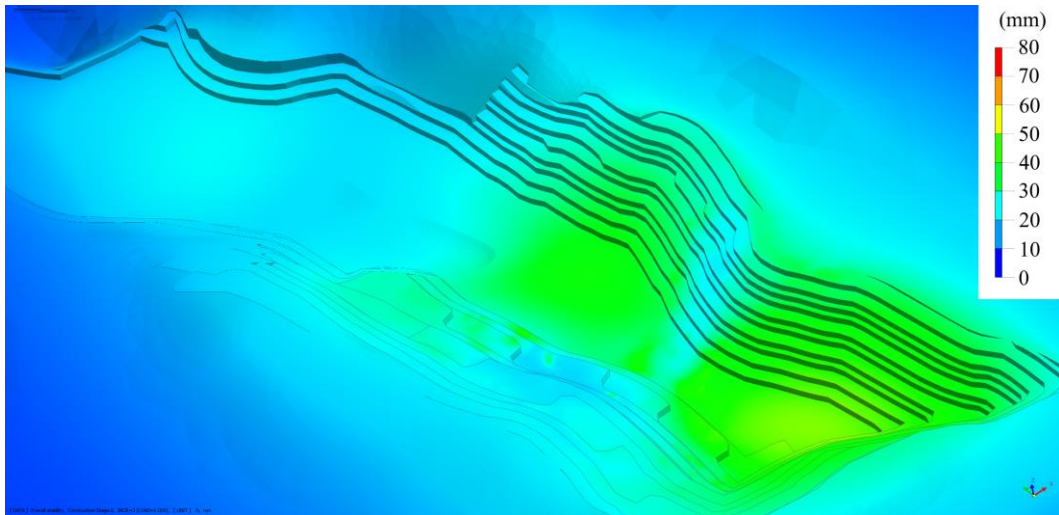
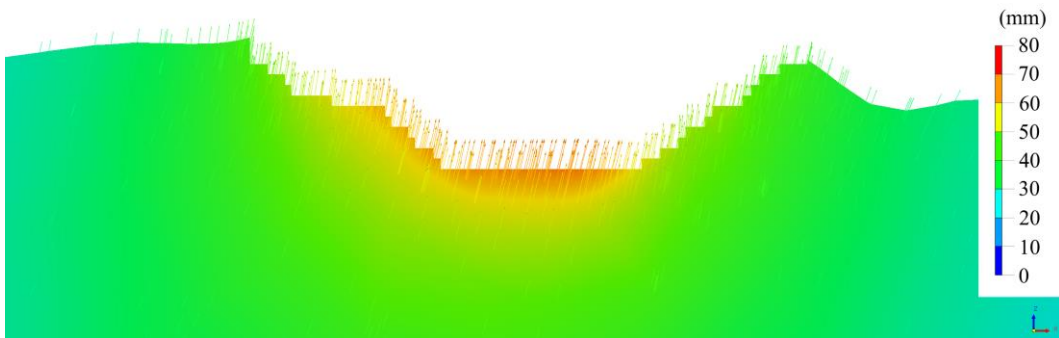


Fig. 5.10 – Total displacement of the slopes (2011 parameters).



**Fig. 5.11 – Total displacement of the slopes (2019 parameters).**



**Fig. 5.12 – Total displacement of the slopes (2011 parameters).**

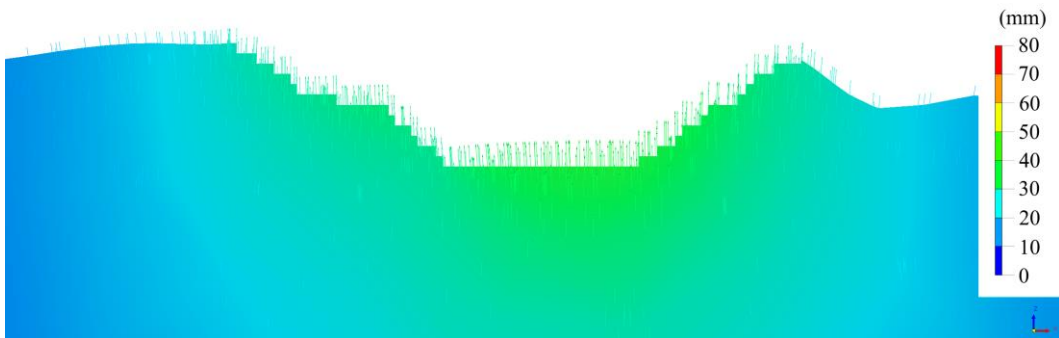


**Fig. 5.13 – Total displacement of the slopes (2019 parameters).**

### 5.3.2 Equivalent plastic strain

The effective plastic strain is also called as yield point and it has contributions from both the volumetric plastic strain and the deviatoric plastic strain. After the stresses beyond this point, the material undergoes a non-elastic deformation; therefore it is

an indicator of an irreversible deformation. This is a common indicator used in slope stability for assessing the sliding surfaces. The results show a trend of possible instabilities forming in the East area for both the data sets, being more evident and critical for the 2011 set (Figure 5.14 and Figure 5.15).

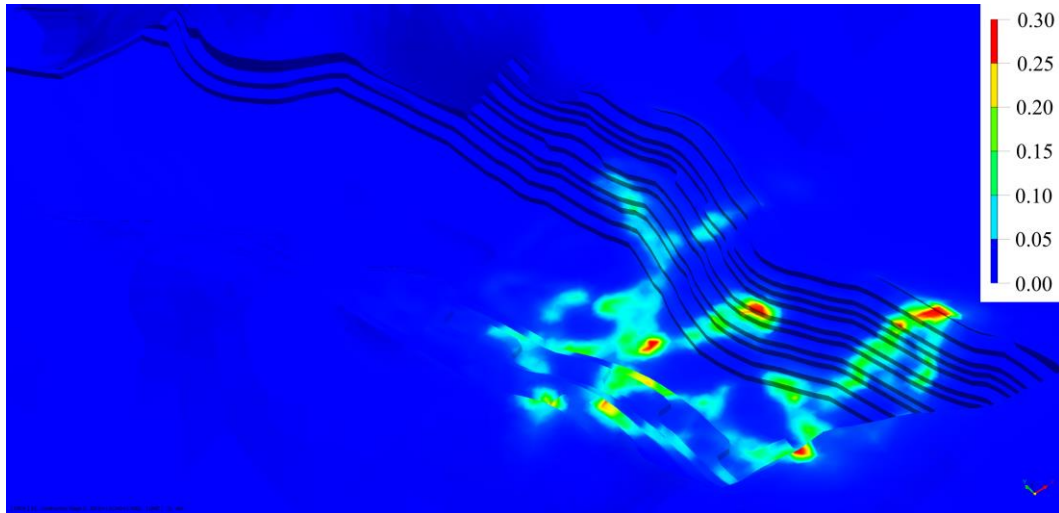


Fig. 5.14 – Equivalent plastic strains of the slopes (2011 parameters).

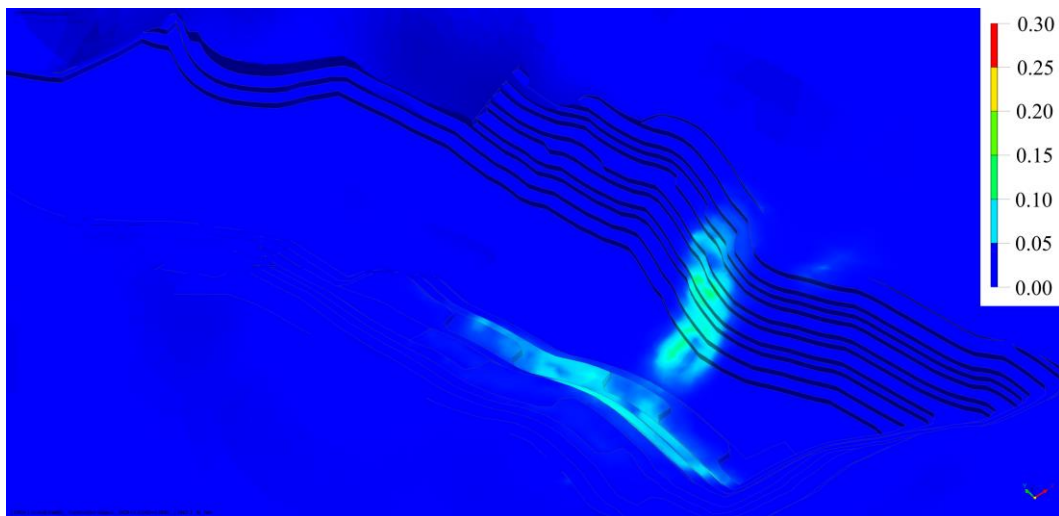
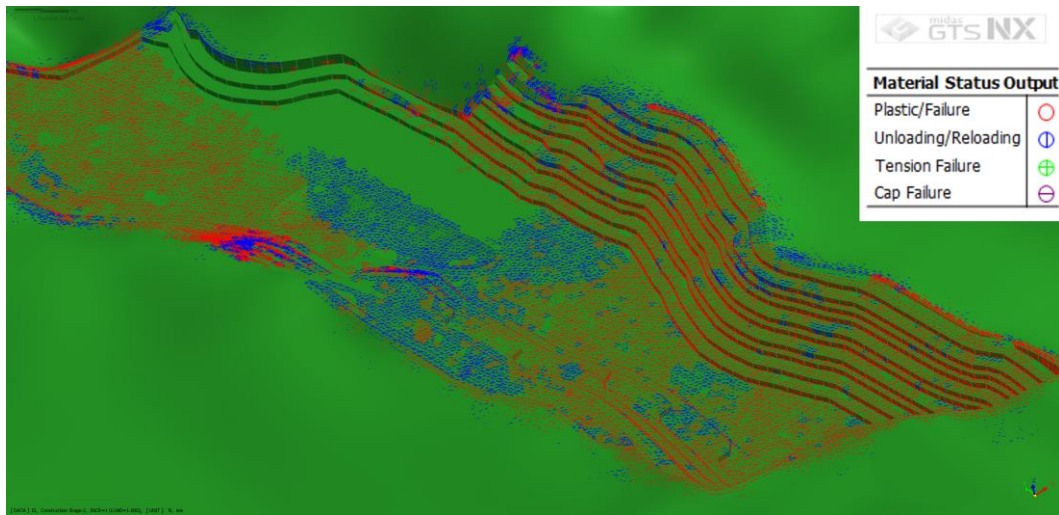


Fig. 5.15 – Equivalent plastic strains of the slopes (2019 parameters).

### 5.3.3 Material status

This result is an indicator for assessing the state of the single element of material. The code is able to identify the material status depending on the strength criterion and especially regarding plastic, unloading/reloading, tension and cap failure.

According to the results obtained, the data set of 2011 appears inadequate to assess the behaviour of the rock slopes based on a continuum modelling approach, as it is evident that the whole slope is yielding (Figure 5.16). The results pertaining to the 2019 set show, on the contrary, a zone of yielded elements according to the results of the plastic strains (Figure 5.17).



**Fig. 5.16 – Material status (2011 parameters).**

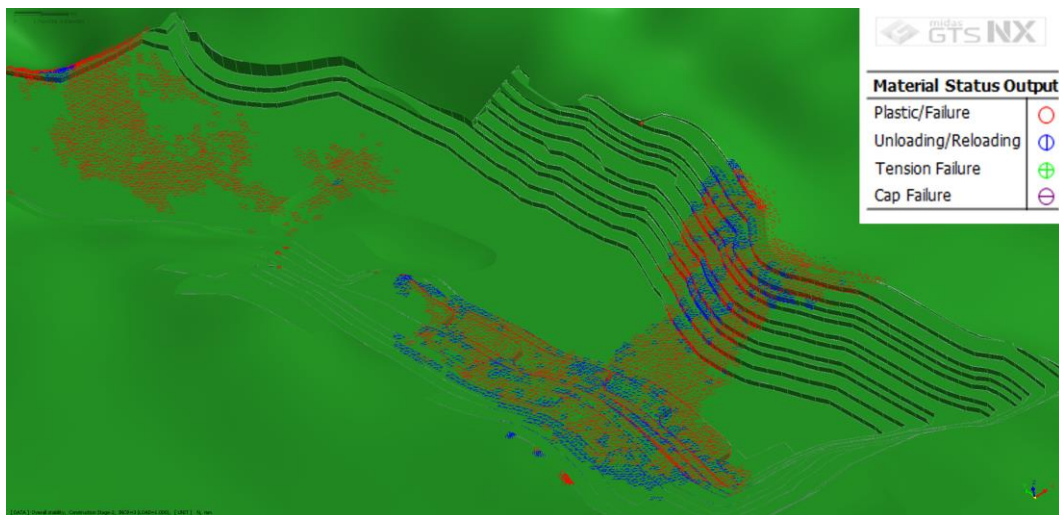


**Fig. 5.17 – Material status (2019 parameters).**

#### **5.4. Remarks on the continuum modelling**

According to the results of the continuum models, the 2019 rock mass characterization represents a suitable starting point for a more detailed modelling of the Faraona quarry. As verified also on site, the East face is identified as the critical zone where the instabilities can take place: this aspect is confirmed by the position of the maximum displacement (Fig. 5.11). Also, the equivalent plastic strain and the material status indicate the same critical zone. This supports even more the need of carrying out a discontinuum model in order to take in account the joints.

## **6. DISCONTINUUM MODELLING OF THE FARAONA QUARRY**

For the discontinuum model of the Faraona quarry, it has been decided to use the Itasca 3DEC code (version 5.2). This software is ideal for analysing potential failure modes directly related to the presence of discontinuities. The code provides numerous material models, joint models, groundwater flow and ground support structural elements. 3DEC simulates the discontinuous model through a set of discrete blocks.

Discontinuities are processed as boundary conditions among the blocks; therefore, important displacements along the discontinuities and rotations between blocks are allowed. The single block can assume a rigid or deformable behaviour. The behaviour of the discontinuities can be governed by linear or non-linear stress-strain relations. This code allows to simulate a representative response of the discontinuous geological model (Itasca 2020). As already stated in Section 4.5.3, this work includes both these typologies (overall model with deformable blocks in this chapter and detailed model of the East area for the back analysis with rigid blocks in Chapter 7).

3DEC is a command-driven program: the input language is based on a command window with intuitive commands. The list of input commands corresponds to the physical sequence of the phenomenon represented. Thanks to a text editor, the commands can be modified in a simple way.

### **6.1. Model preparation**

#### **6.1.1 Geometry**

The preparation of the geometry in 3DEC is more complex compared to that of GTS NX, as it is not possible to directly “draw” the solids using a GUI. An important aspect to consider while modelling in 3DEC is the need of working with

convex blocks, because it cannot handle concave shapes. There are two main techniques to build the geometry in 3DEC: the first consists of starting from a cube representing the external boundary which is cut through different surfaces in order to reproduce the final geometry (Figure 6.1); the second is more complex as it requires a third-party software able to directly prepare the blocks geometry. Thanks to this last method, very detailed and precise models can be built, such as complex slopes, underground constructions and other rock structures. For this work the second method has been used by taking advantage on the existing Midas GTS NX model: the geometry is prepared starting from the mesh elements representing a single block. The blocks are then merged in order to create a continuum geometry that after this step has been sliced by using the proper joint networks (Figure 6.2). The size of the model is equal to the continuum equivalent one carried out in Midas GTS NX (2.5x2.5 km<sup>2</sup>).

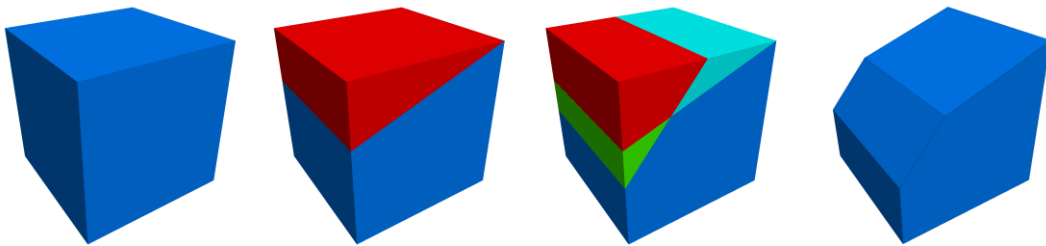


**Fig. 6.1 – Example of preparation of a simple 3D slope by cutting a cube with 2 joint sets (evolution from left to right).**

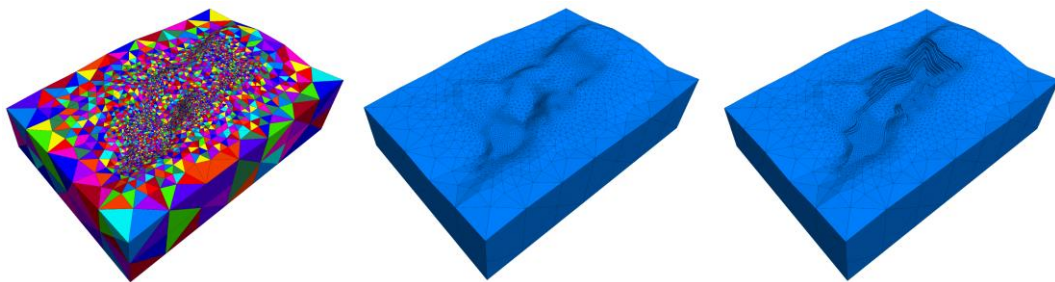


**Fig. 6.2 – Model of the Faraona quarry exported from Midas and split into blocks (represented by the different colours on the left) and joined to create a continuum geometry (right).**

Once created the continuum geometry, the joint sets can be included into the model. Considering the above-mentioned large size of the model, it would be impossible to suitably investigate the stability of the walls, thus the presence of jointing was

limited only to the high wall interested by the instability event previously described (Section 4.3).

For implementing this approach, it is useful to apply a hybrid DEM-FEM approach, where the DEM region is highly fractured and contains the excavation stages, whereas the FEM region is modelled as a continuum equivalent representation (Jing, 2007). A crucial issue is the displacement compatibility at the interface between the 2 regions. Figure 6.3 shows a combined representation of the DEM region (in near field) and of the FEM region (in far field).

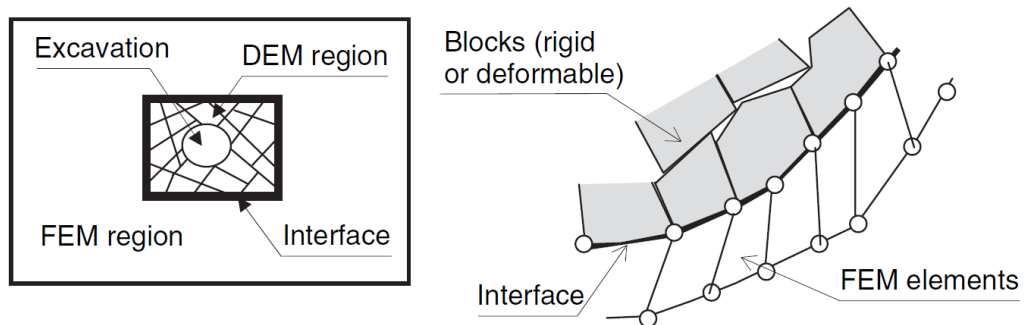


**Fig. 6.3 – Hybrid DEM-FEM model and interface representation (Jing 2007).**

For this overall model, due to the extension of the Faraona quarry, the DEM region includes only a part of the East face (approximate extension 300x300x100 m<sup>3</sup>). Figure 6.4 shows the overall extension of the model, with a whole external block (in green) embedding the jointed part (mixed colours).

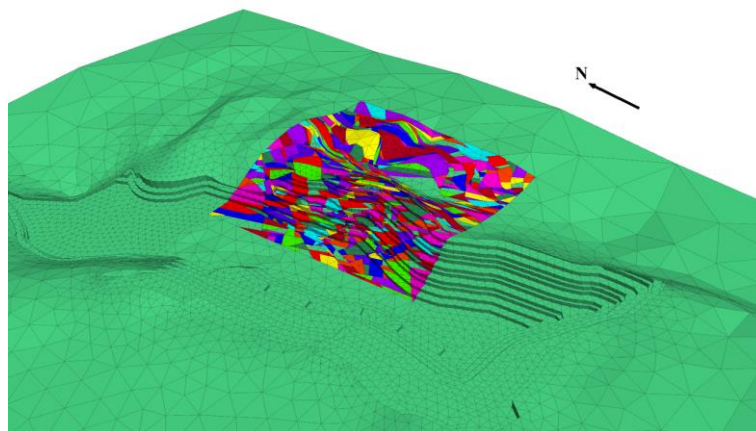


**Fig. 6.4 – Overview of the discontinuum model. The mixed coloured zone represents the East face, where various phenomena of instability have occurred.**

The blocks for this model are set as deformable: in this way the 3DEC code allows the internal deformation of each block of the model. The blocks are internally discretized into finite-difference tetrahedral elements. An example of a possible internal deformation is given in Figure 6.5.

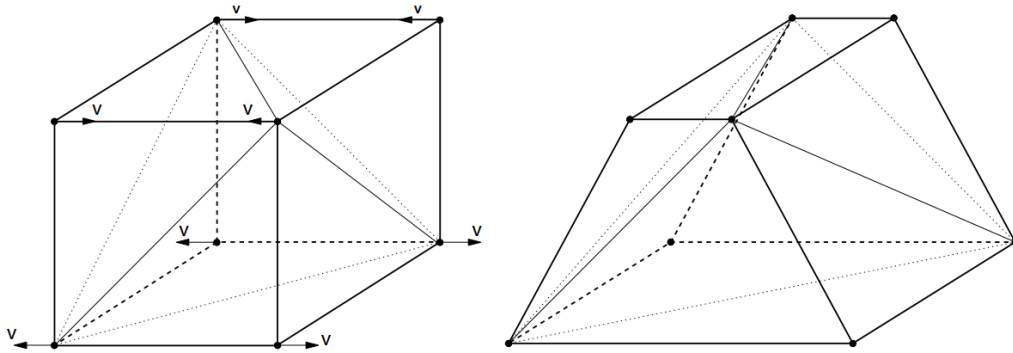


Fig. 6.5 – Example of deformation of a deformable block (Itasca 2020).

### 6.1.2 Meshing

The code allows the creation of a mesh similarly to the previous code, but the mesher is less powerful. For this reason, it is necessary to manually create different areas with different discretization, as the code is not able to handle change in the seed size smoothly. Figure 6.6 shows the different regions depending on the mesh size: the central area, which represents the quarry, has a denser mesh, while the external part has a higher seed size.

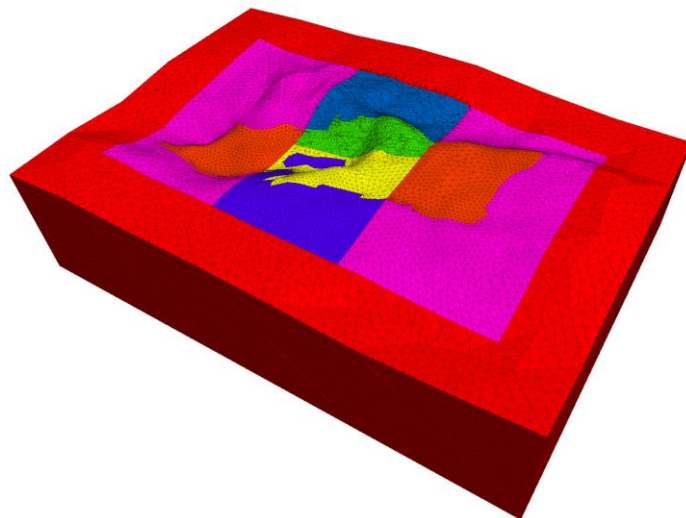


Fig. 6.6 – Regions used for the meshing of the model.

### 6.1.3 Staging

Staging for the first overall model (Figure 6.7) has been done in the same way as for the 3D-FEM model, thus considering an in-situ stage with the initial state and a final stage, representing the end of the exploitation.

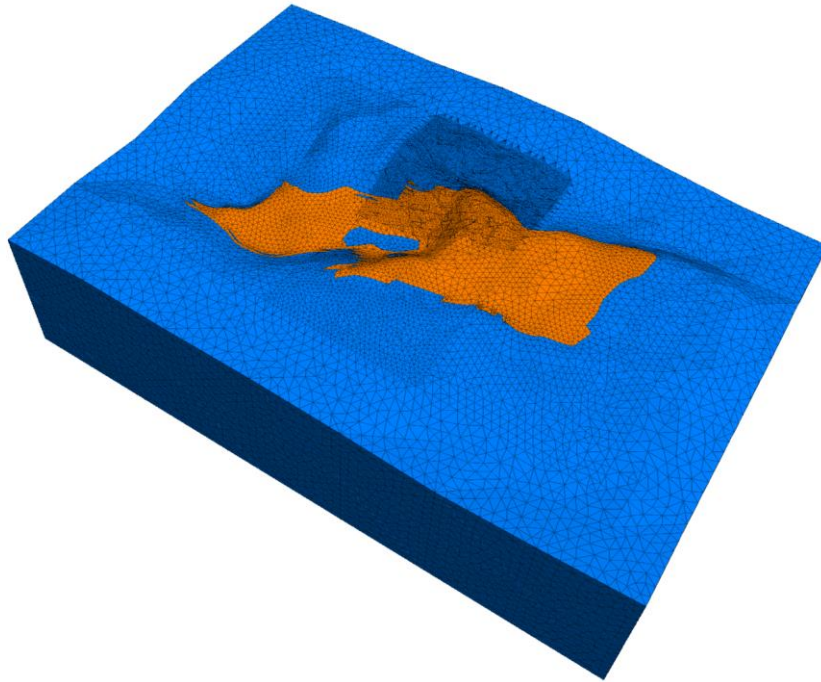


Fig. 6.7 – Stages of the overall 3D-DEM model with deformable blocks: in blue, the residual geometry; in orange the exploited volume.

## 6.2. Input data

3DECcode requires that every single passage is performed by writing a specific string for each operation. The geometry has been input as described before, creating blocks from the previous GTS NX model through the transformation of elements by means of the command POLY FACE. The polyhedron is formed by planar faces with the FACE keyword, where the coordinates  $(x_1, y_1, z_1)$ ,  $(x_2, y_2, z_2)$ , etc. define the boundary of the face.

Once created the geometry, the joints have to be included into the model. The joints are added thanks to the JSET command, which includes all the characteristics of

the joint itself. For adding a joint set, it is necessary to add the spacing and the number of the joints: in this way the model will include all the joints belonging to a certain set. As an example, a string used to add a joint set to the model is reported below:

```
jset o 650, 1000, 310 dip 18 9 dd 268 28 s 3 n 50 p 1 id 2
```

Where:

- “o” is the origin of the initial joint of the set;
- “dip” and “dd” (degrees clockwise from North) are the orientation of the discontinuities with the relative standard deviations in terms of dip (dip) and dip direction (dd);
- “s” is the spacing distance between joints;
- “n” is the number of joints in the set starting from the initial one;
- “p” is the persistence in terms of probability that any given block lying in the path of a joint will be split;
- “id” is the identification number of the joint set and it is helpful to assign the right properties to each set.

### 6.2.1 Joint properties

Table 6.1 summarizes the main parameters of the joint sets used for the overall 3D-DEM model, according to the 2019 structural data (Griffini 2020).

**Tab. 6.1- Principal structural data used into the discontinuum model, with the indication of the colours used for their representation in Figure 6.8.**

ID set	Dip (°)	Dip direction (°)	Spacing (m)	Persistence
J1 (green)	18	268	3	1
J2 (red)	75	50	9	0.6
J3 (purple)	68	135	9	0.4
J4 (cyan)	73	70	9	0.4

Unlike the previous slope stability analyses (see Section 4.5), in this case the model considers all the 4 joint sets characterized by the actual values of persistence (between 40÷100%), for obtaining a more realistic scenario according to the on-site

survey. In the 2D existing model the persistence of the joint sets is set equal to 100%, which overestimates the criticalities.

Figure 6.8 represents a cross section of the 3D-DEM model: the blocks are simulated through the intersection of different joint sets. Due to the variability of the structural parameters, an average value of standard deviation of 10° has been considered for dip and dip direction. With this randomized setting, the model presents blocks with different size.

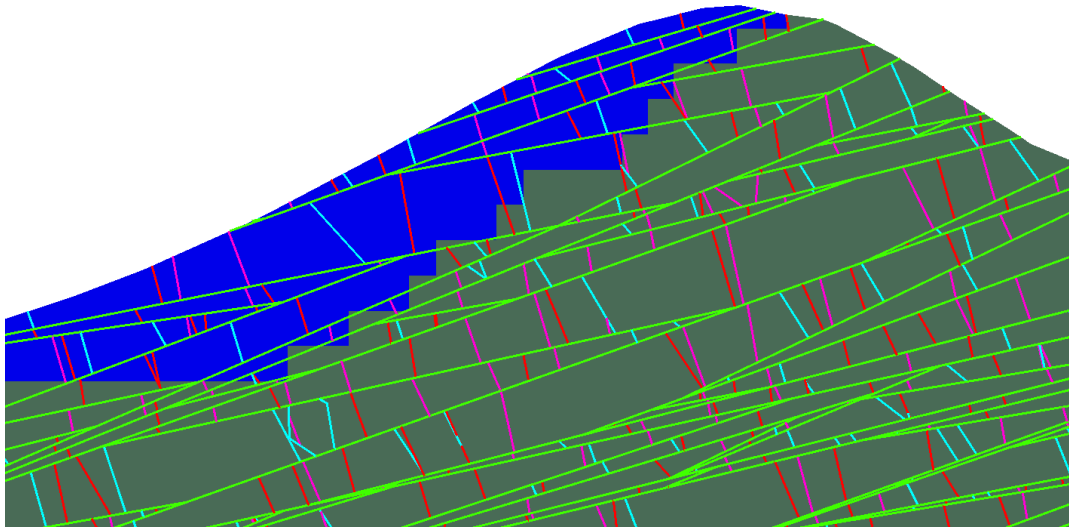


**Fig. 6.8 – Section of the overall 3D-DEM model with blocks created by the joint sets with the colours according to Table 6.1.**

Regarding the mechanical parameters of the joints, the data are taken from the report and modelling work of Griffini (2019). The stiffnesses of the joints (normal and shear) were not indicated, thus they have been calculated by using the formulation from Barton (1972):

$$k_n = \frac{E_i \cdot E_m}{L - (E_i \cdot E_m)}$$

where  $k_n$  is the joint normal stiffness,  $L$  is the mean joint spacing,  $E_i$  is the intact rock modulus and  $E_m$  is the rock mass modulus. The  $k_s$  has been then set to 5% of the normal stiffness. A summary of the parameters used for the joint sets included in this overall model is shown in Table 6.2.

**Table 6.2- Joint parameters used for the overall model.**

<b>Joint parameter</b>	<b>J1 value</b>	<b>J2, J3, J4 values</b>
Normal stiffness	750 MPa	750 MPa
Shear stiffness	37.5 MPa	37.5 MPa
Friction angle	28°	24°
Cohesion	0.05MPa	0.05MPa

### **6.2.2 Material properties**

Regarding the material properties, the model is theoretically composed by 2 materials (in reality it is just a large limestone outcrop): one is the external material (continuum region) that is set as a continuum equivalent material and the other is the investigated zone (DEM region), modelled as a discontinuum.

The most relevant parameter differing between one region and the other is the Young's modulus ( $E_{rm}$ ): in the continuum part has been calculated through the application of the Hoek-Brown GSI method described in Section 5.2.1; whereas in the discontinuum region this value has been set as the 80% of the intact rock Young's modulus ( $E_i$ ), in order to consider that only some of the existing joints are actually modelled (the spacing of the joints in the model is higher than in the reality). Regarding the strength criterion, the materials have been modelled using the linear elasto-plastic Mohr-Coulomb criterion, by using the same approach as the Young's modulus (continuum by linearizing the parameters of the FEM model and discontinuum by using the intact rock values). However, since most of the deformations are expected along the joints, this last aspect is less relevant. An example of the string for setting the material property with the PRO MAT command is given below:

```
pro mat 2 dens 2400 bc 16e6 bt 10.7e6 ph 38 pr 0.25 ym 16000e6
```

Where:

- "dens" is the density of the material ( $\text{kg/m}^3$ );

- “bc” is the cohesion
- “bt” is the tensile strength
- “ph” is the friction angle
- “pr” is the Poisson’s ratio;
- “ym” is the Young’s modulus.

Table 6.3 resumes all the material data.

**Tab. 6.3 – Material data used for the overall model.**

<b>Parameter</b>	<b>Continuum region</b>	<b>DEM region</b>
Density	2400 kg/m <sup>3</sup>	2400 kg/m <sup>3</sup>
Cohesion	0.5 MPa	16 MPa
Tensile strength	0.5 MPa	10.7 MPa
Friction angle	38°	38°
Poisson ratio	0.25	0.25
Young’s modulus – rock mass ( $E_{rm}$ )	3000 MPa	16000 MPa

### **6.2.3 Boundary conditions**

3DEC allows different sets of boundary conditions for deformable blocks (load, stress and velocity boundaries are the most common). In this model, for setting the boundary conditions, a velocity boundary condition has been set: the normal direction velocity for deformable blocks is set to 0 (the normal direction is defined as the normal to the block face) through the following string command (one as an example):

```
bound xvel 0 yvel 0 ran y -370.6 -370.5
```

No external in-situ stress has been added to the model; only the gravity is acting on the movement of the blocks and of the external region (not jointed).

## 6.3. Results

Different typologies of results are available in 3DEC: examples are the maximum displacement, maximum and minimum principal stresses ( $\sigma_1$  and  $\sigma_3$ ) and normal or shear stress of the joints. The results show the behaviour of the deformable blocks in the 3D-DEM model. Since that the excavation is simulated with only one stage, all the results are referred to the end of the exploitation.

The results are presented (also regarding Chapter 7) in the overall 3D view of the East slope and in an average middle cross-section which represents a critical area on the stability point of view (most of the jointing is concentrated in that area). The section is represented in Figure 6.9.

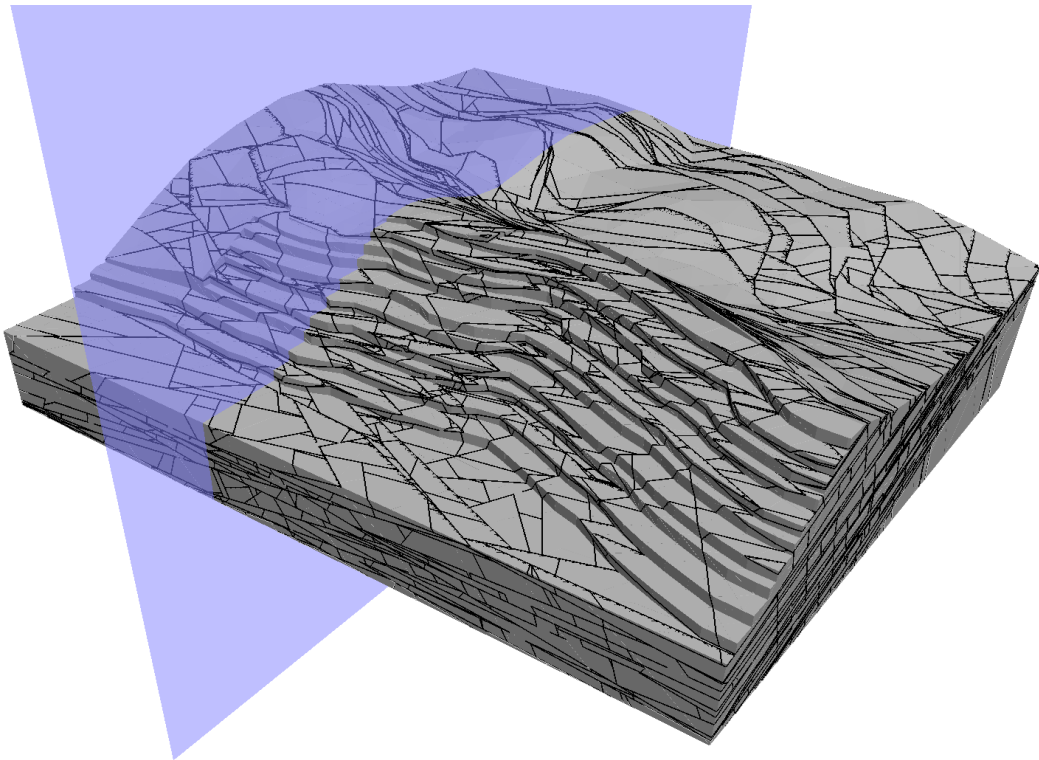


Fig. 6.9 – Cross-section used as a reference section for representing the results.

### 6.3.1 Displacements

The total displacements after the exploitation (Figure 6.10), appear quite reliable with the overall stability of the quarry. The vectors show that the excavation induces a kind of heave effect on the benches, which is quite common in such a large open

pit excavation. The phenomenon is even more marked in the middle crosscut of the slope (Figure 6.11). The maximum displacements are within 50 mm and are limited to some small local blocks that are sliding down from the benches.

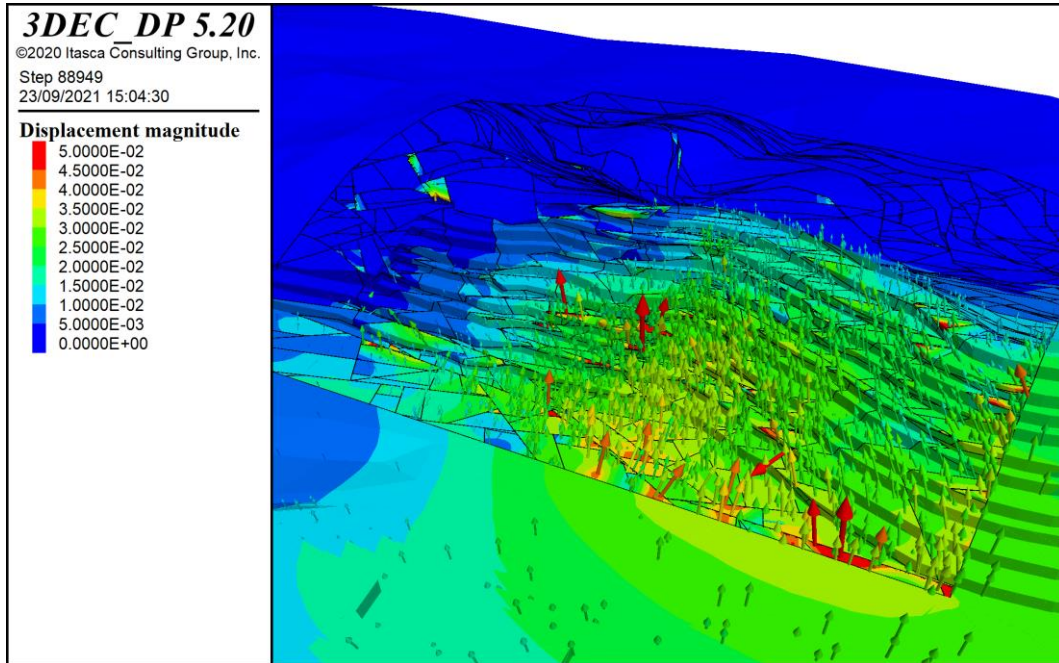


Fig. 6.10 – Total displacements at the end of the exploitation with the vectors.

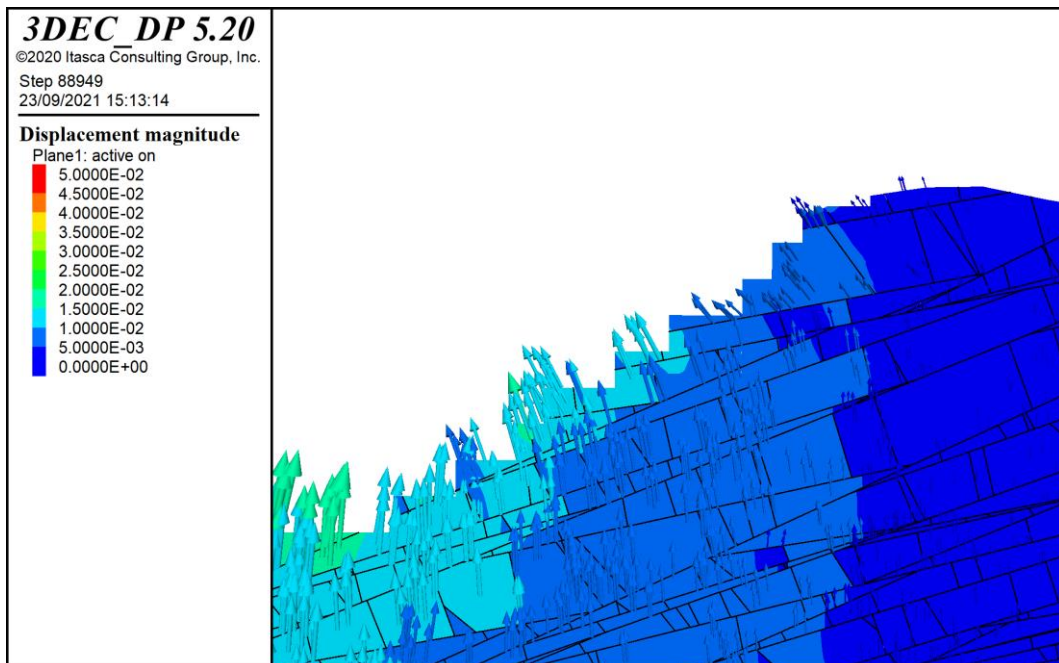


Fig. 6.11 – Total displacements at the end of the exploitation with the vectors in the middle section.

### 6.3.2 Principal stresses

Since that this is a deformable model, the stress induced by the excavation can be plotted. Figure 6.12 shows the maximum principal stress  $\sigma_1$  with a maximum compression stress value of around 10 MPa, while Figure 6.13 shows the minimum principal stress  $\sigma_3$ , with a minimum tensile stress of 0.5 MPa. These values are low which is compatible with the fact that no in-situ stress has been introduced in the model. The peak compressive stress of 10 MPa is limited to the corners of the blocks, where the sliding of the different blocks induce a stress concentration. This is even more marked in Figure 6.14, where the distribution of the maximum principal stress  $\sigma_1$  is represented in the usual middle cross section of the slope. Figure 6.15 shows the minimum principal stress  $\sigma_3$  in the same cross section, and also in this case it is clear that the tensile component is very low.

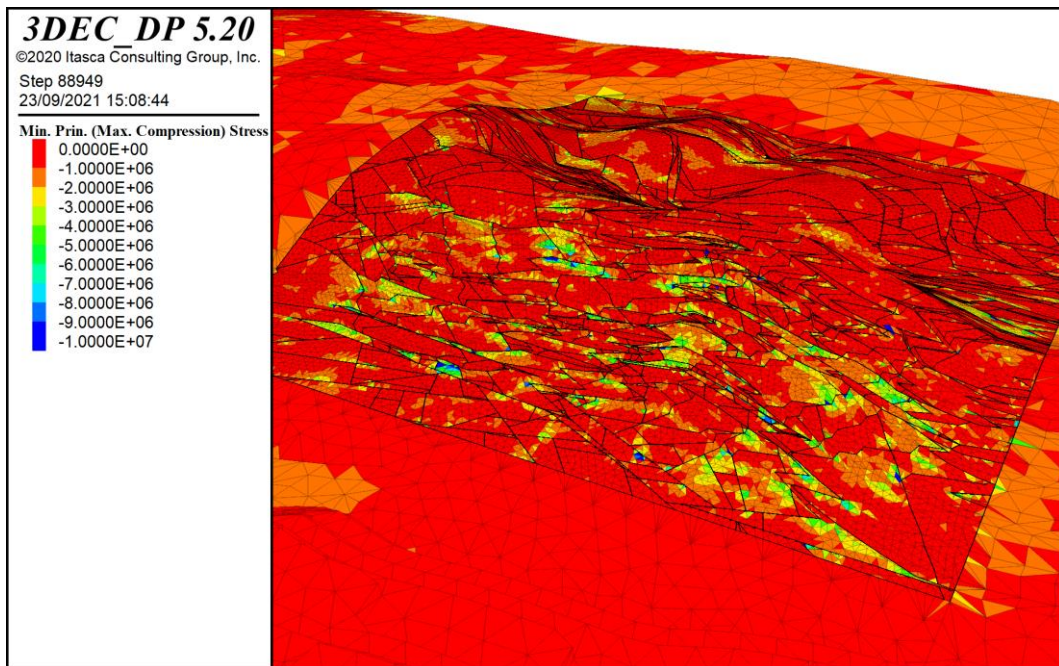


Fig. 6.12 – Maximum compressive stress  $\sigma_1$  in the overall view of the model.

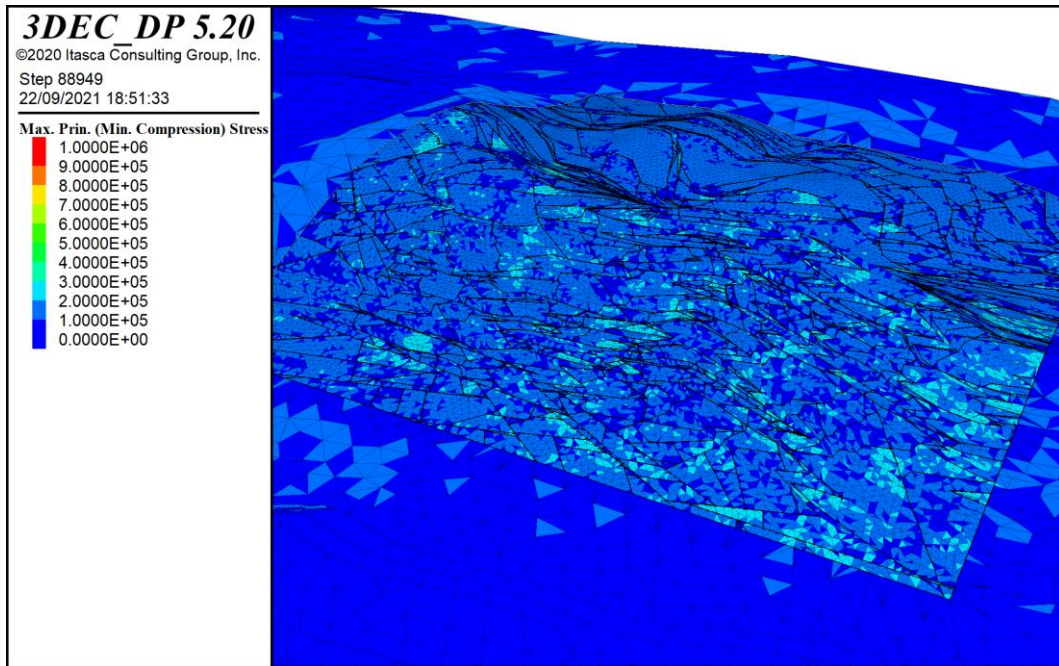


Fig. 6.13 – Minimum tensile stress  $\sigma_3$  in the overall view of the model.

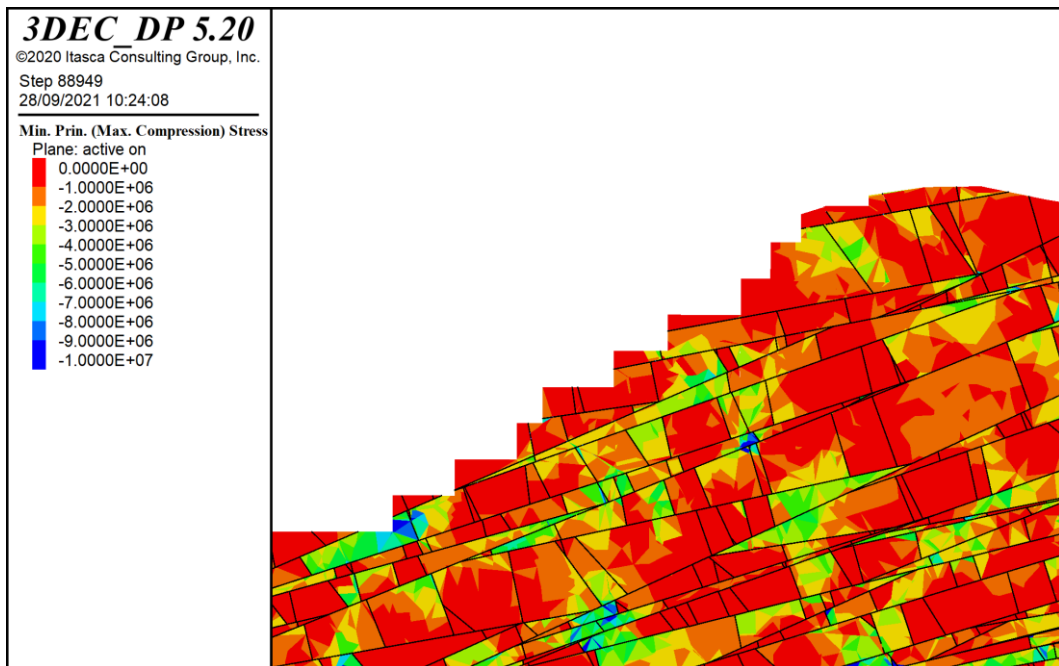


Fig. 6.14 – Maximum compressive stress  $\sigma_1$  in the middle cross section of the slope.

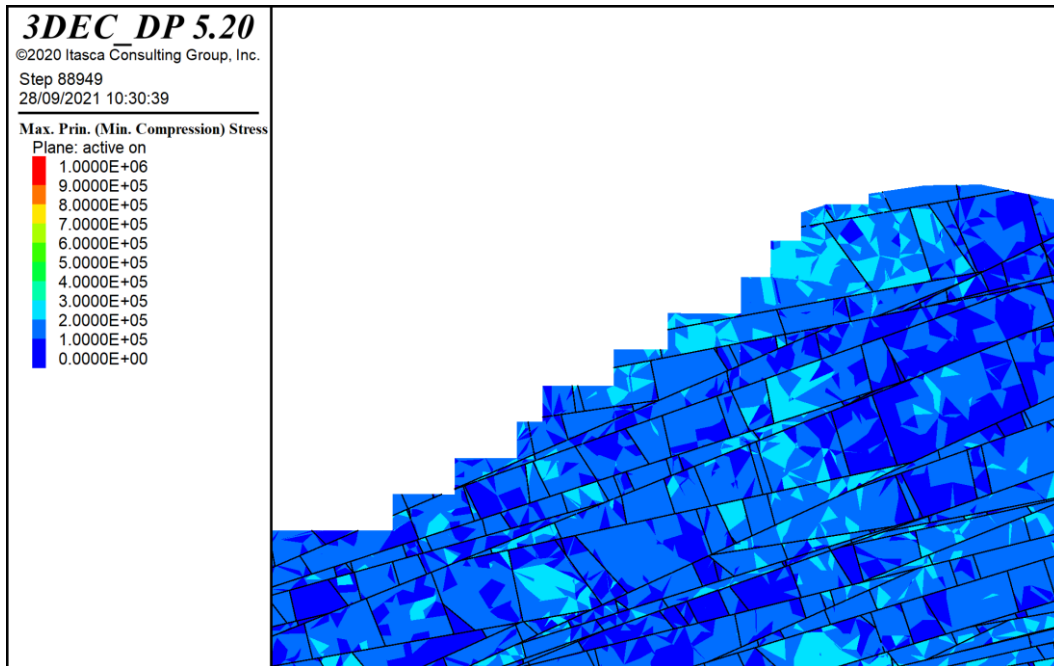


Fig. 6.15 – Minimum tensile stress  $\sigma_3$  in the middle cross section of the slope.

### 6.3.3 Joint stress

The joint stresses (normal and shear) seem to be very low in this model. This is due to the limited sliding of the blocks along the joints. Figure 6.16 shows the results regarding the normal stress, while Figure 6.17 shows the shear stress.

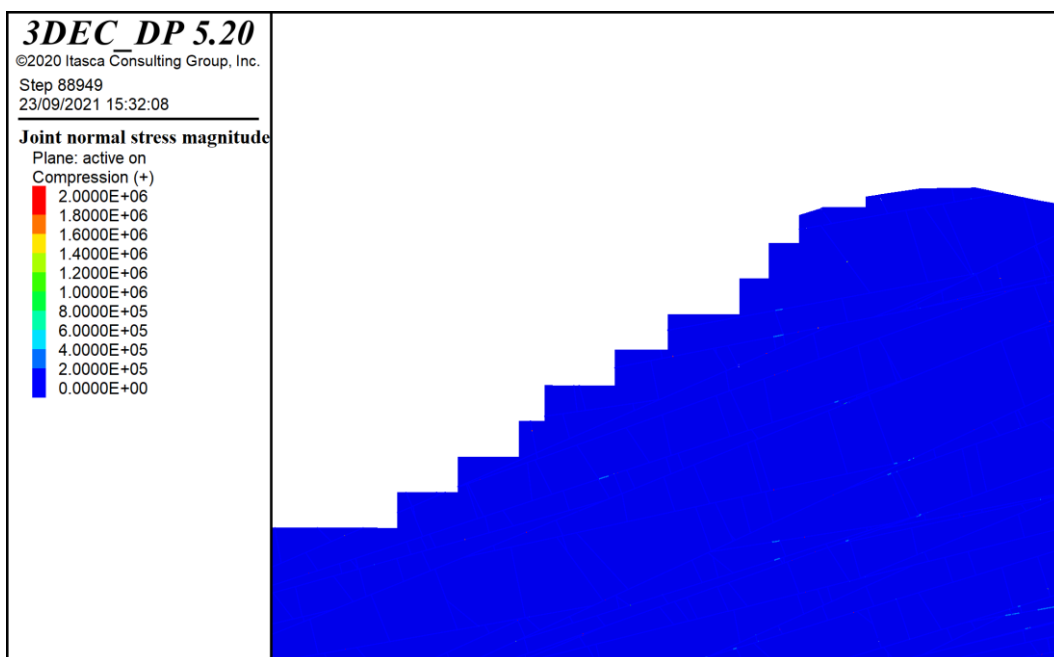


Fig. 6.16 – Joint normal stress in the average cross section of the slope.

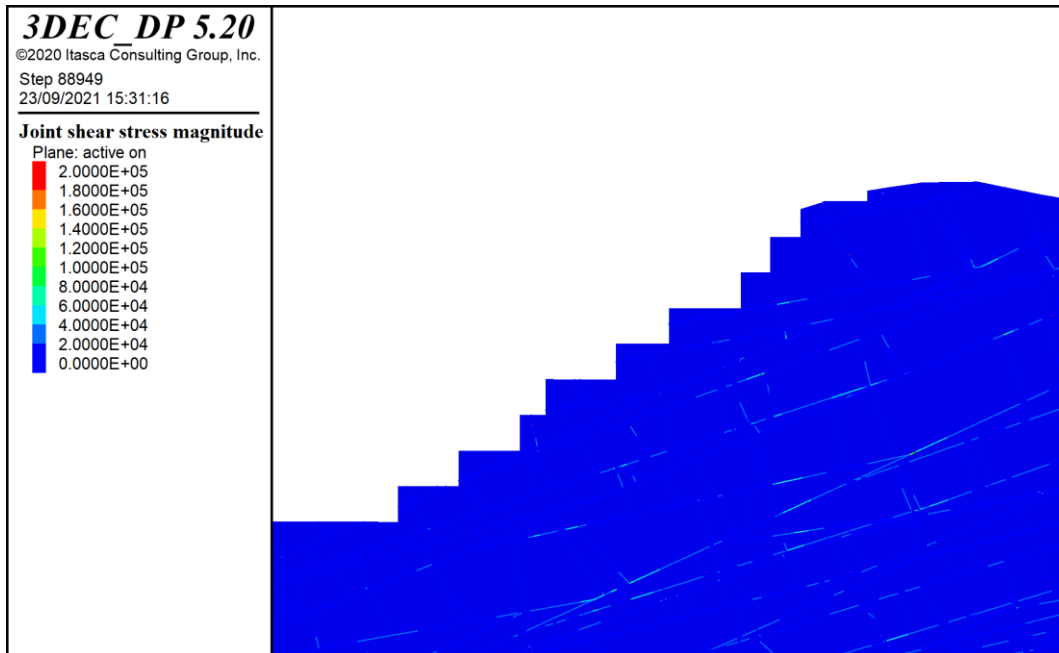


Fig. 6.17 – Joint shear stress in the average cross section of the slope.

#### 6.4. Remarks on the overall discontinuum modelling

The results do not show noticeable criticalities on the overall stability of the Faraona quarry. The displacements are within the expected magnitudes, as already found in the previous studies, especially the one carried out in 2019 (Griffini, 2020). The presence of the block discretization and the induced stress distribution in the rock mass return a heave effect visible in the deformations: this effect is somehow dampening the actual critical failure mechanism of sliding. Moreover, the statistical distribution on the dip and dip direction components of each set, induces the presence of less critical sub-horizontal joints (regarding J1 set). For this reason, the next step of modelling (back-analysis) has been carried out by considering the most critical condition for this set, which is the highest possible dip. This aspect is detailed in Section 7.2.1.

Regarding the stress distribution itself, the movements of the blocks induce the presence of stress peaks around the corners, but with quite low values (maximum 10 MPa). The stress along the joints (normal and shear components) are also very

low, and this is especially due to the small deformations occurring during the excavation with this type of simulation.

All these aspects are relevant to consider the need of producing a more accurate and detailed model of the potentially unstable area, by using rigid blocks and the most critical dip in the J1 set.

## **7. BACK ANALYSIS FOR THE EAST FACE**

The results obtained with the overall 3D-DEM model provide a first validation in the set of rock mass parameters from the 2019 characterization. Nevertheless, it is necessary to deepen the study in terms of the stability analysis of the East face of the Faraona quarry. Example of rock mechanics studies for slope stability conditions in the quarry basin are suggested by Deangeli et al. (1996): a back analysis is useful to better understand the failure mechanism of the slope. Also, Coggan et. al. (2007) used a similar methodology.

Using the same approach, this part of the thesis is devoted to a detailed 3D-DEM model with a back analysis of the main parameters that influence the stability of the rock mass. Specifically, with an iterative method, by setting worse and worse values of cohesion and friction angle of the material, the numerical modelling provides some representative results of the instable scenarios that occurred during the exploitation.

### **7.1. Model preparation**

#### **7.1.1 Geometry**

In order to create a denser joint pattern for the detailed model used in the back-analysis, the external part has been removed to lighten the calculation. Moreover, rigid blocks have been considered, so that the model is lighter also because there is no possibility of including stress distribution (Figure 7.1). The individual blocks are set as rigid bodies: in case of low stresses and negligible internal deformations, this approximation can be adopted as suggested by Jing (2007). In fact, in this case, most of the deformations occur along the joints, thus the block deformability plays a minor role, that can be neglected.

The number of potentially sliding blocks is therefore much larger than in the previous model; in this way, it would be possible to simulate more effectively what occurs in the reality with small local instability (Section 4.3.4).

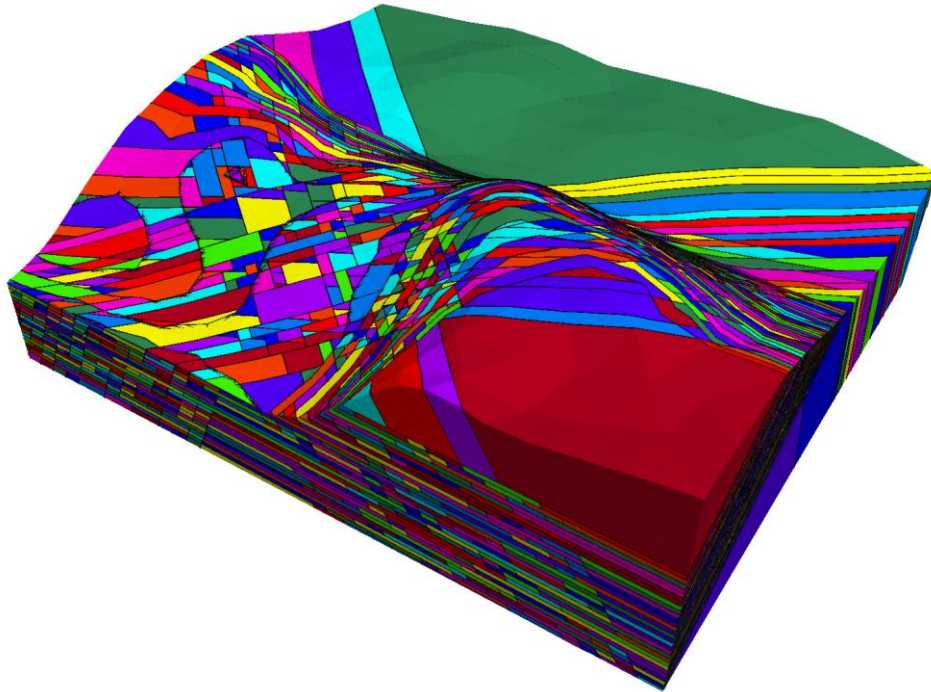


Fig. 7.1 – Detailed 3D-DEM model at the initial state (before exploitation).

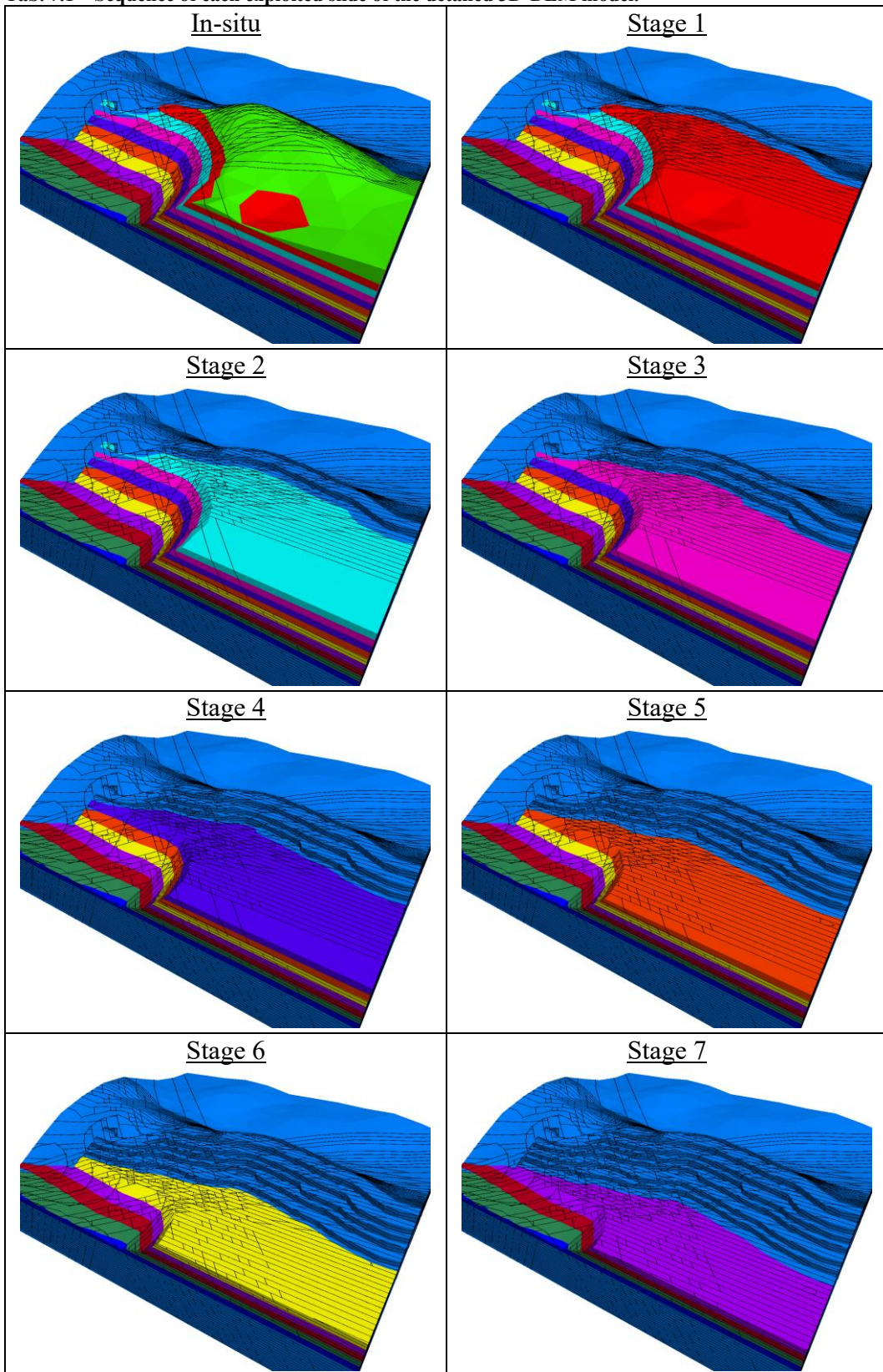
### **7.1.2 Meshing**

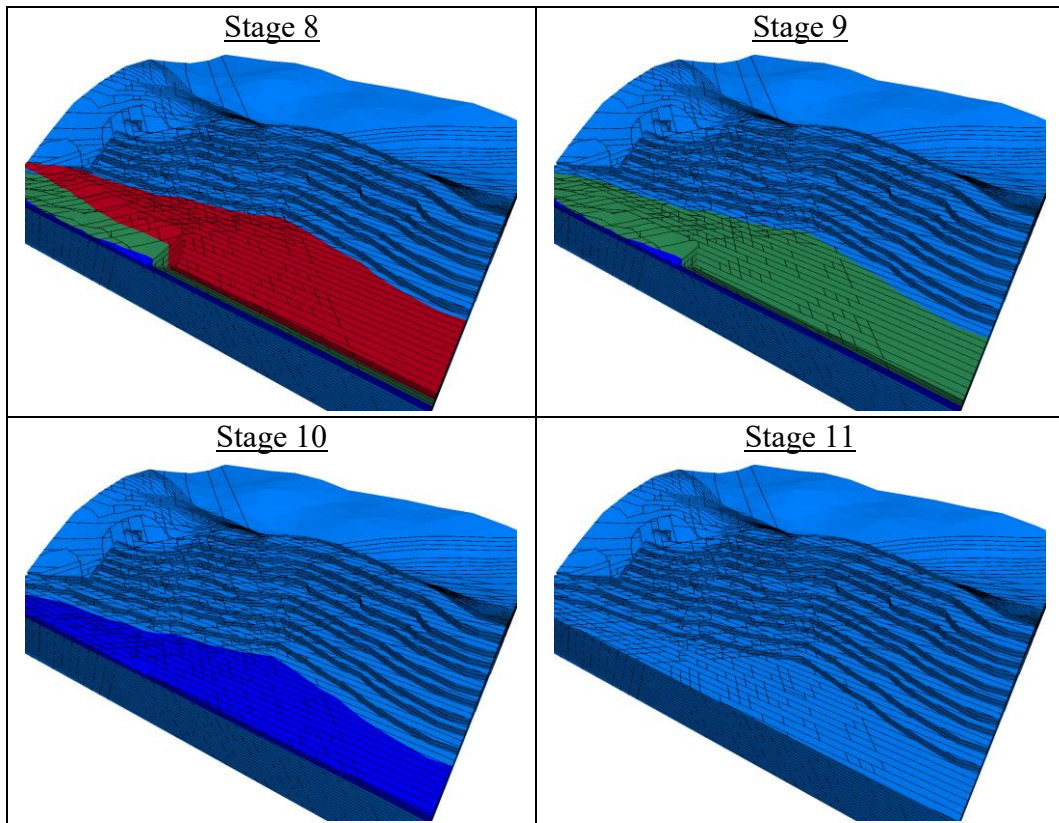
Rigid blocks have no mesh as the deformations occur only along the joints and the blocks cannot handle internal deformations and stress fields.

### **7.1.3 Staging**

For the detailed model, the exploitation is simulated through 11 different 5 m thick slices, in order to verify the stability at each deepening (Table 7.1). Each stage consists of a 5 m thick slice.

**Tab. 7.1 – Sequence of each exploited slide of the detailed 3D-DEM model.**





## 7.2. Input data

Most of the input data coincide with the ones used for the detailed model (Section 6.2). Based on the considerations coming from the previous results (Section 6.4), some data have been adjusted in order to investigate more in detail some aspects that were not evident from the overall model due to the limitations already described.

### 7.2.1 Joint properties

As already said, in this model the parameters coming from the 2019 rock mass characterization have been used, but with a more conservative approach. As a matter of fact, the large deviation on the dip of the main critical joint set (J1, with a dip of  $18^{\circ} \pm 9^{\circ}$ ) allowed the formation of sub-horizontal planes where sliding cannot occur. For this reason, it has been decided to consider the maximum possible dip value of  $27^{\circ}$ . Also, as the model is lighter, the spacing can be decreased in order to

recreate a more discretized pattern in the area close to the slope, avoiding useless joints in the deeper region. Table 7.2 resumes all the joint sets geometrical data for the detailed model.

**Table 7.2 – Joint sets geometrical data for the detailed model.**

ID set	Dip (°)	Dip direction (°)	Spacing (m)	Persistence
1	27	268	2	1
2	75	50	5	0.6
3	68	135	5	0.4
4	73	70	5	0.4

Using rigid blocks, the code allows to add the same parameters for the joints, in terms of normal and shear stiffness, friction angle, cohesion. For this detailed model the initial joint parameters are the same as the ones used in the overall model (Table 6.2). Figure 7.2 represents a comparison between the overall model and the detailed model: in the second model, more joint sets and therefore more blocks are visible.

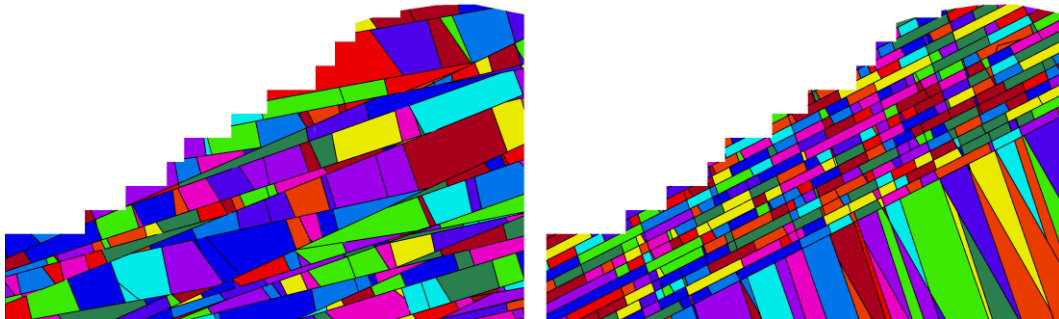


**Fig. 7.2 –Comparison between jointing of the overall model (left) and detailed model (right).**

### 7.2.2 Material properties

In this detailed model, the analysis is focused on the joints; compared to the previous model, the constitutive behaviour is considered as elastic and therefore the blocks are characterized by a density, Young’s modulus and Poisson’s ratio that are the same of the ones used in the overall model.

### 7.2.3 Boundary conditions

In the rigid models, the command BOUND is not working, thus the easiest way is to include an external bounding block that is then fixed through the command FIX, in order to properly constrain the internal blocks (Figure 7.3). The interface between the two regions has the same properties of the J1 set.

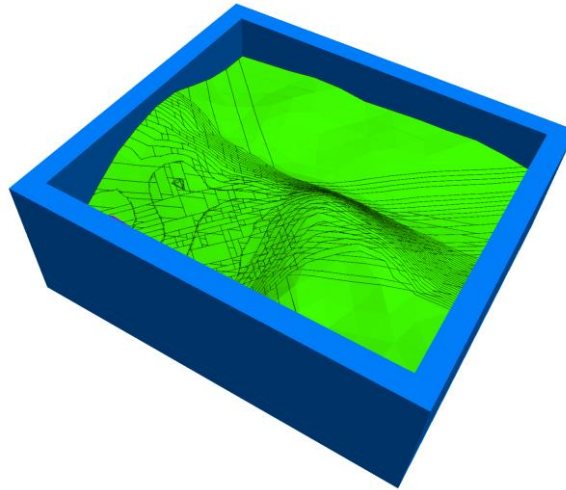


Fig. 7.3 – Fixed external block (blue) used to constrain the internal model (green).

### 7.2.4 Back-analysis data

In order to proceed with the back-analysis, the joint parameters have been weakened after the first excavation stages showed in Table 7.1. In particular, only the J1 set has been considered for this back-analysis, as it represents the most critical one. First, the cohesion has been reduced to zero (simulating weathering or weakening due to water flowing through the cracks), then the friction angle has been reduced by 1° step to a minimum of 20° if there will not be any collapse before that value. In that case, the iterative process will stop. In Table 7.3 the joint J1 parameters of the iterative process are listed, starting from Stage 11 which is the last of the “regular” detailed model.

Table 7.3 – Joint sets geometrical data for the detailed model.

Stage	Friction angle	Cohesion
11	28°	0.05 MPa
12	28°	0 MPa

13	27°	0 MPa
...	...	0 MPa
20	20°	0 MPa

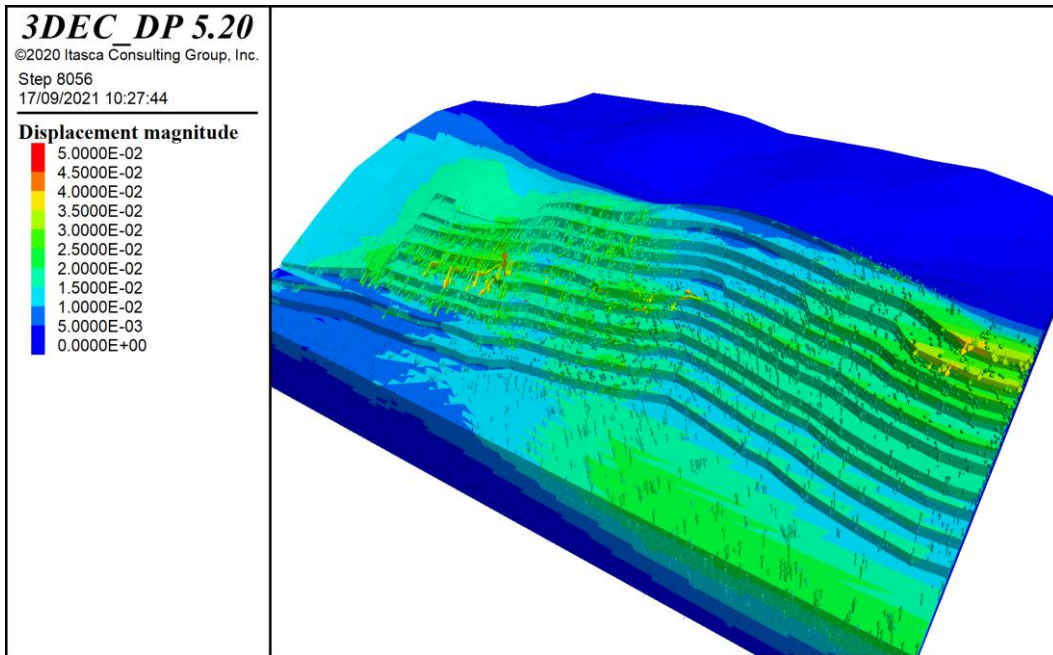
### 7.3. Results

This model can provide a large range of results which can help to assess the behaviour of the rock mass after the exploitation of the quarry, proceeding downwards according to smaller slices (5 m). The most important result to assess the stability of the Faraona quarry is the magnitude and direction of the blocks displacement, in order to verify both the local and global stability of the slopes.

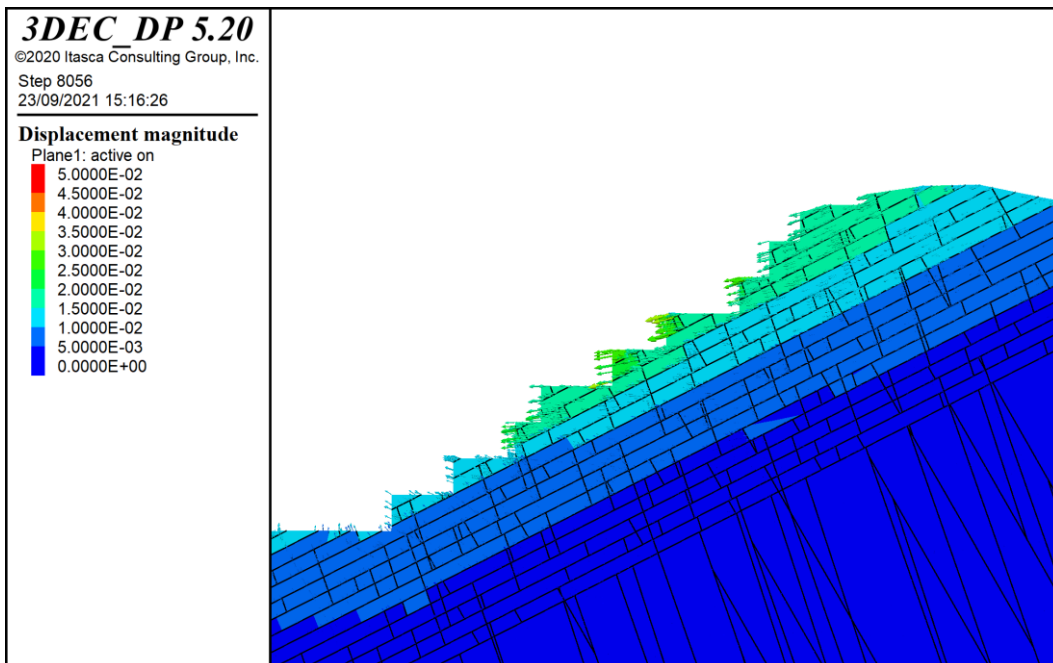
Regarding the modelling after Stage 11, which consists in the back-analysis part, the iterative process stopped at Stage 17 (cohesion 0 MPa, friction angle 23°) due to the collapse of the whole slope.

#### 7.3.1 Displacements

Considering the “regular” part of the model (up to Stage 11), the results return a scenario similar to the overall model, without having the heave effect. This is due to the fact that there is no stress field affecting the block movements, that are in this case just caused by the gravity. Therefore, the deformations recorded by the model are caused by the sliding of the blocks (as it actually occurs). Figure 7.4 and Figure 7.5 show the total displacements at the end of the exploitation (Stage 11) respectively in the 3D overall view and the middle cross section. The maximum magnitude of displacement is 41 mm. Table 7.4 collects all the pictures of the displacements and their directions, while Figure 7.6 resumes the magnitude of the displacements after each excavation stage. The maximum displacement at the end of the exploitation is aligned with the value obtained by the 2019 model: in this case, it is slightly higher than 40 mm at the lowest excavation level (285 m).

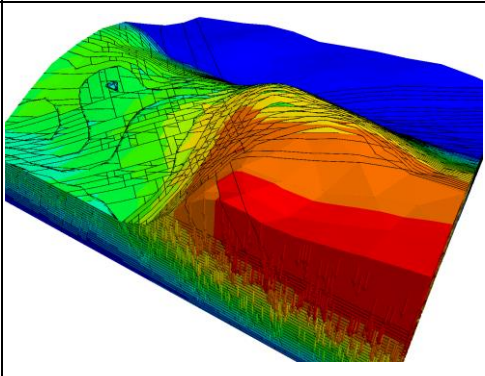
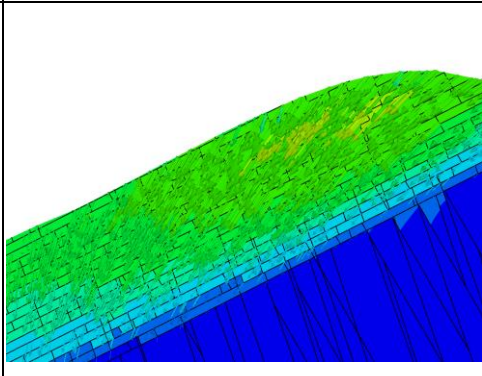
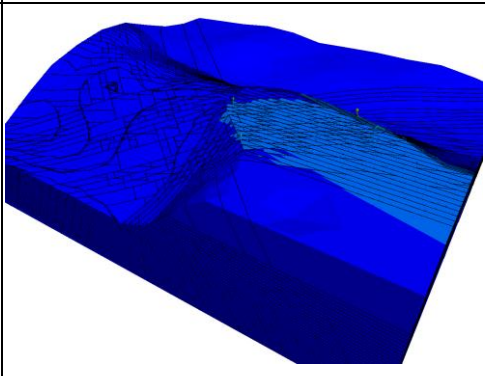
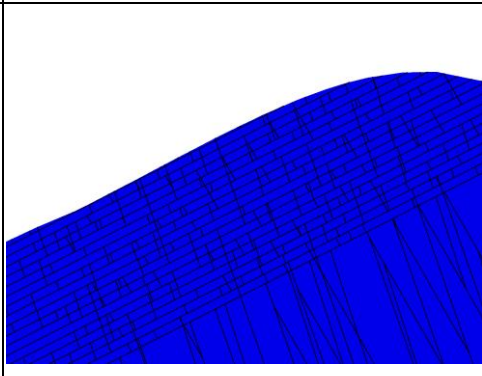
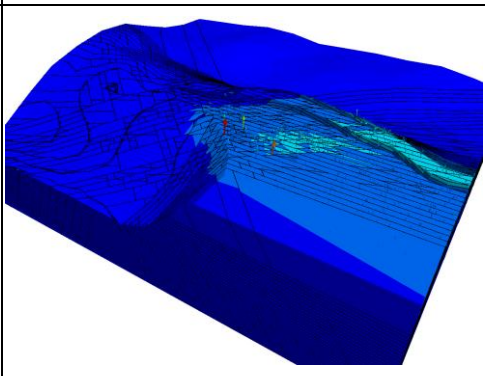
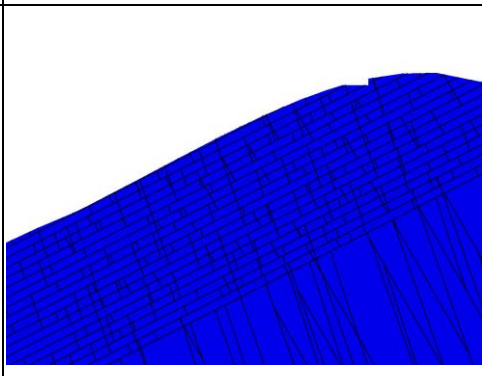
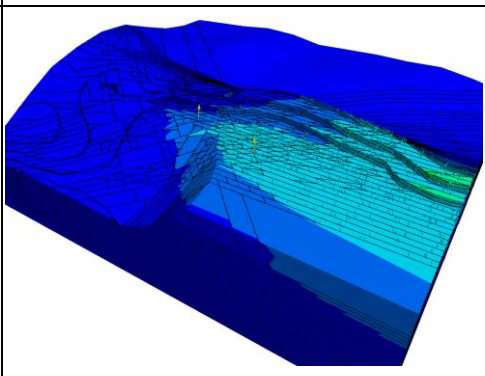
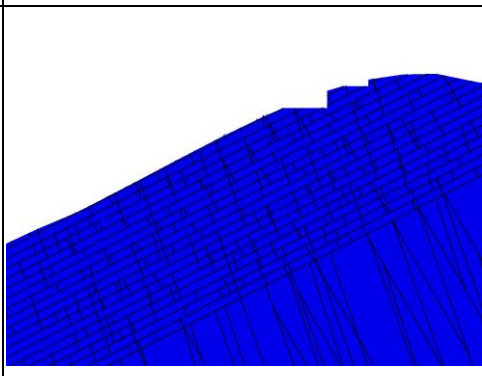


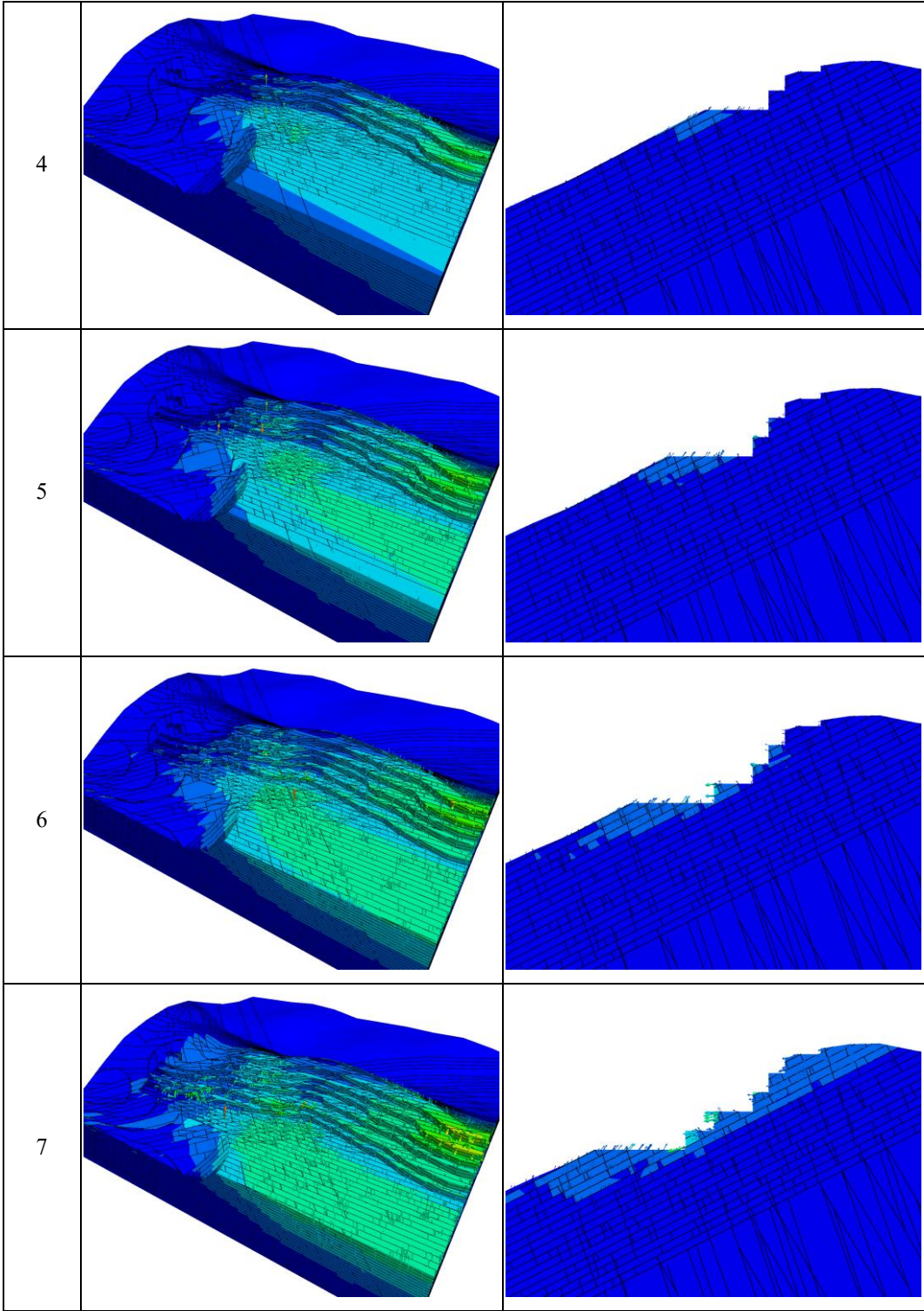
**Fig. 7.4 – Fixed external block (blue) used to constrain the internal model (green); 3D overall view.**

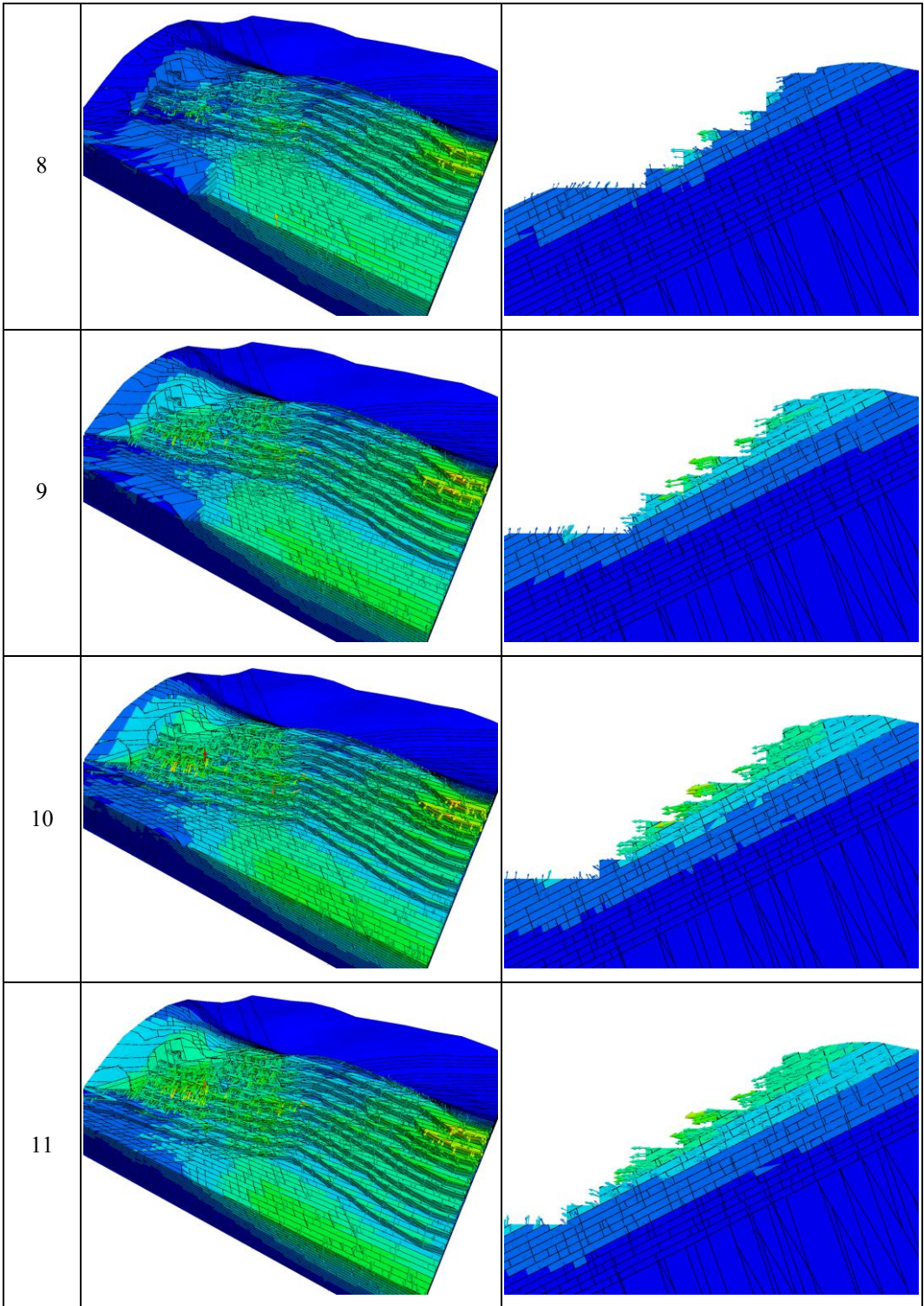


**Fig. 7.5 – Fixed external block (blue) used to constrain the internal model (green); middle cross section.**

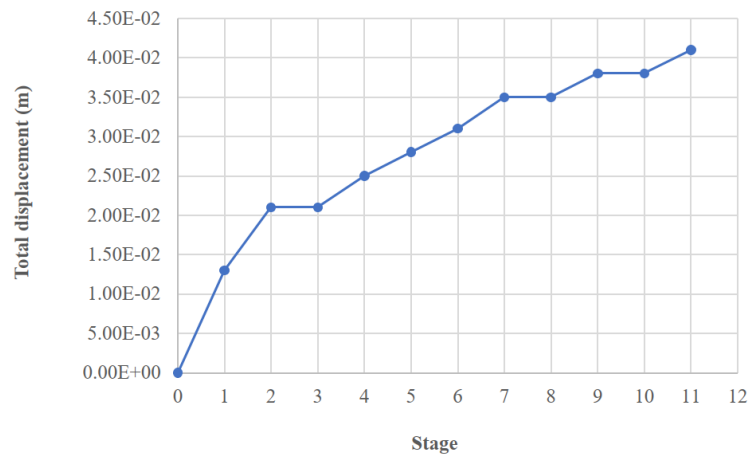
**Table 7.4 – Total displacements with vectors after each excavation stages in the 2 views. The in-situ displacements are not reset, while from Stage 1 the in-situ displacement is removed. The legend is the same as for Figure 7.4, both for the solids and the vectors.**

Stage	3D overall view	Cross section
IS		
1		
2		
3		





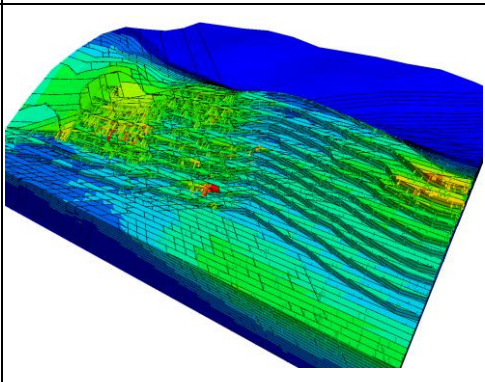
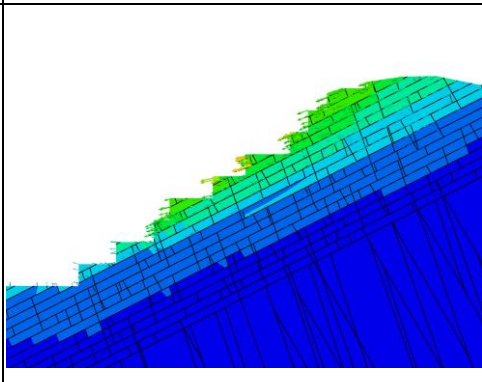
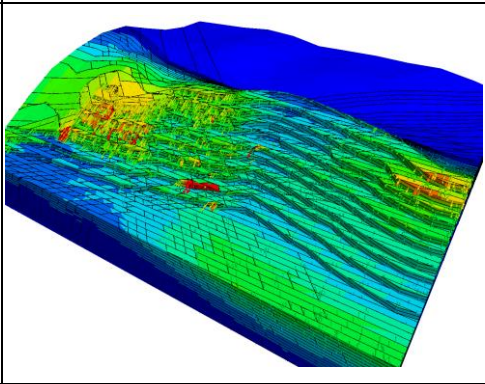
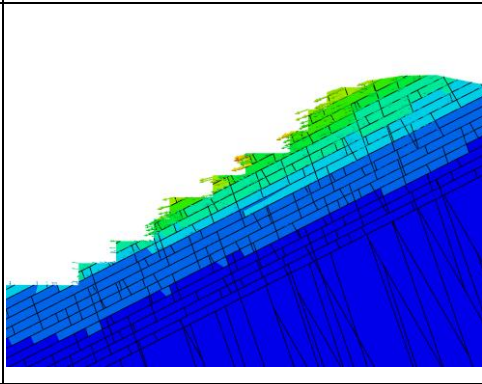
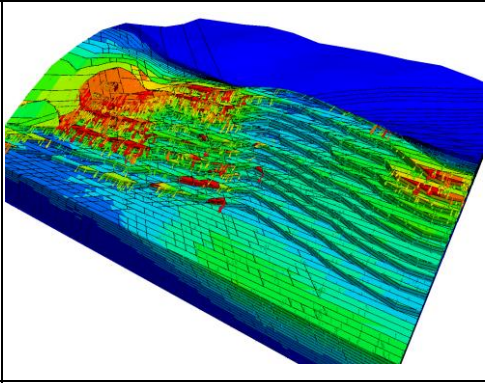
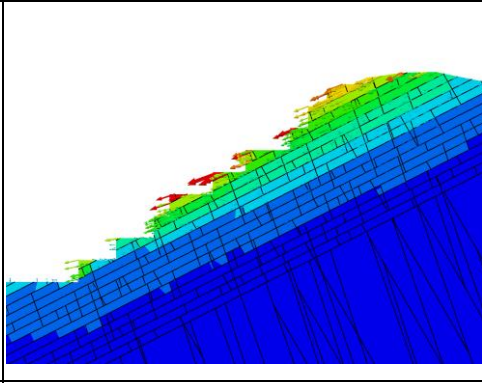
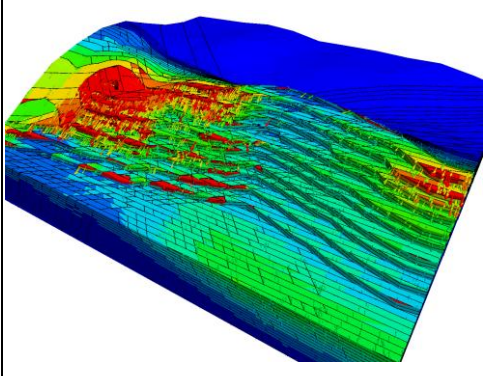
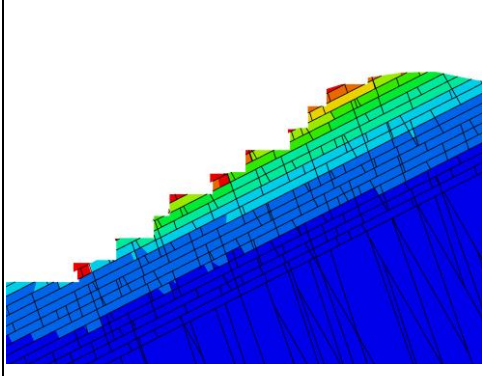
Stage	Displacement (m)
In-situ	0.00E+00
Stage 1	1.30E-02
Stage 2	2.10E-02
Stage 3	2.10E-02
Stage 4	2.50E-02
Stage 5	2.80E-02
Stage 6	3.10E-02
Stage 7	3.50E-02
Stage 8	3.50E-02
Stage 9	3.80E-02
Stage 10	3.80E-02
Stage 11	4.10E-02



**Fig. 7.6 – Magnitude of the maximum total displacements after each stage of the exploitation.**

As for the back-analysis, the excavation appears stable until Stage 13 ( $\phi=27^\circ$  and  $c=0$  MPa), with a maximum displacement of 76 mm. In Stage 14, several blocks start to move, especially in the upper part of the bench, reaching a maximum displacement of 111 mm. This value appears high in terms of benches stability and seems to describe effectively the present situation at the Faraona quarry, with several small edge blocks sliding down by the formation of tension cracks (e.g. Figure 4.9 and Figure 4.10). With the next 2 steps (Stage 15 and 16), the total displacement assumes a pseudo-exponential trend respect to the previous stages and this means that the collapse is imminent. The last iteration is Stage 17, in which the friction angle is  $23^\circ$ , when the model collapses. Table 7.5 collects all the results of the back-analysis in both the 3D overall view and cross section view, where the increasing number of unstable blocks with the gradual reduction of the strength parameters of the joints can be appreciated. This is even more visible in Figure 7.7, where the magnitudes of the maximum displacement are plotted into a graph and where the pseudo-exponential trend of the displacement is easily identifiable.

**Table 7.5 – Total displacements in the back-analysis stages in the 2 views. The legend is the same as for Figure 7.4. From Stage 15 in the cross section view and in Stage 17 for the 3D overall view, vectors are not included due to large deformations visible plainly.**

Stage	3D overall view	Cross section view
12		
13		
14		
15		

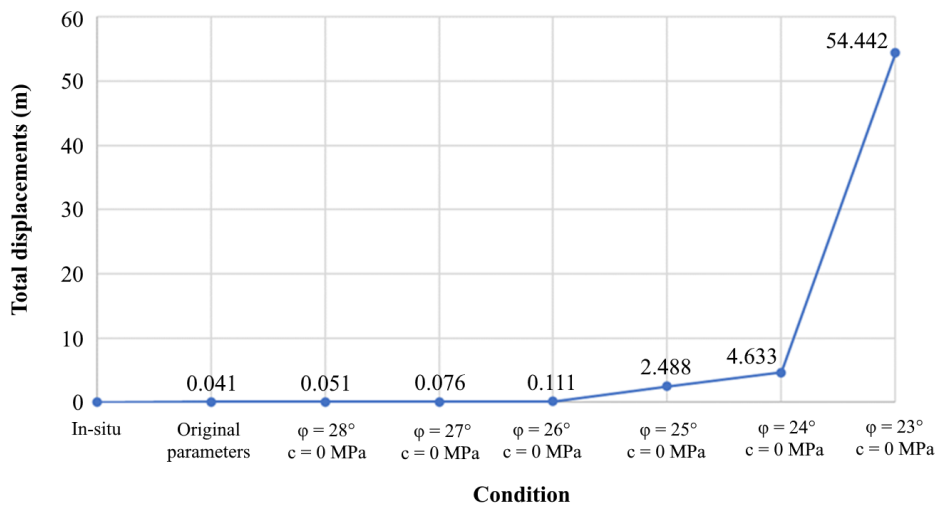
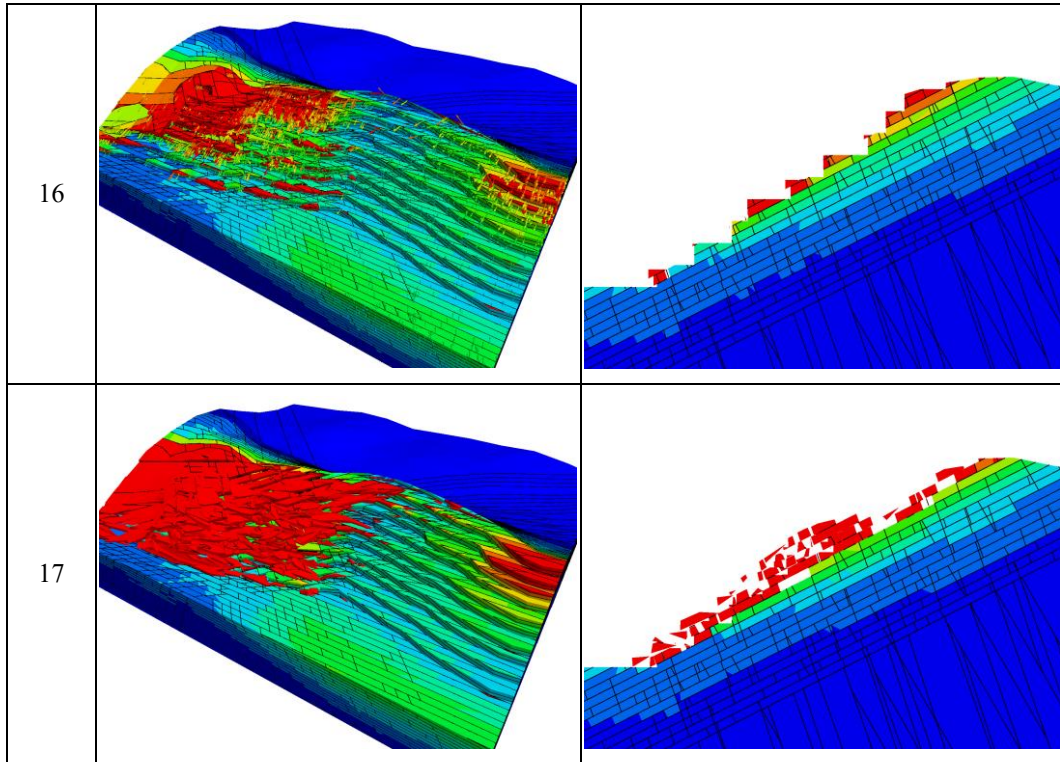


Fig. 7.7 – Magnitude of the maximum total displacements in the back-analysis.

### 7.3.2 Joint stress

Compared to Section 6.3, the joint stresses (normal and shear) appear higher than in the previous model: the presence of rigid blocks and the absence of in-situ stress determine a more evident sliding of the blocks along the joints with a higher stress

concentration along them. Figure 7.8 shows the results as for the normal stress, whereas Figure 7.9 shows the shear stress.

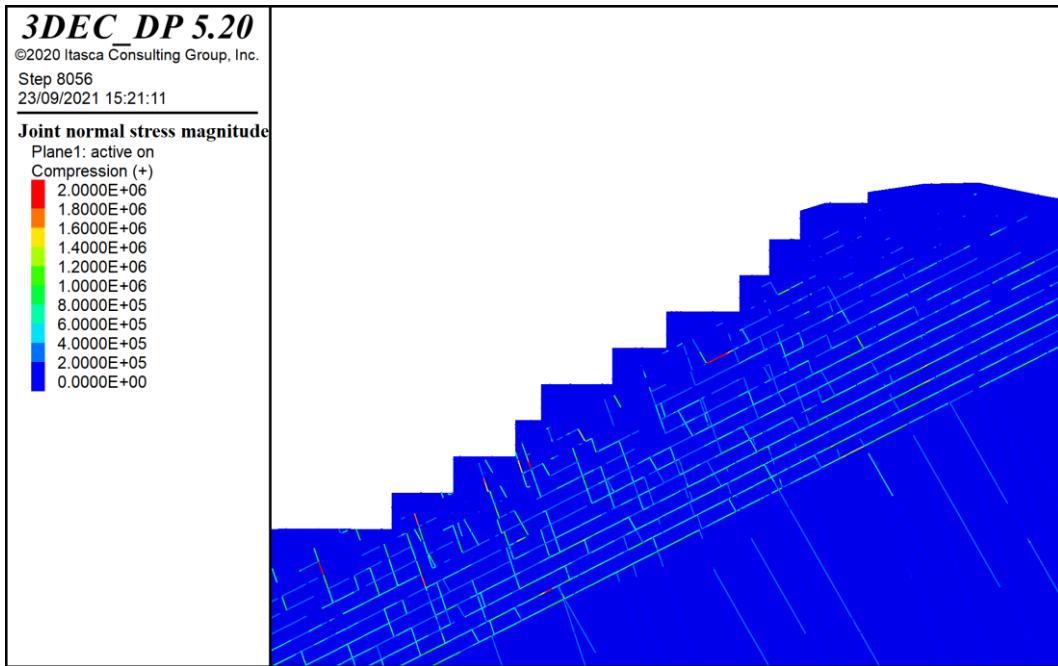


Fig. 7.8 – Joint normal stress in the average cross section of the slope.

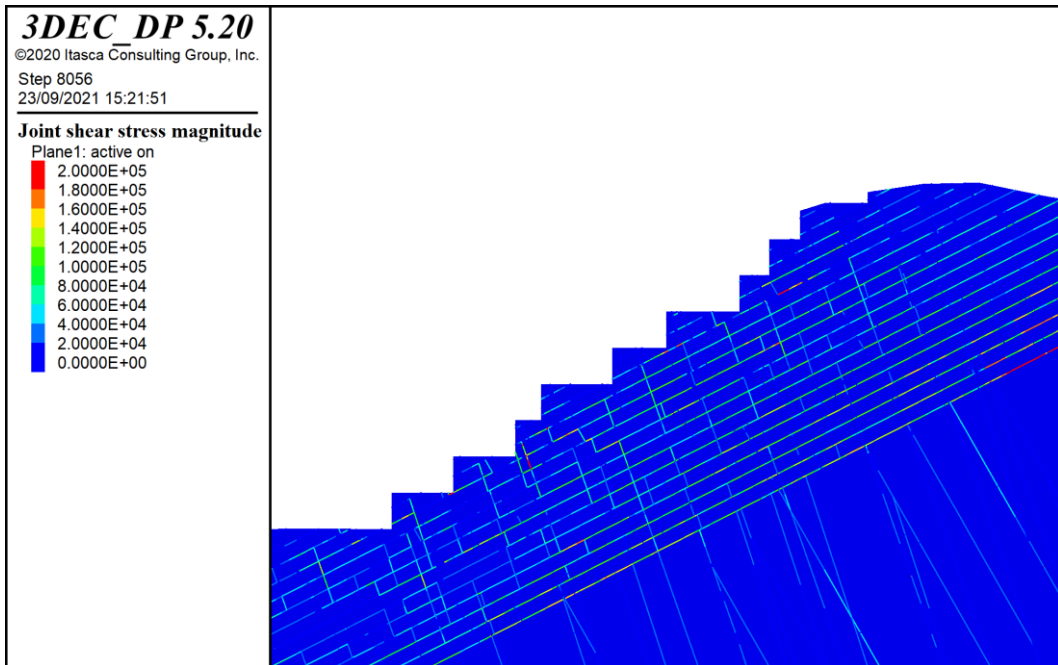


Fig. 7.9 – Joint shear stress in the average cross section of the slope.

#### **7.4. Remarks on the detailed discontinuum modelling and back-analysis**

The detailed model returned a good approximation of what is occurring in the reality, with the principal failure mechanisms arising due to sliding. The results in terms of displacements describe much better the situation, especially in presence of the reduced stage size (5 m thick); this helps a lot on understanding the specific failure mechanisms, which might occur only from the shallow blocks at the slope corners. The joint stress in this case is higher than in the previous overall model, due to larger deformations in the slope (block sliding). Therefore, the overall stability of the Faraona quarry is verified also by this model.

The back-analysis subsequently carried out starting from the final stage of the detailed model gave very good indications on the possible additional failure mechanisms by reducing more and more the strength parameters of the joints for reaching the collapse (borderline condition). The overall stability is guaranteed even when the cohesion is reduced to zero, which might occur in case on intense rainfall or other extreme events. The limit friction angle guaranteeing the stability is  $27^\circ$ , while lower values trigger more local instabilities up to the failure which occurs with a friction angle of  $23^\circ$ .

## 8. CONCLUSIONS

During the exploitation of the open pit Faraona quarry, various phenomena of instability occurred, which required in-depth investigations on the material. Starting from the existing rock mass characterizations and stability analyses, this work identifies some critical issues respect to the previous numerical modelling and develops a three-dimensional approach.

As a first approach, a continuous model with Midas GTS NX code was created to evaluate the global stress-strain behaviour of the quarry, considering some simplifications adopted in order to obtain a manageable model (i.e. the slopes were considered vertical with a height of 5 m, different levels of discretization, only 2 stages have been considered: in-situ stage and residual slopes). As for the input data, a back-analysis was carried out to verify the most effective datasets considering both 2011 and 2019 rock mass characterizations. The FEM results confirm the 2019 parameters as the most representative, with a maximum displacement of 45 mm. The equivalent plastic strains and the plastic state of the material (yielded zones) underline the inadequacy of the 2011 parameters due to an unrealistic extension of the yielded and unstable zones.

After this first stage, a discontinuum model of the quarry was prepared using the Itasca 3DEC code, to take into account the presence of the joints. Due to the large size of the model, the analysis was focused by setting the presence of the joints in the East zone (the unstable face): the model follows a hybrid DEM-FEM approach, where the DEM region is highly fractured and the FEM region is modelled as a continuum equivalent representation. The elements are discretized, like tetrahedra, and each block is deformable and the same meshing, staging and input data (2019) conditions of the previous model were used. In this case, the maximum displacements are within 50 mm and refer to small local blocks that slide off the benches. The maximum compression stress is 10 MPa, limited to the edges of the blocks. The rock mass parameters determine the formation of some sub-horizontal joints (J1) due to the statistical distribution of dip and dip direction.

The last model is a detailed DEM of the East wall of the Faraona quarry, where sliding phenomena are localized. The geometry is focused on setting a denser joint pattern and the blocks are rigid: with this method the deformations occur along the joints. Furthermore, the staging is more detailed: 11 stages describe the evolution of the exploitation in order to obtain a more realistic scenario. The input data are chosen with a conservative approach (i.e. higher dip value for J1) and the back analysis is performed by reducing the cohesion and friction angle values. The maximum displacements are compatible with the overall FEM model, without the heave effect, that affects the 2 previous models. The deformations are caused by the block sliding and the maximum value is 41 mm (less than the overall FEM model). Joint stress appears greater due to the different type of blocks (rigid). With the back-analysis, by reducing the strength parameters of the joints, a simulation of intense rainfalls or extreme events can be simulated. Stability is guaranteed with a friction angle of  $27^\circ$ , whereas some instabilities are evident with lower values.

Numerical modelling of a real case presents a challenge in term of geometry, meshing, staging, input data, boundary conditions and simplification of the problem. The comparison between different models can be used in the design phase but also in case of problems during the exploitation. Applying a 3D model allows to represent the reality more accurately, but it requires a greater level of information in terms of parameters and geometry and a greater effort in terms of model preparation. The results here presented show the effectiveness of using this powerful tool for assessing the stability of the open pit quarry analysed, as it can return a much more reliable and clearer picture of the possible instabilities and criticalities that might occur during the exploitation of the slopes.

## REFERENCES

- Altair (2011). Piano di coltivazione e verifiche di stabilità per Holcim Italia SpA. Rapporto n. 009a-09-Rev.3
- Barton, N.R. (1972). A model study of rock-joint deformation, *Int. J. Rock Mech. Min. Sci.*, Vol. 9, 579-602.
- Coletti G., Vezzoli G., Di Capua A. & Basso D. (2016). Reconstruction of a lost carbonate factory based on its biogenic detritus (Ternate-Travedona Formation and Gonfolite Lombarda Group - Northern Italy). *Riv. It. Paleontol. Strat.* 122(3): 1-22
- Coggan J.S., Pine R.J., Styles T.D., Stead D. (2007). Application of Hybrid Finite/Discrete Element Modelling for Back-Analysis of Rock Slope Failure Mechanisms. *Slope Stability 2007* - Y. Potvin (ed).
- Cruden, D.M. (1991). A simple definition of a landslide. *Bulletin of the International Association of Engineering Geology* 43, 27–29
- Deangeli C., Del Greco O., Ferrero A.M. & Pancotti G. (1996). Rock mechanics studies to improve intact rock block exploitation and slope stability conditions in a quarry basin, Paper presented at the ISRM International Symposium - EUROCK 96, Turin - Italy.
- Gattinoni P., Pizzarotti E., Scattolini E. & Scesi L. (2004). Stabilità dei pendii e dei fronti di scavo in roccia, Eds Edizioni Pei srl
- Goodman R.E. (1989). *Introduction to Rock Mechanics*, John Wiley & Sons, New York
- Griffini L. (2018). Polo 6 - ATE C2 “Cava Faraona” - Travedona-Monate (VA) - Monitoraggio periodico condizioni di stabilità dei fronti in fase di coltivazione - Rapporto di sintesi Dicembre 2018

- Griffini L. (2020). Polo 6 - ATE C2 “Cava Faraona” - Travedona-Monate (VA) Sistemazione Frana Fronte Est - Piano di messa in sicurezza
- Hoek E. (2007). Practical Rock Engineering, Rocscience, Vancouver
- Hoek, E. & Bray, J.W. (1981). Rock Slope Engineering. Revised 3rd Edition, The Institution of Mining and Metallurgy, London, 341-351
- Hoek, E. & Brown, E.T. (2018). The Hoek-Brown failure criterion and GSI - 2018 edition, Journal of Rock Mechanics and Geotechnical Engineering 11 (3): 445-463
- Holcim Italia SpA (2012). Progetto attuativo ATEc2 – Aut. N.1358 del 04.04.2012
- Hudson J. A., Harrison J. P. (1997). Engineering Rock Mechanics - An Introduction to the Principles. Elsevier Science Publishers
- Jing L., (2003). A review of techniques, advances and outstanding issues in numerical modelling for rock mechanics and rock engineering, International Journal of Rock Mechanics and Mining Sciences, Volume 40, Issue 3, 2003, Pages 283-353
- Jing L., (2007). Fundamentals of Discrete Element Methods for rock engineering theory and applications, Lanru Jing, Ove Stephansson (Developments in Geotechnical Engineering, Vol. 85). Elsevier Science Publishers
- Itasca (2020). Itasca 3DEC Online Manual (version 5.2) Itasca Consulting Group, Inc
- Lancellotta R. (2008). Geotechnical Engineering, Taylor and Francis
- Lorig L., Stacey P. & Read J. (2009). Slope design methods. In: Guidelines for open pit slope design. Eds. Read J. & Stacey P. CRC Press/Balkema.
- Mancin, N. (2001). La Formazione di Ternate (Italia Settentrionale): contenuto micropaleontologico e caratterizzazione petrografica). Atti Ticinensi di Scienze della Terra. 42. 37-46.

Midas (2019). Midas GTS NX Online Manual (version 1.1 September 2019)  
MIDAS Information Technology Co., Ltd

Varese quarry plan (2004). Piano Cave della Provincia di Varese - Relazione  
tecnica

Varese quarry plan (2018). Scheda e Cartografia dell'ATEc2 - Proposta di modifica  
del Piano cave della Provincia di Varese relativa all'ATEc2 nei Comuni di  
Travedona Monate e Ternate. Ottemperanza alla sentenza TAR n. 5015/2009  
passata in giudicato, Provincia di Varese

## **ACKNOWLEDGEMENTS**

My gratitude goes to Dr. Marcelino Linarez Gonzales and Holcim Italia S.p.A. for allowing the possibility to develop my work on the instability analysis of the Faraona quarry and for having provided me fundamental data for my project.

I would like to thank my supervisor Prof. Marilena Cardu for all her help and advice with this thesis. The passion that she puts into her teaching made me understand that the choice to resume my studies was right for me.

My heartfelt thanks to my co-supervisor Dr. Daniele Martinelli for his assistance, infinite patience and advice during the modelling phases.

Lastly, I would also like to thank my Daniele, who first beliefs in me and supports me in my madness. Your support for me is vital.

I dedicate this work to my father and my mother, who gave me the tenacity without which I would not be where I am now.